Fast Time Scale Dynamics of Protein Backbones: NMR Relaxation Methods, Applications, and Functional Consequences

Virginia A. Jarymowycz and Martin J. Stone*

Department of Chemistry and Interdisciplinary Biochemistry Program, Indiana University, Bloomington, Indiana 47405-0001

Received January 7, 2005

Contents

* Author to whom correspondence should be addressed [telephone (812) 855-6779; fax (812) 855-8300; e-mail mastone@indiana.edu].

1. Overview

Over the past 15 years there has been an explosion of research on the dynamical properties of proteins, largely driven by the emergence of a handful of techniques that are sensitive to protein motion.[1] One of these methods, nuclear magnetic relaxation (NMR), has now been applied to hundreds of proteins. These studies have indicated which aspects of dynamics are conserved or variant throughout a protein structure or between different proteins. More importantly, they have allowed us to observe specific changes in protein dynamics related to the chemical or physical state of the protein. Ongoing studies are providing insights into the possible functional consequences of these dynamical properties. However, despite the many successes, NMR relaxation methods are plagued by a number of limitations and assumptions that make the functional interpretation of the data very difficult.

A number of previous reviews have appeared describing NMR relaxation and dynamics methods and/or their applications.[1−14] While reiterating many of the central points from these previous reviews, the present paper is intended to focus attention on the potential functional consequences of dynamics on a fast (picosecond−nanosecond) time scale. We hope that this review will prove useful not only to established NMR spectroscopists but also to other biochemical researchers seeking to understand the importance of dynamics in their own systems. In section 2 we present a variety of ways in which fast time scale dynamics could potentially influence protein function. We hope that this discussion will be helpful in formulating hypotheses with regard to specific systems and provide a framework for interpretation of results. In section 3 we present a summary of the theory behind protein backbone ($^{15}N_H$ and $^{13}C_H$) NMR relaxation methods and the relationship of relaxation to dynamics. We also discuss several practical aspects of implementing these techniques. This section is written at a level that should not require much expertise in physics or mathematics but is nevertheless sufficiently thorough for the reader to understand and apply the most commonly used methods. We anticipate that this section will be of particular interest to graduate students and other researchers who are using these methods for the first time. In section 4, we present an exhaustive list of previous NMR studies of backbone dynamics and we discuss several of these studies in more detail, focusing on those for which there appear to be relationships between dynamics and function. Finally, in section 5, we summarize the current progress with reference to the goals put forward in section 2, and we discuss the future challenges.

10.1021/cr040421p CCC: $59.00
Published on Web 04/25/2006

Virginia A. Jarymowycz (née Goehlert) received her B.S. degree in biochemistry from Indiana University in 2001. She is currently pursuing a Ph.D. through the Interdisciplinary Biochemistry Program at Indiana University in the laboratory of Dr. Martin J. Stone. Her thesis research is focused on using NMR relaxation techniques to investigate the potential contributions of fast time scale dynamics to observed protein stability and function.

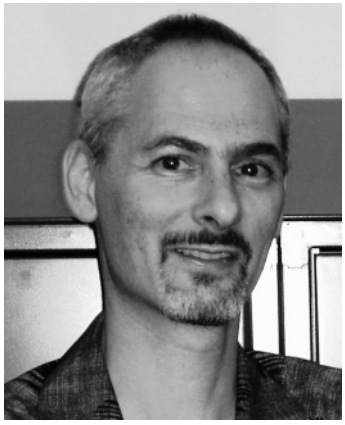

Martin J. Stone received his B.Sc. and M.Sc. (honors) degrees (in 1986 and 1987, respectively) from the University of Auckland (New Zealand) and his Ph.D. degree in 1991 from the University of Cambridge (United Kingdom), where he studied with Prof. Dudley H. Williams. He performed postdoctoral research with Prof. Peter Wright at the Scripps Research Institute (La Jolla, CA) and then joined the Department of Chemistry and Program in Biochemistry at Indiana University, Bloomington, IN. His research spans two major areas: understanding the relationships of protein dynamics to structure, stability, and function and studying the structural basis of receptor recognition by chemokine proteins.

2. Potential Functional Importance of Fast Dynamics

2.1. Kinetics and Thermodynamics of Structural Ensembles

It has long been recognized that the chemical properties of proteins are intimately related to their internal molecular structures. In the classical "lock-and-key" model of molecular interactions,[15,16] it is implicitly assumed that each protein molecule has a static internal structure. This assumption is incorrect. In fact, proteins (and other biomolecules) exist as complex ensembles of structural states (conformations) that are continuously interconverting due to thermal fluctuations. Only a subset of these structures is competent for any particular function (catalysis, ligand-binding, etc.) so the observed (bulk) functional properties of the protein are a manifestation of the functional properties of each competent state, the populations of these states (thermodynamics of the ensemble), and the rates of interconversion between the different conformations (kinetics of the ensemble).

Dynamics (or molecular motion) is the process of interconversion between conformational states. However, the prevalence of any particular motional mode depends not only on the relevant energy barrier (intrinsic rate constant for the event) but also on the population of the starting conformation. Therefore, studies of protein "dynamics" offer information about both the time scales of motions and the population distribution of conformational states, that is, both the thermodynamics and the kinetics of the ensemble. In this paper we will use the term "dynamics" in this broader sense.

The energy barriers separating different conformations of a protein can vary dramatically, so interconversion between states can be as fast as a few picoseconds (for librations and rotations of small, relatively unhindered groups) and as slow as many seconds (for large conformational rearrangements such as unfolding).[14] In this paper, we focus exclusively on the fast (picosecond to nanosecond) motions, with particular emphasis on the protein backbone; several other papers in this issue discuss the dynamics of side-chain groups and/or protein motions on slower time scales. Most of the chemical reactions and interactions of proteins occur on time scales much slower than nanoseconds. Nevertheless, it is possible that fast time scale dynamics underlie some of these slower fluctuations (vide infra). Moreover, the thermodynamics of protein−ligand binding and of large conformational rearrangements (equilibria between two distinct conformational ensembles) depend on the population distributions of substates within these ensembles. Consequently, studies of fast time scale dynamics can provide information relevant to both the kinetics and the thermodynamics of protein function.

2.2. Importance of Conformational Entropy

In many biochemical studies, a goal is to understand and/or manipulate the positions of equilibria—between free and bound states, between reduced and oxidized forms, between folded and unfolded ensembles, between ground states and transition states, etc. These equilibria are influenced by a large number of physicochemical factors such as strain energy, hydrogen bonding, charge−charge and other electrostatic interactions (including dispersion forces), the interactions and structure of the solvent, solvent entropy, etc.[17−21] An important additional factor is the intrinsic conformational entropy of the protein molecule, which represents the distribution of conformational states discussed above.[11,12,22,23] High conformational entropy indicates a larger number of states or a more evenly distributed population, whereas low conformational entropy represents few states or unequal distributions.

Consider for illustrative purposes an idealized protein molecule containing 100 amino acid residues, each with three accessible conformations, and assume that all conformations are equally likely and independent of each other. The conformational entropy of the free state will be $R \ln(3^{100})$. If, upon binding to a ligand, 5 of the 100 residues completely lose their conformational freedom, the conformational entropy of the bound ensemble will be $R \ln(3^{95})$, so the conformational entropy will have decreased by $R \ln(3^5)$ or $\sim$3.2 kcal mol^{-1} at 25 °C. This will decrease the association equilibrium constant by a factor of $\sim$240 relative to its value if no conformational freedom has been lost. Thus, conformational entropy can potentially have a substantial effect on binding affinity, and any attempt to predict or rationalize

binding constants or protein stability should take this into account if possible.

The literature reviewed in section 4 (vide infra) clearly indicates that substantial changes in fast time scale dynamics can indeed occur when a protein binds to a ligand or for certain other changes in the state of the protein. A major goal of NMR dynamics studies is to evaluate the thermodynamic importance of these changes, that is, to convert the NMR observables to a measure of conformational entropy.[11] Section 3.7 describes several approaches to accomplishing this and discusses the limitations of these methods. One limitation is that the conformational entropy of the system depends not only on the motions of each group but also on the coupling between motions of different groups in the protein. For this reason, as well as others discussed below, another major goal of NMR studies of fast dynamics is to characterize the relationships between the motions of different groups within protein structures.

2.3. Coupled or Correlated Motions

In the illustrative example presented above, we concluded that immobilization of five amino acid residues each with three accessible conformational states was associated with a reduction in conformation free energy of $\sim$3.2 kcal mol^{-1} at 25 °C. However, we assumed that each of these five residues was moving independently of the others. Now consider the situation if the motions of these residues were tightly coupled with each other; that is, a change in conformational state of one residue would be linked to a change in conformational state of one or more other residue(s). For example, the five residues might consist of two groups, one of three residues and the other of two residues. Within each group the motions of the different residues might be tightly synchronized, but the two groups of residues might be independent of each other. In this situation each coupled group of n residues would have a total of only three conformational states (not 3^n). Instead of the number of conformations lost upon binding being 3^5 (= 243), it would now be only 3^2 (= 9), with an associated free energy cost of only 1.3 kcal mol^{-1}. Although this reduction in conformational entropy will still affect the association equilibrium constant for binding, the influence of this term is much less substantial than if the motions of the immobilized groups were independent. Thus, to obtain accurate estimates of conformational entropy, it is essential to determine whether coupled motions exist.

One can consider the question of whether coupled motions exist from a teleological perspective. Most proteins are marginally stable; typically only $\sim$5−15 kcal mol^{-1} separate the native and denatured ensembles.[24,25] Although denatured proteins are not completely without structural order,[26−28] it is reasonable to assume that most residues move independently of each other if they are separated by more than a few residues in the primary sequence.[29] Formation of the native state unavoidably involves loss of many degrees of freedom. However, the introduction of coupled motions will cause an additional reduction in the conformational entropy and hence the stability of the native ensemble. This reduction could easily be large enough to tip the equilibrium in favor of the denatured ensemble. Therefore, we might expect evolutionary pressure to have selected natural folded (stable) proteins in which there are relatively few coupled motions.

Counter to the above argument, there are two situations in which we might expect proteins to have evolved with substantial correlated internal motions. One scenario is that it is physically impossible to accomplish well-defined secondary and tertiary structure (a functional folded state) without packing groups against each other such that their motions become interdependent. This is a reasonable proposal, but at present we do not know whether it is correct. Indeed, it could be the case for certain folds but not others. The second possibility is that the coupling of internal motions has a favorable influence on protein function, which might override the negative selective pressure associated with entropy reduction. It is important then to consider what types of functional properties might be reliant on coupled internal motions of proteins. We discuss several possibilities below.

We first propose a way in which coupled motions could provide a thermodynamic driving force in favor of binding. The above discussion of the relationship between conformational entropy and binding focuses on the case in which binding reduces the number of conformational states accessible to a protein, originally referred to as "configurational adaptability"[30] but subsequently dubbed "induced fit" binding.[31] Imagine, however, that the motions of certain residues in an unbound protein are strongly coupled but that binding interferes with the coupling mechanism. In this case, although some of the residues involved in the coupling network might become immobilized upon binding, others might be "released" from the coupling network undergoing increased motions and therefore contributing favorably to the entropy of binding. Depending on the details, this could cancel or even outweigh the entropic penalty of induced fit binding. Thus, *the disruption of a dynamical coupling network is a possible mechanism to promote ligand binding*.

Coupled motions could also be involved in regulating allosteric (or cooperative) ligand binding by a protein, the thermodynamic linkage of binding two ligand molecules at different sites.[32] If the motions of groups in the two sites were coupled, either directly or through an intervening network of other groups, then binding at one site might change the distribution of conformations at the other site.[13,33] If the dynamical coupling resulted in both binding sites accessing binding-competent conformations simultaneously, then the binding at one site would increase the population of binding-competent conformations in the second site, resulting in positive binding cooperativity. Alternatively, the linkage of binding competent conformations at one site with noncompetent conformations at the second site would give rise to negative cooperativity. Finally, the binding at one site could potentially disrupt the coupling mechanism, with the effect at the second site depending on the change in the structural ensemble at this site.

In addition to influencing the thermodynamics of binding, it has been proposed that coupled motions on picosecond−nanosecond time scales can influence the kinetics of enzyme-catalyzed reactions.[34−36] This is at first counterintuitive because turnover rates for enzymes typically occur on much slower time scales, for example, milliseconds. How can motions occurring on a time scale of picoseconds regulate chemical reactions occurring with rate constants in the millisecond regime? This can be understood in terms of the theory of "near-active conformations" (NACs).[37] This theory postulates that the intrinsic turnover rate of an enzyme, k_{cat}, is related to the frequency (or probability) with which the enzyme populates conformations that are competent to catalyze the reaction (NACs). The NACs might be quite rare, and they might occur only when each of several functional

groups in the enzyme moves into the appropriate position relative to the substrate. Therefore, the probability with which NACs are attained is related to the probabilities with which each of the necessary groups occupies the appropriate conformation. If the groups move independently, then the NAC probability will be the product of the individual functional group probabilities. Even if the individual groups move rapidly, the NAC probability could be very low, resulting in slow catalytic chemistry. This is akin to the interference of two high-frequency sound waves, which gives rise to a resultant wave the amplitude of which oscillates at a much lower frequency ("beat frequency") than that of either of the two underlying oscillations. On the other hand, if the motions of two active site functional groups are appropriately coupled, the NAC probability will no longer be the product of the individual functional group probabilities, but will instead be higher, resulting in more efficient catalysis. Thus, it is not difficult to imagine that natural selection may have yielded enzymes in which coupled motions occur at the active site. Similarly, the kinetics of multisubstrate or allosterically regulated enzymes might be regulated by dynamical coupling between the different binding sites.

A special case in which fast time scale dynamics have been implicated in enzyme function is the class of enzymes that catalyze electron or proton transfer by using quantum tunneling mechanisms as opposed to thermally crossing classical activation barriers. In these enzymes the efficiency of tunneling is extremely sensitive to the distance between the original and final positions of the tunneling particle.[38] Consequently, molecular motions that modulate this distance have a substantial influence upon tunneling rates.[38−43] In addition, molecular motions can potentially influence the mechanisms through which tunneling occurs.[44] It is clear that efficient tunneling could be promoted by the simultaneous movement of two or more groups (especially the origin and destination groups), so synchronization of fast motions could potentially influence the rate of tunneling.

2.4. Summary

The above discussion lays out a variety of ways in which fast time scale dynamics could influence the interactions and functions of proteins. However, until recently the only experimental techniques available to characterize these motions did not provide sufficiently detailed or reliable information to assess the functional importance of the motions.[1] This situation has now changed. A "revolution"[36] (*sic*) in the study of fast protein dynamics by NMR spectroscopy has been stimulated by two important developments. First, Lipari and Szabo constructed a new theoretical framework for representing the relationship between fast dynamics and heteronuclear NMR relaxation rates.[45,46] Second, Kay et al. developed experimental methods to determine the necessary relaxation parameters using biosynthetically isotope-labeled proteins and ^{1}H-detected heteronuclear correlation spectra.[47] These and a series of subsequent extensions and developments (discussed in section 3) have made it possible to characterize the internal motions of proteins at an unprecedented level of detail. Moreover, the application of these methods to numerous proteins (reviewed in section 4) has vastly increased our knowledge of high-frequency motions in proteins and has revealed a number of cases in which these motions appear to play a functional role. Nevertheless, there remain several important challenges in unequivocally identifying the functional consequences of fast dynamics in proteins; these are discussed in the section 5 of this review.

3. NMR Relaxation Methods for Characterizing Fast Dynamics

In this section we discuss the methods that are most commonly used for the analysis of fast backbone dynamics in proteins. The physics relating nuclear magnetic relaxation to molecular motion is quite complex, so a thorough discussion of the topic requires presentation of rather complicated mathematical relationships. In an attempt to make this section more readable and accessible to biochemical researchers, we present most of the necessary equations in several tables and use the text and figures to highlight the key features of the relationships in conceptual rather than rigorous mathematical terms. Much of the relevant physics has been presented in previous reviews.[3−5,7]

3.1. Nuclear Magnetic Relaxation and Its Relationship to Dynamics

In any modern NMR experiment, the bulk magnetization of the sample is perturbed from its equilibrium state (along the *z*-axis, parallel to the permanent magnetic field), and the emitted signal is observed as the sample returns to equilibrium. Relaxation is the process by which nonequilibrium magnetization returns to the equilibrium state (or transforms to another nonequilibrium state). Considering that there are many different nonequilibrium states (different nuclei, in-phase versus anti-phase, single- versus multiple-quantum, etc.), there are many corresponding relaxation processes that could potentially be measured. In studies of backbone NH group dynamics in proteins, it is typical to measure the ^{15}N longitudinal relaxation rate ($R_1 = 1/T_1$), the in-phase ^{15}N transverse relaxation rate ($R_2 = 1/T_2$), and the heteronuclear nuclear Overhauser effect ($\{^{1}H\}-^{15}N$ NOE). Several additional parameters are also described below in reference to specific applications. All of these parameters are typically measured using two-dimensional (HSQC type) experiments in which the intensities of peaks are modulated as a function of a time delay placed at a point in the sequence when the relevant relaxation process is active.

Each observable relaxation process involves transitions between quantized magnetic energy levels. Such transitions are stimulated by magnetic fields that oscillate at the transition frequencies. Thus, the relaxation rates are determined by the likelihood that the relevant nuclei experience appropriate oscillating magnetic fields. Such oscillating fields in proteins result from the movements of magnetic nuclei relative to each other or relative to the overall permanent field of the NMR magnet. Consequently, relaxation is exquisitely sensitive to molecular motion.

For the two heteronuclei of primary interest in terms of backbone dynamics studies, ^{13}C and ^{15}N, there are two dominant mechanisms by which molecular motion on the picosecond to nanosecond time scale influences magnetic relaxation, dipole−dipole interactions, and chemical shift anisotropy (CSA). We present here a brief conceptual description of each mechanism; for a more theoretical discussion we refer readers to the excellent review by Fischer et al.[7]

The dipole−dipole mechanism results from the fluctuating interaction (coupling) between a pair of magnetic nuclei as

Table 1. Rotational Correlation Functions $C(t)$ for Various Motional Models Discussed in the Text

motional model	rotational correlation function	eq
isotropic molecular tumbling with no internal motion[a]	$C(t) = \frac{1}{5} e^{-t/\tau_m}$	1
slow isotropic tumbling with faster isotropic internal motions[a,b]	$C(t) = \frac{1}{5} e^{-t/\tau}$	2
slow isotropic tumbling with faster, spatially restricted internal motions[a-c]	$C(t) = \frac{1}{5} S^2 e^{-t/\tau_m} + \frac{1}{5}(1 - S^2) e^{-t/\tau}$	3
axially symmetric tumbling with no internal motion[d]	$C(t) = \frac{1}{5} A_1 e^{-t/\tau_1} + \frac{1}{5} A_2 e^{-t/\tau_2} + \left(\frac{1}{5}\right) A_3 e^{-t/\tau_3}$	4

[a] τ_m is the overall correlation time of the molecule.[45] [b] $\tau^{-1} = \tau_m^{-1} + \tau_e^{-1}$, where τ_e is the effective internal correlation time of the X−H bond vector.[45] [c] S^2 (the squared order parameter) is a model-independent measure of the degree of spatial restriction of internal motion of the X−H bond vector.[45] [d] The coefficients are defined as $A_1 = (0.75) \sin^4 \alpha$, $A_2 = 3 \sin^2 \alpha \cos^2 \alpha$, $A_3 = (1.5 \cos^2 \alpha - 0.5)^2$, in which α is the angle between the X−H bond vector and the unique axis of the principal frame of the diffusion tensor. The time constants are defined as $\tau_1 = (4D_{||} + 2D_\perp)^{-1}$, $\tau_2 = (D_{||} + 5D_\perp)^{-1}$, and $\tau_3 = (6D_\perp)^{-1}$, where $D_{||}$ and $D_\perp$ are rotational diffusion constants around the unique (parallel) and perpendicular axes, respectively. In some cases the diffusion constants are presented as an effective isotropic diffusion constant $D_{iso} = (1/3)D_{||} + (2/3)D_\perp$ or correlation time $\tau_m = (6D_{iso})^{-1}$ and the ratio of parallel to perpendicular diffusion constants $(D_{||}/D_\perp)$.[72]

the internuclear vector rotates relative to the permanent magnetic field. Consider a pair of bonded ^{15}N and ^{1}H nuclei in the backbone of a protein in an NMR magnet. As the $^{15}N-^{1}H$ bond vector rotates, due to either molecular tumbling or internal structural fluctuations of the protein, the magnetic field that the ^{1}H nucleus induces at the position of the ^{15}N nucleus will vary. If this field fluctuates at the appropriate frequency, it will induce relaxation of the ^{15}N nucleus.[48] Importantly, the strength of the dipolar coupling is extremely dependent on the internuclear distance, so the attached proton dominates over all other nuclei in effecting the dipolar relaxation of a protonated ^{15}N nucleus.

The CSA relaxation mechanism results from the fluctuating magnetic field that is experienced by a nucleus due to variations in shielding from the permanent magnetic field. Again, consider a protonated backbone amide ^{15}N nucleus in a protein. As the molecule tumbles or the rigid amide group oscillates relative to the remainder of the molecule, the ^{15}N nucleus is shielded to varying extents. The fluctuation of this shielding can induce relaxation of the ^{15}N nucleus. Because the chemical shift of the ^{15}N is dominated by the amide group in which it is located, this relaxation component can again be expressed in terms of the fluctuations of the NH bond vector. Both ^{13}C and ^{15}N, the nuclei of primary interest in protein NMR relaxation studies, have considerable contributions to relaxation from CSA.[48]

In addition to the above two mechanisms, the measured transverse relaxation rate constant (R_2) can also be influenced by conformational exchange. During the variable delay period for R_2 measurements, the magnetization is transverse and is typically repeatedly refocused using a series of 180° pulses separated by a short (~1 ms) delay. If the ^{15}N nucleus exchanges between different conformations on the time scale of this short delay (microseconds to milliseconds), then the resulting chemical shift change can lead to dephasing of the transverse magnetization, which is observed as apparent R_2 relaxation. In the model-free approach discussed in this review, this exchange contribution to R_2 (designated R_{ex}) can often be identified, but its detailed physical interpretation remains obscure. If the microsecond to millisecond motions are of primary interest, the powerful relaxation dispersion experiments can be applied to characterize the time scales of these events and the populations of the exchanging conformations; readers are referred to the recent review by Palmer for a discussion of these methods.[14]

Molecular motions can be exceedingly complex. Thus, a very large number of parameters would be required to accurately describe their time scales, amplitudes, and directionalities. Considering that it is generally not practical to observe more than a handful of relaxation parameters for each nucleus and that observable relaxation parameters are not sensitive to all molecular motions, obtaining a full description of molecular motions is not feasible. Therefore, the three approaches discussed below all provide limited but still useful views of the motions of nuclei within proteins. The spectral density mapping approach yields accurate information about the prevalence of motions at each of a limited number of frequencies, but not much insight into the nature of these motions. The model-free approach separates the overall tumbling of the protein molecule from the internal motions of each group and provides a useful estimate of the degree of order at each site. However, this approach makes certain assumptions about the frequency-dependence of both internal and overall motions, limiting the potential accuracy of the method. The final approach discussed assumes a specific motional model, allowing a very precise description of the motions, again at the probable expense of accuracy. As discussed in section 4.1, the model-free approach has been by far the most popular, although spectral density mapping has often been applied in cases for which the assumptions of the model-free approach are inappropriate. The analysis of dynamics in terms of specific motional models has not been widely applied.

3.2. Correlation Functions and Spectral Density Functions

The most general approach to rigorously describing the rotational motions of a bond vector (e.g., NH group) is to define a time-dependent rotational correlation function $C(t)$, a measure of the probability that a bond vector has the same position (angle) relative to the permanent magnetic field at arbitrarily defined time zero and a later time t. This function decays from a value of one-fifth[45] at $t = 0$ to a value of zero at infinite t, but the shape of the function between these extremes defines the likelihood of motions on different *time scales*. Several simple examples are given in Table 1 and Figure 1. If a bond vector rotates isotropically with a single characteristic time scale, the correlation function is a single exponential decay. This would be the case for a rigid NH bond vector within an isotropically rotating protein, in which

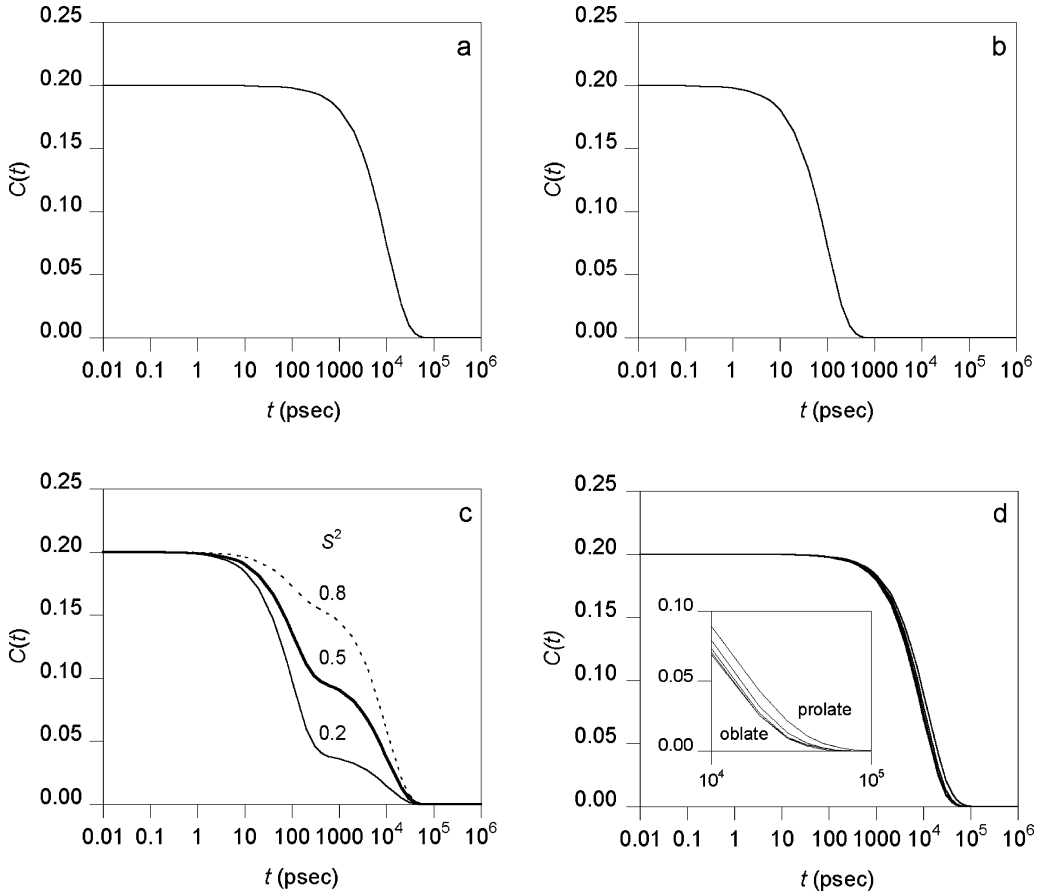

Figure 1. Graphical representations of the rotational correlation functions listed in Table 1: (a) isotropic tumbling with one characteristic time ($\tau_m = 10$ ns), simulated using eq 1; (b) slow isotropic tumbling ($\tau_m = 10$ ns) with hypothetical faster ($\tau_e = 100$ ps) isotropic internal motions, simulated using eq 2; (c) slow isotropic tumbling ($\tau_m = 10$ ns) with faster ($\tau_e = 100$ ps), spatially restricted isotropic internal motions simulated using eq 3 and S^2 values of 0.2, 0.5, and 0.8, as indicated; (d) axially symmetric tumbling simulated using eq 4 for $\alpha = 45°$, $\tau_m = 10$ ns, and $D_{||}/D_\perp$ values of 0.2 (labeled "oblate"), 0.5, 1, 2, and 5 (labeled "prolate").

case the characteristic time scale is the rotational correlation time of the molecule τ_m; this correlation function is shown in eq 1 (Table 1) and Figure 1a. If the bond vector is subject to isotropic motions at two different characteristic time scales [e.g., relatively slow isotropic overall motions (time scale τ_m) and faster isotropic internal motions (effective time scale τ_e)—a hypothetical situation], then the decay is a single exponential with a decay constant dominated by the fast motions ($\tau^{-1} = \tau_m^{-1} + \tau_e^{-1}$; eq 2; Figure 1b). If the faster time scale is spatially restricted (not isotropic), then the fast decay phase accounts for only a fraction of the total decay of $C(t)$, as shown in eq 3 and Figure 1c; in these relationships the degree of spatial restriction is represented by the squared order parameter S^2 ($0 \leq S^2 \leq 1$). Finally, if there is no internal motion but the overall motion is axially symmetric rather than isotropic (e.g., a rigid NH group within an elongated protein), $C(t)$ depends on the time scales of motions about axial and orthogonal axes as well as the angle of the bond vector relative to these axes (eq 4; Figure 1d).

The correlation functions discussed above can be readily related to simple models for rotational motions of bond vectors and are particularly well suited to separating motions that occur on substantially different time scales (e.g., overall tumbling versus internal motions). However, the measurable relaxation parameters are more easily understood in terms of the probabilities of motions at specific *frequencies* rather than *times*. Therefore, it is convenient to redefine correlation functions on a frequency scale, which is readily achieved by Fourier transformation of the correlation function $C(t)$ to give the spectral density function $J(\omega)$; note that this is the same transformation used to convert time domain NMR data (free induction decays) to frequency domain data (spectra). The spectral density functions corresponding to the four simple correlation functions discussed above are given in Table 2 (eqs 5−7 and10) and presented graphically in Figure 2; Table 2 also lists several additional spectral density functions that are discussed below.

In panels a−c of Figure 2 we have labeled the spectral densities at three critical frequencies (for $^{15}N-^{1}H$ bond vectors) discussed below: a frequency of zero (i.e., very slow motions), the Larmor frequency of the ^{15}N nucleus (60 MHz on a 14.1 T magnet), and the Larmor frequency of the ^{1}H nucleus (600 MHz on a 14.1 T magnet). For the spectral density function representing isotropic rotation of a protein (Figure 2a), the value of the spectral density function at the low frequency is much larger than those at the ^{15}N or ^{1}H Larmor frequencies. For the model dominated by internal motions (Figure 2b), the high-frequency spectral densities are comparable to the $J(0)$ value. For the model representing restricted internal motions (Figure 2c), the relative magnitudes of high- and low-frequency spectral densities are dependent on the degree of motional restriction (S^2). Finally, panels d−f of Figure 2 indicate that, for axially symmetric overall motions, the spectral density functions are dependent on the ratios of diffusion rates around unique and perpendicular axes (different curves within each panel) and also on the angle (α) between a bond vector and the unique axis (different panels).

Table 2. Spectral Density Functions $J(\omega)$ for Various Motional Models Discussed in the Text

motional model	spectral density function, $J(\omega)$	eq
isotropic molecular tumbling with no internal motion[a]	$J(\omega)=\frac{2}{5}\left(\frac{\tau_m}{1+(\omega\tau_m)^2}\right)$	5
slow isotropic tumbling with faster isotropic internal motions[a]	$J(\omega)=\frac{2}{5}\left(\frac{\tau}{1+(\omega\tau)^2}\right)$	6
slow isotropic tumbling with faster, spatially restricted internal motions ("original" model-free formalism)[a]	$J(\omega)=\frac{2}{5}\left(\frac{S^2\tau_m}{1+(\omega\tau_m)^2}+\frac{(1-S^2)\tau}{1+(\omega\tau)^2}\right)$	7
"simplified" model-free formalism ($\tau_e \ll \tau_m$) with isotropic tumbling[b]	$J(\omega)=\frac{2}{5}\left(\frac{S^2\tau_m}{1+(\omega\tau_m)^2}\right)$	8
"extended" model-free formalism (two time scales of internal motion) with isotropic tumbling[c]	$J(\omega)=\frac{2}{5}\left(\frac{S^2\tau_m}{1+(\omega\tau_m)^2}+\frac{(S_f^2)\tau_s'}{1+(\omega\tau_s')^2}\right)$	9
axially symmetric tumbling with no internal motion[a]	$J(\omega)=\frac{2}{5}\sum_{j=1}^{3}A_j\left(\frac{\tau_j}{1+(\omega\tau_j)^2}\right)$	10
"original" model-free formalism with axially symmetric tumbling[d]	$J(\omega)=\frac{2}{5}\sum_{j=1}^{3}A_j\left(\frac{S^2\tau_j}{1+(\omega\tau_j)^2}+\frac{\tau_j'(1-S^2)}{1+(\omega\tau_j')^2}\right)$	11
fully anisotropic tumbling with no internal motion[e]	$J(\omega)=\frac{2}{5}\sum_{j=1}^{5}A_j\left(\frac{\tau_j}{1+(\omega\tau_j)^2}\right)$	12
"original" model-free formalism with fully anisotropic tumbling[e]	$J(\omega)=\frac{2}{5}\sum_{j=1}^{5}A_j\left(\frac{S^2\tau_j}{1+(\omega\tau_j)^2}+\frac{\tau_j'(1-S^2)}{1+(\omega\tau_j')^2}\right)$	13

[a] These spectral density functions correspond to the four correlation functions listed in Table 1. Symbols are defined in the footnotes to Table 1. [b] Symbols are as defined for the "original" model-free formalism. [c] The generalized squared order parameter is defined as $S^2 = S_f^2 S_s^2$, in which S_f^2 is the squared order parameter for fast time scale (<20 ps) internal motions and S_s^2 is the order parameter for slow internal motions occurring on a time scale τ_s longer than ~500 ps. The reduced time constant τ_s' is defined as $(\tau_s')^{-1} = (\tau_m)^{-1} + (\tau_s)^{-1}$. [d] Most symbols are as defined for the case of axially symmetric tumbling with no internal motion. In addition, this equation contains the internal motional parameters (S^2 and τ_e) and three reduced time scales defined as $\tau_j' = \tau_j\tau_e/(\tau_j + \tau_e)$. [e] The coefficients are defined as $A_1 = 6m^2n^2$, $A_2 = 6l^2n^2$, $A_3 = 6l^2m^2$, $A_4 = d - e$, $A_5 = d + e$, in which $d = [3(l^4 + m^4 + n^4) - 1]/2$ and $e = [\delta_x(3l^4 + 6m^2n^2 - 1) + \delta_y(3m^4 + 6l^2n^2 - 1) + \delta_z(3n^4 + 6l^2m^2 - 1)]/6$; l, m, and n are the direction cosines of the X−H bond vector with respect to the diffusion axes, x, y, and z, respectively; $\delta_i = (D_i - D)/(D^2 - L^2)^{1/2}$; D_x, D_y, and D_z are the diffusion constants around the three principal axes; $D = (1/3)(D_x + D_y + D_z)$; and $L^2 = (1/3)(D_xD_y + D_xD_z + D_yD_z)$. The time constants are defined as $\tau_1 = (4D_x + D_y + D_z)^{-1}$, $\tau_2 = (4D_y + D_x + D_z)^{-1}$, $\tau_3 = (4D_z + D_x + D_y)^{-1}$, $\tau_4 = [6(D + (D^2 - L^2)^{1/2})]^{-1}$, and $\tau_5 = [6(D - (D^2 - L^2)^{1/2})]^{-1}$; and the reduced time constants are defined as $\tau_j' = \tau_j\tau_e/(\tau_j + \tau_e)$.[73]

3.3. Spectral Density Mapping and Reduced Spectral Density Mapping

Relationship of Relaxation Parameters to Spectral Densities. Considering that the correlation function and corresponding spectral density function are the most general ways to describe bond vector motions, a goal of dynamics studies is to completely define these functions for each bond vector. The relationships between the three commonly measured relaxation parameters for NH or CH groups and the relevant values of the spectral density function are listed in Table 3A. Note that the relaxation rates are divided into dipolar and CSA components but that both are dependent on linear combinations of the spectral density function evaluated at five critical frequencies, $J(0)$, $J(\omega_X)$, $J(\omega_H)$, $J(\omega_H + \omega_X)$ and $J(\omega_H - \omega_X)$.

Simple inspection of the relationships in Table 3A highlights two important points. First, because these equations contain only the spectral densities at five frequencies, any rotational motions at other frequencies do not directly affect these relaxation parameters. Therefore, inferences regarding motion at other frequencies can be made only if we assume some simple relationship between the observed and unobserved frequencies. Second, it is not possible to unambiguously evaluate the five unknown spectral density values for each bond vector from the three most commonly measured relaxation parameters; at least five independent parameters would be needed.

Full Spectral Density Mapping. To overcome the latter limitation, Peng and Wagner developed the spectral density mapping (SDM) method, in which an expanded set of six relaxation parameters is measured, allowing the spectral density values at all five frequencies to be uniquely determined directly from measured relaxation parameters.[49,50] The six parameters measured in this approach are the three listed in Table 3A and also the antiphase transverse relaxation rate $R_{2,anti}$, the decay rate of longitudinal two-spin order R_{DQ}, and the amide proton longitudinal relaxation rate $R_{1,H}$. The relationships between these parameters and the relevant spectral density values are given in Table 3B, and the relationships for calculating the five critical spectral density values are given in Table 4.

The initial implementation of SDM for $^{15}N-^{1}H$ bond vectors in the protease inhibitor eglin C[50] indicated that the three high-frequency spectral densities [$J(\omega_H - \omega_N)$, $J(\omega_H)$, and $J(\omega_H + \omega_N)$] have very similar values to each other but that these differ substantially from the $J(\omega)$ values at the two low frequencies [$J(0)$ and $J(\omega_N)$]. This trend can also

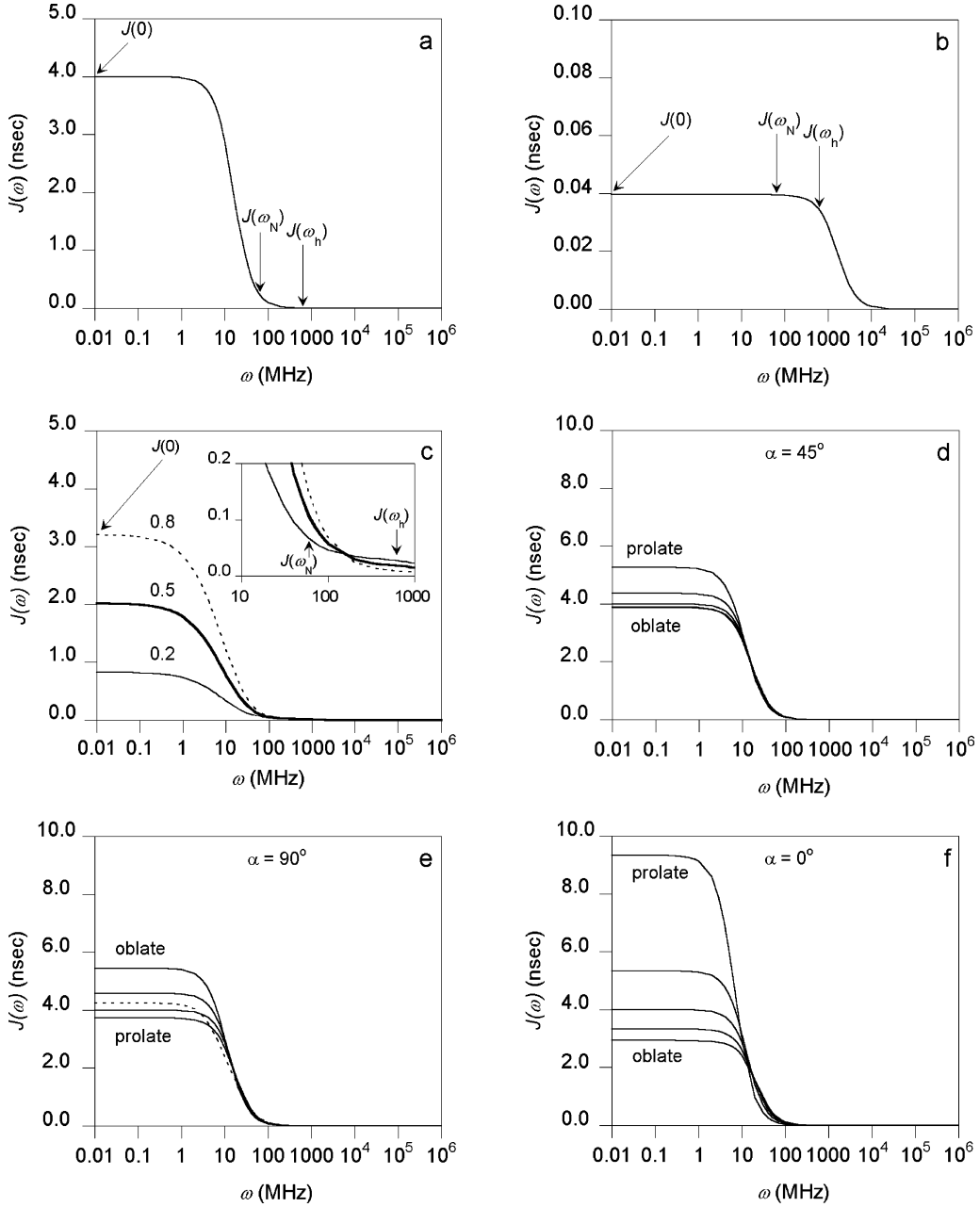

Figure 2. Graphical representations of the spectral density functions corresponding to the correlation functions presented in Figure 1. Panels a−d correspond to eqs 5, 6, 7, and 10, respectively, with the values of the parameters as listed in the footnotes for panels a−d, respectively of Figure 1. Panels e and f illustrate the same spectral density function as panel d for $\alpha = 90°$ and $\alpha = 0°$, respectively. Panels d and f show five curves corresponding to $D_{||}/D_{\perp}$ values of 0.2 (labeled "oblate"), 0.5, 1, 2, and 5 (labeled "prolate"). Panel e shows five curves corresponding to $D_{||}/D_{\perp}$ values of 0.2 (labeled "oblate"), 0.5, 1, 2 (labeled "prolate"), and 5 (dotted line). The $J(\omega)$ values at the three critical frequencies (0, ω_N, and ω_h) for a 600 MHz spectrometer are indicated by arrows; because the three high frequencies are nearly indistinguishable on the scale shown and because $J(\omega)$ values evaluated at these frequencies are extremely similar, $J(\omega_h)$ is used to indicate the spectral density values at frequencies of ω_H, ω_{H+N}, and ω_{H-N}, assuming $J(\omega)$ is effectively constant at $\omega \approx \omega_H$. The inset in panel c is an expansion of the indicated region to illustrate that the three curves cross between ω_N and ω_h. Note that the *y*-axis scales vary between panels.

be observed in the simple spectral density functions simulated in Figure 2; note that the three high frequencies occur in almost identical positions on the logarithmic scale (symbolized by ω_h). In addition, Peng and Wagner noted that $J(0)$ and $J(\omega_N)$ were the most variable spectral densities across the eglin C sequence, indicating that they are particularly sensitive to internal dynamics; this trend can also be seen in the simulation of Figure 2c. These observations prompted the subsequent development of simplified versions of the SDM approach, referred to as "reduced spectral density mapping" techniques.[51−54]

Reduced Spectral Density Mapping. In the simplest version of reduced SDM,[51] $J(\omega)$ values at the three high frequencies ($\omega_H - \omega_N$, ω_H, and $\omega_H + \omega_N$) are combined into a single spectral density value $J(\omega_h)$ due to their negligible variation in comparison with the $J(\omega)$ values at the two low frequencies (0, ω_N). In this case, the equations relating the heteronuclear R_1 and R_2 and the $\{^1H\}-^{15}N$ NOE to the spectral density values (Table 3A) can be simplified to those listed in Table 5A, allowing the three reduced spectral densities to be calculated directly from the three commonly measured relaxation parameters (Table 5B). An alternative version of

Table 3. Relationships between Relaxation Parameters and Relevant Values of the Spectral Density Function

A. Relationships between the Three Commonly Measured Relaxation Parameters for NH or CH Groups and the Relevant Values of the Spectral Density Function

parameter[a]	relationship to spectral density function[a,b]	eq
longitudinal relaxation rate constant for nucleus X	$R_1^{DD} = \frac{1}{4} d^2[J(\omega_H - \omega_X) + 3J(\omega_X) + 6J(\omega_H + \omega_X)]$	14a
$R_1 = R_1^{DD} + R_1^{CSA}$	$R_1^{CSA} = c^2 J(\omega_X)$	14b
transverse relaxation rate constant for nucleus X	$R_2^{DD} = \frac{1}{8} d^2[4J(0) + J(\omega_H - \omega_X) + 3J(\omega_X) + 6J(\omega_H) + 6J(\omega_H + \omega_X)]$	15a
$R_2 = R_2^{DD} + R_2^{CSA} + R_{ex}$	$R_2^{CSA} = \frac{1}{6} c^2[4J(0) + 3J(\omega_X)]$	15b
	R_{ex} = conformational exchange broadening contribution	
^{1}H−X nuclear Overhauser effect (NOE) or cross-relaxation rate constant (σ_{XH})	$\mathrm{NOE} = 1 + \frac{1}{4} d^2 T_1(\gamma_H/\gamma_X)[6J(\omega_H + \omega_X) - J(\omega_H - \omega_X)]$	16a
	$\sigma_{XH} = \frac{1}{4} d^2[6J(\omega_H + \omega_X) - J(\omega_H - \omega_X)]$	16b

B. Relationships between the Three Additional Relaxation Parameters Required for Full Spectral Density Mapping and the Relevant Values of the Spectral Density Function

parameter[a,c]	relationship to spectral density function[a,b,d]	eq
antiphase transverse relaxation rate constant for nucleus X	$R_{2,anti}^{DD} = \frac{1}{8} d^2[4J(0) + J(\omega_H - \omega_X) + 3J(\omega_X) + 6J(\omega_H + \omega_X)]$	17a
$R_{2,anti} = R_{2,anti}^{DD} + R_{2,anti}^{CSA} + \rho_{H^xH^i}$	$R_{2,anti}^{CSA} = \frac{1}{6} c^2[4J(0) + 3J(\omega_X)]$	17b
longitudinal two-spin order relaxation rate constant	$R_{DQ}^{DD} = \frac{3}{4} d^2[J(\omega_X) + J(\omega_H)]$	18a
$R_{DQ} = R_{DQ}^{DD} + R_{DQ}^{CSA} + \rho_{H^xH^i}$	$R_{DQ}^{CSA} = c^2 J(\omega_X)$	18b
^{1}H longitudinal relaxation rate constant	$R_{1,H}^{DD} = \frac{1}{4} d^2[J(\omega_H - \omega_X) + 3J(\omega_H) + 6J(\omega_H + \omega_X)]$	19a
$R_{1,H} = R_{1,H}^{DD} + \rho_{H^xH^i}$	$\rho_{H^xH^i} = \sum_i 2d^2[J_{H^xH^i}(\omega_{H^x} - \omega_{H^i}) + 3J_{H^xH^i}(\omega_{H^x}) + 6J_{H^xH^i}(\omega_{H^x} + \omega_{H^i})]$	19b

[a] Superscripts "DD" and "CSA" refer to dipole−dipole and chemical shift anisotropy relaxation mechanisms, respectively. [b] ω_H and ω_X are the angular Larmor frequencies for ^{1}H and X (= ^{13}C or ^{15}N) spins, respectively. The constants d and c are defined as follows: $d = (\mu_0 h \gamma_X \gamma_H/8\pi^2)\langle 1/r_{XH}^3\rangle$; $c = \omega_X \Delta\sigma/\sqrt{3}$; μ_0 is the permeability of free space; h is Planck's constant; γ_X and γ_H are the gyromagnetic ratios of X and ^{1}H nuclei, respectively; r_{XH} is the length of an X−H bond vector, and the angular brackets indicate the time-averaged value; and $\Delta\sigma$ is the chemical shift anisotropy of the X spin.[202] In some cases, the constants d and c were defined differently in the cited articles; in these cases, we have redefined these constants so that the definitions are consistent throughout the current paper. [c] $R_{2,anti}$, R_{DQ}, and $R_{1,H}$ represent the antiphase transverse relaxation rate $R_{XH}(2H_z^X X_y)$, the decay rate of longitudinal two-spin order $R_{XH}(2H_z^X X_z)$, and the amide proton longitudinal relaxation rate $R_H(H_z^X)$, respectively; in which using the nomenclature $R_{obs}(Q)$ the "obs" refers to the observed nucleus or nuclei and Q refers to the type of spin undergoing relaxation.[49,50] [d] $\rho_{H^xH^i}$ is the net spin−lattice relaxation rate of a given H^X proton, due to other protons, H^i, where the two protons have angular Larmor frequencies of ω_{H^x} and ω_{H^i}, respectively, and spin−spin coupling of $J_{H^xH^i}$.[49,500]

Table 4. Equations for Explicit Calculation of the Five Critical Spectral Density Values from Six Measured Relaxation Parameters According to the Full Spectral Density Mapping Approach of Peng and Wagner[49,50]

relationship of spectral density function to relaxation parameters[a]	eq
$J(0) = \frac{3}{3d^2 + 4c^2}\left(-\frac{1}{2}R_1 + R_2 + R_{2,anti} - \frac{1}{2}R_{DQ} - \frac{1}{2}R_{1,H}\right)$	20
$J(\omega_N) = \frac{2}{3d^2 + c^2}(R_1 + R_{DQ} - R_{1,H})$	21
$J(\omega_H + \omega_N) = \frac{1}{6d^2}(R_1 - R_{DQ} + R_{1,H} + 2\sigma_{XH})$	22
$J(\omega_H) = \frac{1}{3d^2}(-R_1 + 2R_2 - 2R_{2,anti} + R_{DQ} + R_{1,H})$	22
$J(\omega_H - \omega_N) = \frac{1}{d^2}(R_1 - R_{DQ} + R_{1,H} - 2\sigma_{XH})$	23

[a] Symbols are as defined in the footnotes to Table 3.

the reduced SDM approach involves the assumption that the high-frequency spectral densities are related to each other in a simple manner: for example, $J(\omega) = \lambda_1/\omega^2 + \lambda_2$, in which λ_1/ω^2 and λ_2 are the contributions to $J(\omega)$ from overall rotation and internal motion, respectively.[52] Using relaxation parameters collected at multiple field strengths, it is then possible to calculate the spectral densities at each high frequency. Although this is attractive, it should be noted that

Table 5. Relationships between Relaxation Parameters and Reduced Spectral Density Values and Equations for Calculation of the Reduced Spectral Density Values

A. Relationships between the Three Commonly Measured Relaxation Parameters and the Reduced Spectral Density Values $J(0)$, $J(\omega_N)$, and $J(\omega_h)$[52]

relationship of relaxation parameters to reduced spectral density values[a,b]	eq
$R_1 = \frac{1}{4} d^2[3J(\omega_N) + 7J(\omega_h)] + c^2 J(\omega_N)$	24
$R_2 = \frac{1}{8} d^2[4J(0) + 3J(\omega_N) + 13J(\omega_h)] + \frac{1}{6} c^2[4J(0) + 3J(\omega_N)]$	25
$\mathrm{NOE} = 1 + \frac{1}{4} T_1 d^2(\gamma_H/\gamma_N)[5J(\omega_h)]$	26

B. Equations for Explicit Calculation of the Three Reduced Spectral Density Values from the Three Commonly Measured Relaxation Parameters

relationship of reduced spectral density values to relaxation parameters[a,b]	eq
$J(0) = \frac{1}{3d^2 + 4c^2}\left(6R_2 - R_1\left(3 + \frac{18}{5}(\gamma_N/\gamma_H)(\mathrm{NOE} - 1)\right)\right)$	27
$J(\omega_N) = \frac{4}{3d^2 + 4c^2}\left(R_1\left(1 - \frac{7}{5}(\gamma_N/\gamma_H)(\mathrm{NOE} - 1)\right)\right)$	28
$J(\omega_h) = \frac{4}{5d^2}(R_1(\gamma_N/\gamma_H)(\mathrm{NOE} - 1))$	29

[a] Unless otherwise noted, symbols are as defined in the footnotes to Table 3. Again, the constants d and c have been redefined to maintain consistency throughout the current paper. [b] ω_h represents the value of the spectral density function at frequencies of ω_H, $(\omega_H + \omega_N)$, and $(\omega_H - \omega_N)$, assuming $J(\omega)$ is effectively constant over this frequency range.[52]

the variations between the different high-frequency $J(\omega)$ values are completely reliant on the assumed relationship between these values. Furthermore, unless the proportionality constants (λ_1 and λ_2) differ substantially between residues, the calculated high-frequency spectral densities would all be expected to display similar variations across the protein sequence, so this method may not provide any more structural or mechanistic insights than the simple reduced SDM method.

The reduced SDM approach has the obvious advantage that it requires roughly half the primary data relative to the full SDM method. An additional benefit is that the reduced SDM method requires the same relaxation parameters to be measured as for the model-free formalism discussed below. Commonly, one does not know prior to data collection whether the assumptions of the model-free approach will hold for a particular protein. Therefore, if one finds that the data cannot be adequately fit using the model-free method, the reduced SDM analysis can be applied without recourse to additional data collection.

Spectral density values calculated using either the full or reduced SDM methods indicate whether the motions of a particular bond vector are dominated by high- or low-frequency oscillations. A qualitative assessment of the same factors can often be made directly by observation of variations in the primary relaxation data across a protein sequence or between similar proteins. The simulated data shown in Figure 3 illustrate the relationships between the three reduced spectral density values, $J(0)$, $J(\omega_N)$, and $J(\omega_h)$, and the three commonly measured relaxation parameters, R_1, R_2, and the NOE for a protonated ^{15}N nucleus. The following points are noteworthy.

(1) On the basis of the formulas in Tables 3A and 5A, it is clear that $J(\omega_h)$ and $J(\omega_N)$ influence all three relaxation parameters, whereas $J(0)$ influences only R_2.

(2) Increased motions close to either the ^{15}N or ^{1}H Larmor frequency enhance R_1 relaxation of the ^{15}N nucleus, although R_1 is most sensitive to changes in $J(\omega_N)$. For example, in Figure 3a, doubling $J(\omega_N)$ increases R_1 ~1.85-fold, whereas doubling $J(\omega_h)$ increases R_1 only ~1.15-fold. This is in part because the value of $J(\omega_N)$ is typically much larger than $J(\omega_h)$. However, another relevant factor is that spin flips of the ^{1}H itself do not affect the population of ^{15}N spins; the dependence of R_1 on $J(\omega_h)$ is entirely due to zero-quantum and double-quantum transitions (see the definition of R_1; eq 14a in Table 3A).

(3) Because the NOE is a function of R_1, it should not be surprising that the NOE is also influenced by motions close to both the ^{15}N and ^{1}H Larmor frequencies. However, the effects of these two terms are distinguishable because increasing $J(\omega_h)$ leads to a reduction in the NOE, whereas increasing $J(\omega_N)$ causes an increase in the NOE as shown in Figure 3b. NOE values approach the theoretical maximum of unity when $J(\omega_h)$ approaches zero but can become negative when extensive high-frequency motions are present, that is, high values of $J(\omega_h)$. The influence of $J(\omega_N)$ on the NOE is a consequence of the variation in R_1 values with varying $J(\omega_N)$ (Table 5A). Consequently, the product $R_1(1 - \mathrm{NOE})$ is independent of $J(\omega_N)$ and is simply proportional to $J(\omega_h)$ (Figure 3e). Elevated values of this product are a direct indication of extensive high-frequency motion.

(4) R_2 relaxation is affected by motions throughout the frequency spectrum but is dramatically more sensitive to low-frequency motions. For example, in the simulations of Figure 3c,d, doubling the value of $J(\omega_N)$ or $J(\omega_h)$ causes a very small (<2%) increase in R_2, whereas doubling the value of $J(0)$ increases R_2 by 83−96%. Considering that R_1 and R_2 are influenced similarly by $J(\omega_h)$ but only R_2 is affected by $J(0)$ and only R_1 is influenced significantly by $J(\omega_N)$, the ratio R_2/R_1 is most sensitive to variations in the latter two spectral densities (Figure 3f).

An important caveat of the SDM approach involves the influence of slow conformational exchange on transverse ^{15}N or ^{13}C relaxation. If conformational exchange is present, measured R_2 values will contain contributions from both the spectral densities discussed above and the exchange broaden-

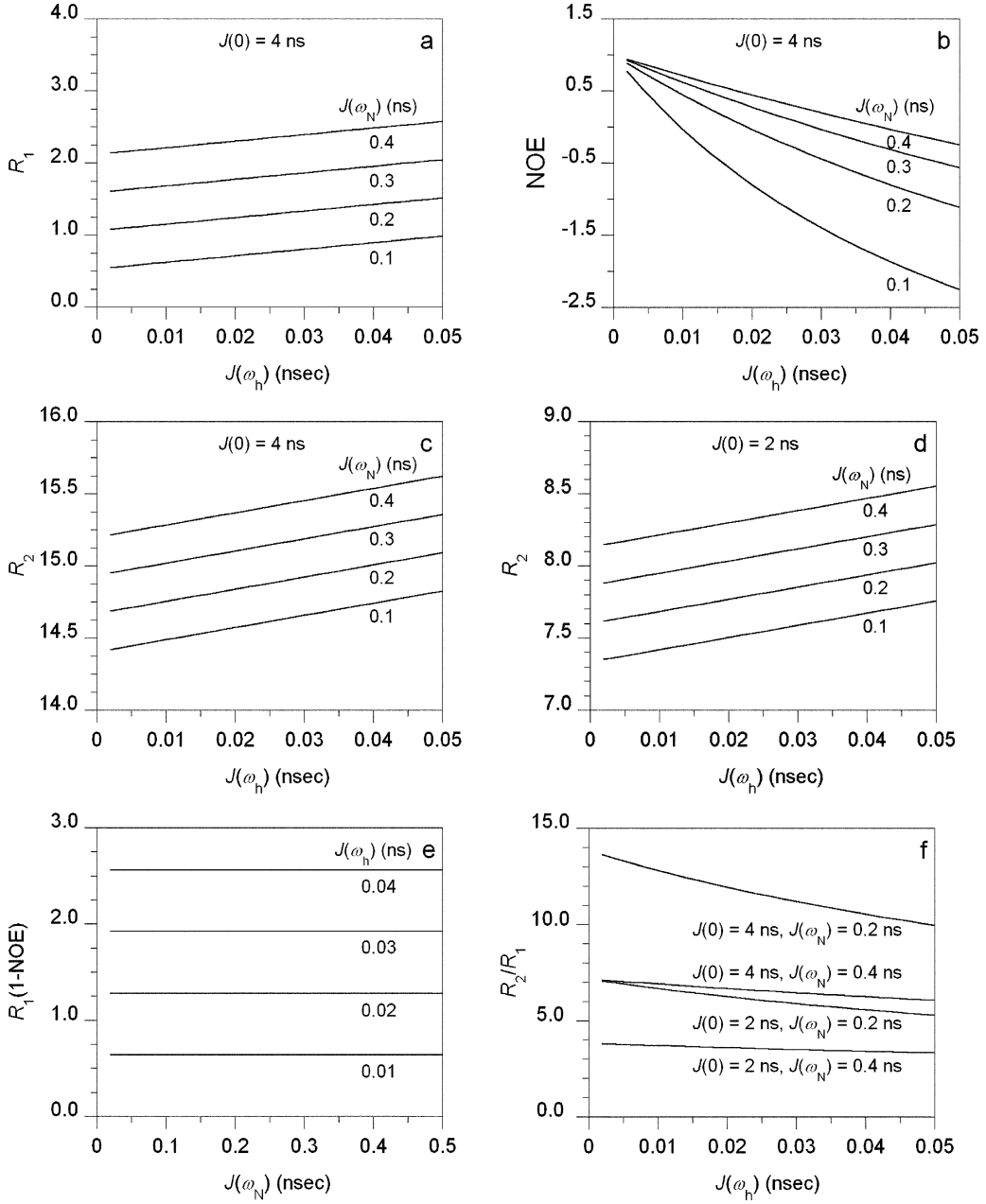

Figure 3. Simulated data showing the relationships between the three reduced spectral density values, $J(0)$, $J(\omega_N)$, and $J(\omega_h)$, and the three commonly measured relaxation parameters, R_1, R_2, and the NOE for a protonated ^{15}N nucleus. Shown in each panel is the dependence on $J(\omega_h)$ of (a) R_1, (b) NOE, (c, d) R_2, (e) $R_1(1\text{-NOE})$, and (f) the R_2/R_1 ratio for the indicated values of $J(0)$ and $J(\omega_N)$. Note that $J(\omega_h)$ represents the value of the spectral density function at the frequencies ω_H, ω_{H+N}, and ω_{H-N}, assuming $J(\omega)$ is effectively constant over this frequency range.

ing term R_{ex} (Table 3A). Consequently, if exchange broadening is assumed to be absent, the calculated $J(\omega)$ values will be incorrect. In particular, $J(0)$ values will be overestimated.[55] To separate these two effects, relaxation data can be measured at multiple magnetic field strengths.[56] In the absence of such data, $J(0)$ should be interpreted as representing a combination of slow motions (such as molecular tumbling) and conformational exchange.

3.4. Lipari–Szabo Model-free Formalism

The spectral density values discussed above represent the probabilities with which a bond vector is oscillating at each specified frequency. However, they do not directly indicate whether these oscillations are associated with global molecular rotation or the local or segmental internal motions affecting the bond vector. To gain a mechanistic understanding of protein dynamics, it is beneficial to separate the internal dynamics from the global motions. The so-called "model-free" formalism, introduced by Lipari and Szabo in 1982,[45,46] is an attempt to do just this and has gained widespread popularity since it was first applied to ^1H-detected ^{15}N relaxation data by Kay, Torchia, and Bax in 1989.[47]

The basic premise of the model-free formalism is that the internal motions of bond vectors in proteins are independent of the overall rotational diffusion of the molecule as a whole. In addition, the rotational diffusion of the molecule influences each bond vector identically (for isotropic rotation) or in a manner that is related through the relative orientations of the bond vectors in the molecule (for nonisotropic rotation), whereas the internal motions of any two bond vectors are independent of each other or at least unrelated in any predictable way. Recently, an alternative approach dubbed

"slowly relaxing local structure" (SRLS), has been developed in an effort to also incorporate coupling between global and local motions.[57] Below we discuss several variations of the model-free formalism, which differ from each in two main respects: (1) whether the overall tumbling is assumed to be isotropic, axially symmetric, or completely anisotropic and (2) whether the internal motions are assumed to occur on a single time scale or two separable time scales. Irrespective of these details, the correlation function for each bond vector can now be represented as the product of the correlation functions for overall (global) and internal motions: $C(t) = C_{global}(t)C_{internal}(t)$. These component correlation functions can, in turn, be written as functions of the characteristic time scales of overall and internal motions and the degree of spatial restriction of internal motions. The spectral density functions (and hence the relaxation parameters) can then be reformulated in terms of these same motional parameters so that the observed relaxation parameters can be fit to yield values for the dynamics parameters. Typically, the internal motions of bond vectors are substantially faster than the rate of molecular rotational diffusion. However, the model-free approach remains valid, albeit less precise, even for internal motions on time scales somewhat slower than molecular tumbling;[58] characterization of substantially (>50-fold) slower motions is not practical. The discussion below refers to the situation in which three relaxation parameters (R_1, R_2, and NOE) are measured at a single magnetic field strength for each nucleus of interest. In laboratories where it is possible, it has become common to repeat some or all of these measurements at one or two additional field strengths, which yields a proportionately greater number of measured relaxation parameters for each nucleus, allowing the model-free parameters to be determined with greater precision or allowing a larger number of adjustable parameters to be determined.

(1) Isotropic Tumbling with a Single Time Scale of Internal Motion. In this "original" model-free formalism, the overall motions are assumed to be unrestricted with a correlation function that decays exponentially to zero with a single characteristic (typically slow) time scale (τ_m), as illustrated in Figure 1a. The internal motions, on the other hand, are assumed to be spatially restricted so that the correlation function for internal motions decays to a finite (plateau) value with a characteristic (typically fast) time scale (τ_e, where the subscript denotes the effective time scale of internal motions). The resulting total correlation function (Figure 1c) is a double exponential with the fast and slow phases representing the internal and global motions, respectively. The relative amplitude of the slow (global) phase, that is, the plateau value divided by the initial value $C(0)$, is defined as the square of the order parameter (S^2) and represents the degree of spatial restriction of internal motions; completely restricted motions have $S^2 = 1$, and completely unrestricted motions have $S^2 = 0$. Thus, there are three fitted parameters for each bond vector (τ_m, τ_e, and S^2). Because one of them (τ_m) is the same for all n bond vectors, the problem is overdetermined ($2n + 1$ fitted dynamics parameters and $3n$ measured relaxation parameters), so unique solutions can be obtained for all of the dynamics parameters. Alternatively, if τ_m has been determined (see section 3.5, subsection 4)) there are only $2n$ fitted parameters (τ_e and S^2 for each residue), which can be adequately determined from the R_1 and NOE data without need for R_2 data.[59]

(2) Simplified Model-Free Formalism: Extremely Fast Internal Motions. If the internal motions of a bond vector are extremely fast in comparison to the overall tumbling ($\tau_m/\tau_e > 100$), then the spectral density function in the relevant frequency range becomes insensitive to the time scale of internal motions but remains sensitive to their degree of restriction (Figures 2c and 4a−c). Consequently, $J(\omega)$ reduces to the form shown in eq 8 (Table 2), and the relaxation data can still be fit to yield S^2 for each bond vector and τ_m for the molecule.

(3) Extended Model-free Formalism: Two Time Scales of Internal Motions. In cases when the internal motions of a protein cannot be adequately described using the original model-free formalism, it may be possible to account for the observed relaxation data by adding an additional fitting parameter to the model-free formalism. A common approach, first proposed by Clore and co-workers,[60,61] is to assume that the internal motions occur on two separable time scales (τ_f and τ_s, where the subscripts denote fast and slow), each with a corresponding squared order parameter (S_f^2 and S_s^2). By necessity, τ_f is assumed to be too fast to affect the relaxation parameters, leaving only three dynamics parameters to be determined for each residue (eq 9, Table 2). Although extension of the model-free formalism in this manner often gives a statistically significant improvement in the fits,[62] interpretation of the results is not straightforward. The slow time scale is often found to approach the correlation time for overall motions, indicating that the overall tumbling and internal dynamics are no longer well-separated.[63] In addition, one can imagine alternative methods for increasing the number of fitted parameters that might also result in improved fits over the original model-free formalism, so the observation of improved fits using this common extended method does not necessarily indicate that the extended model is realistic.

(4) Original Model-free Formalism with Anisotropic Tumbling. The assumption that rotational diffusion is isotropic is adequate for proteins having shapes (including the hydration shell) that are close to spherical. However, many proteins have one dimension that is elongated (prolate ellipsoid, the shape of a rugby ball) or shortened (oblate ellipsoid, approaching a disk shape) relative to the other two, whereas others have three distinguishable principal axes of rotation. Because rotational diffusion is faster around a long axis than a short axis, the relaxation of a nucleus will be differentially affected depending on whether the associated bond vector is aligned with the long or the short axis of the molecule. Consequently, it is necessary to extend the correlation function to account for rotation around the different axes and the orientation of each bond vector with respect to the principal axes. This can be accomplished if the structure of the molecule is known. The correlation function and spectral density function for axially symmetric molecular tumbling are given in Tables 1 and 2 (eqs 4 and 10). The resulting form of the overall spectral density function, incorporating spatially restricted internal motions, is given in Table 2 (eq 11). For axially symmetric molecular diffusion, four parameters must be optimized to define the rotational diffusion of the molecule: the two time scales and two angles specifying the position of the unique axis relative to a reference axis system.[64] For the fully anisotropic case it is necessary to define six parameters: three time scales and three angles. Once these parameters have been established, the angle of each bond vector to each principal rotational

axis can be obtained from the structure.[45] Considering that the same two internal parameters (S^2 and τ_e) must be determined for each of the *n* bond vectors, the fitting problem remains overdetermined ($2n + 4$ or $2n + 6$ fitted dynamics parameters and $3n$ measured relaxation parameters for data collected at a single field strength).

(5) Incorporation of Conformational Exchange Broadening. As discussed above, conformational exchange in the microsecond−millisecond time regime can increase the apparent transverse relaxation rate constant relative to the value defined by the dipolar and CSA mechanisms. If such a contribution is present, it must be accounted for during fitting of the relaxation data. Thus, the observed R_2 value is expressed as the sum of dipolar, CSA, and exchange broadening contributions, with the latter designated R_{ex} (eq 15, Table 3A). In this case, R_{ex} is treated as an adjustable parameter during the fitting of relaxation data to the original or simplified form of the model-free formalism. The fitted value of R_{ex} will depend entirely on the observed R_2 value, and the fitted values of S^2 and τ_e will be determined by the values of R_1 and NOE (as well as the rotational diffusion tensor).

(6) Anisotropic Tumbling with Alternative Formalisms for Internal Motions. Because the model-free approach assumes independence of overall and internal motions, it is straightforward to develop correlation functions that account for both the anisotropic molecular rotation and either the simplified or extended formalisms for internal motions (Table 2). The one caveat is that as the number of fitted parameters increases it may approach the number of measured relaxation parameters, resulting in increased uncertainties or, in the extreme, an inability to uniquely define the dynamical parameters. In reality, there are usually very few residues in a protein that require the extended model-free formalism. However, in some cases, slow conformational exchange can be spread throughout a protein, leading to difficulty defining the rotational diffusion parameters. In the latter case, the SDM approach may be preferred over model-free analysis.[65,66]

Figure 4 illustrates the relationships of the internal NH group model-free parameters (S^2 and τ_e) to the spectral density values $J(0)$, $J(\omega_N)$, and $J(\omega_H)$ and to the primary relaxation parameters. These simulations were performed according to the original model-free formalism for a protein that tumbles isotropically with a correlation time of $\tau_m = 10$ ns, which is typical for a protein of molecular mass around 20 kDa. For most values of τ_e shown, the values of $J(0)$ and $J(\omega_N)$ increase as the motions become more restricted (higher S^2), whereas the value of $J(\omega_H)$ decreases as S^2 increases (Figure 4a−c). $J(0)$ is dominated by the global tumbling and so is very insensitive to the time scale of internal motions (τ_e), whereas $J(\omega_N)$ increases substantially as the internal motions become slower (higher τ_e). The dependence of $J(\omega_H)$ on τ_e is more complex. $J(\omega_H)$ increases with increasing τ_e until τ_e reaches a value of $1/\omega_H$ (265 ps for a ^{1}H frequency of 600 MHz) and then begins to decrease again. The dependence of R_1 on the internal model-free parameters (Figure 4d) is similar to the dependence of $J(\omega_N)$ on these parameters, with longitudinal relaxation reaching a maximum as motions become slower and more restricted (dominated by global tumbling). Similarly, R_2 relaxation is dominated by the low-frequency oscillations, $J(0)$, and so is most efficient when internal motions are highly restricted (Figure 4e). Because R_1 is more sensitive than R_2 to the time scale of internal motions, low values of the ratio R_2/R_1 provide a useful indication of slow internal motions (high values of τ_e) (Figure 4f). Finally, the heteronuclear NOE has a maximum value (close to unity) when internal motions are highly restricted; the precise value of this maximum is a function of τ_m. As motions become less restricted, the NOE decreases, with the decrease being most pronounced for τ_e values close to the inverse of the ^{1}H Larmor frequency (Figure 4g). For extremely fast internal motions, approximated by the simplified model-free formalism, the NOE becomes independent of S^2 (top curve in Figure 4g).

The model-free approach is particularly attractive because it assists us in understanding the mechanistic consequences of molecular motion. The global tumbling parameters provide information about the apparent size and shape of the molecule, indicating the presence of quaternary structure and providing useful comparisons to other physical measurements such as viscosity, sedimentation data, fluorescence anisotropy, and gel filtration retention times. On the other hand, the internal motions of the molecule are more likely to influence the chemical interactions dictating binding or catalysis. In particular, the order parameter represents the range of motion of each bond vector and so is conceptually related to the number of conformational states or the conformational entropy (vide infra).

Despite the utility of separating global and local motions, it is important to recognize the limitations of the model-free approach. First, there is the possibility that internal motions can occur on a time scale similar to that of overall tumbling. The extended model-free formalism may indicate the presence of such slow motions, but they could be superimposed on faster internal motions that do not satisfy the assumption of this formalism (i.e., that τ_f is extremely small). In this case, the extended model-free formalism may be unable to fit the data (which is sometimes observed) or it may yield parameters that do fit the data yet are not a realistic representation of the actual molecular motions. A second possible scenario is that the internal motions of a particular bond vector are all fast but they are not adequately described by a single time scale of motion and a single spatial parameter. In this case the correlation function for internal motion would be multiexponential and the spectral densities at the high frequencies would be related in some complex manner to the time scales and degrees of restriction of the various internal motions. Indeed, the energy landscapes for structural fluctuations in proteins are far from simple, so this more complicated scenario is probably more realistic in most cases. Nevertheless, the observations that the model-free formalism satisfies relaxation data for many proteins and that the spectral densities obtained by SDM at multiple fields are in good agreement with the model-free spectral density function[55] suggest that this formalism is a reasonable first-order approximation for describing fast internal motions. Finally, we reiterate the caveat that, with the exception of conformational exchange terms (R_{ex}), NMR relaxation measurements are not sensitive to rotational motions substantially slower than the time scale of molecular tumbling, to rotational motions around the bond vector of interest, or to translational motions. This is simply because such motions will make an insignificant contribution to the correlation function so it should not be considered a specific limitation of the model-free approach.

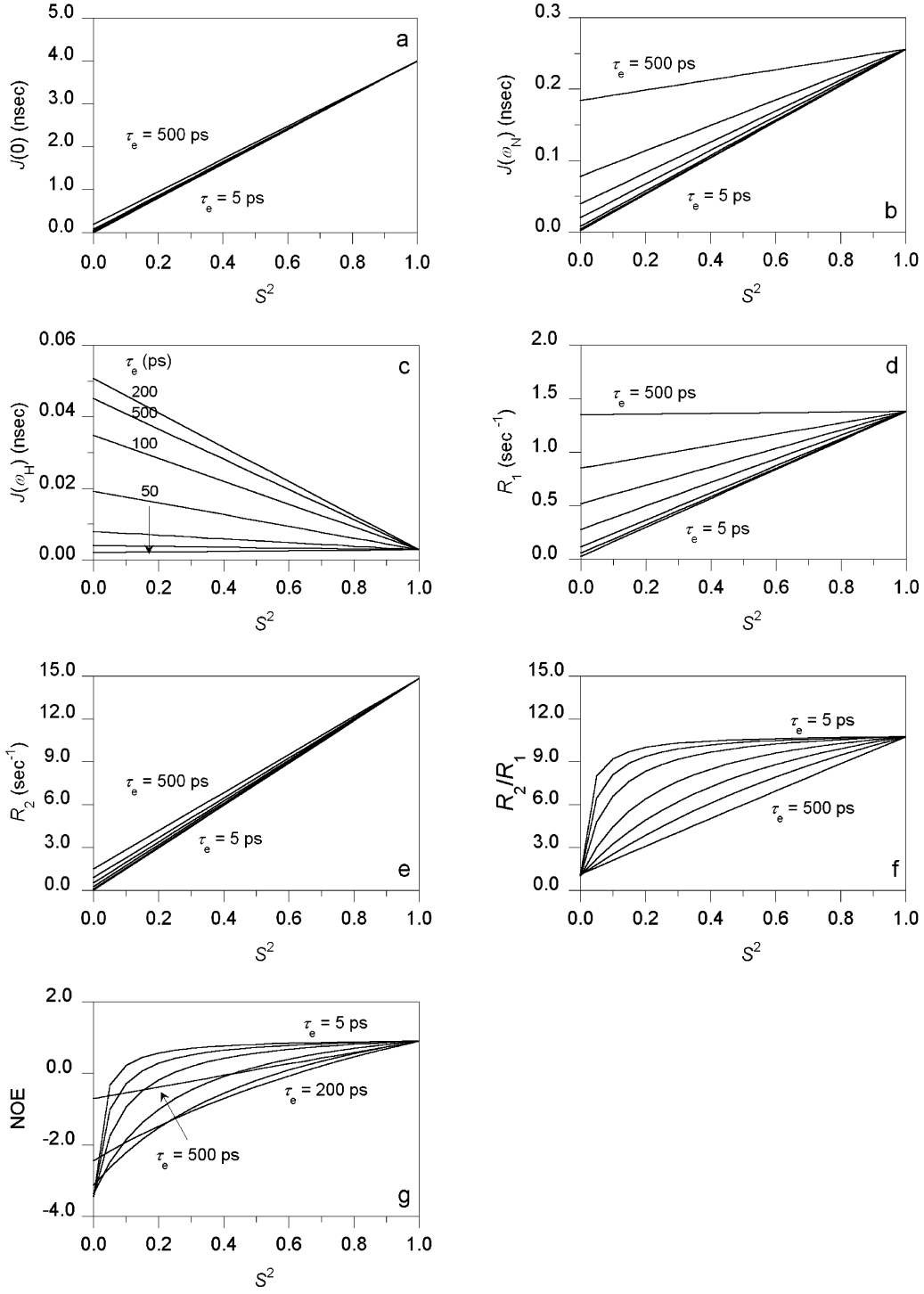

Figure 4. Simulations showing the relationships of model-free dynamics parameters to spectral density values and relaxation parameters for a protonated ^{15}N nucleus: (a, b) dependence of $J(0)$ and $J(\omega_N)$ on S^2 for τ_e values of 5 (bottom), 10, 20, 50, 100, 200, and 500 (top) ps; (c) dependence of $J(\omega_H)$ on S^2 for the indicated τ_e values; (d, e) dependence of R_1 and R_2 on S^2 for τ_e values of 5 (bottom), 10, 20, 50, 100, 200, and 500 (top) ps; (f) dependence of R_2/R_1 on S^2 for τ_e values of 5 (top), 10, 20, 50, 100, 200, and 500 (bottom) ps; (g) dependence of NOE on S^2 for the indicated τ_e values. All simulations were performed using the original model-free formalism (eq 7) with $\tau_m = 10$ ns and a magnetic field strength of 14.1 T, corresponding to a ^{1}H Larmor frequency of 600 MHz.

3.5. Practical Implementation of the Model-free Formalism

This section is intended as a brief guide to researchers who plan on using model-free analysis for the first time to study the dynamics of backbone amide bond vectors. We outline the main steps in the process and attempt to highlight important considerations in optimizing the precision and reliability of the results.

(1) Collection of NMR Relaxation Data. Longitudinal (R_1) and transverse (R_2) relaxation rate constants and $\{^1H\}-^{15}N$ steady-state nuclear NOEs are typically measured from 2D $^1H-^{15}N$ correlation spectra recorded at one or more magnetic field strength(s) using pulsed-field gradient sensitivity-enhanced pulse sequences, such as those developed by Farrow and co-workers.[2,67,68] If data are limited to a single field strength, it is advisable to collect additional relaxation

Table 6. Functions for Determination of Relaxation Rate Constants R_1, R_2, and η_{xy} for a Protonated ^{15}N Nucleus

relaxation parameter	relationship of peak intensities to relaxation rate constants	eq
longitudinal relaxation rate constant (R_1)[a,b]	$I(\tau) = \exp(-R_1\tau)$	30
transverse (auto)relaxation rate constant (R_2)[a]	$I(\tau) = \exp(-R_2\tau)$	31
transverse cross-correlated relaxation rate constant (η_{xy})[c]	$I_{cross}(\tau)/I_{auto}(\tau) = \tanh(\eta_{xy}\tau)$	32

[a] $I(\tau)$ is the peak intensity in the spectrum for which the relaxation delay time is τ. [b] Although the longitudinal relaxation does not naturally decay to zero, it is typical to use phase cycling to cancel the nondecaying component, resulting in a signal that decays exponentially to zero.[203] [c] $I_{cross}(\tau)$ is the peak intensity for the component of antiphase ^{15}N magnetization ($2I_zS_y$) that cross-relaxes to in-phase (S_y) magnetization during the relaxation delay (τ), whereas $I_{auto}(\tau)$ is the peak intensity for the component that remains antiphase.[69,70] The utility of the cross-correlated relaxation method may be limited by the low sensitivity of the former component for short time delays.

data such as the ^{15}N transverse cross-corrrelated relaxation rate constants (η_{xy})[69,70] to facilitate identification of bond vectors that are subject to conformational exchange broadening. Pulse sequences for measuring spin relaxation have been reviewed elsewhere.[1,7] Briefly, R_1 and R_2 data are recorded as a series of spectra in which a relaxation delay (τ) is varied between spectra. η_{xy} data are recorded as two parallel series of spectra. One spectrum of each pair detects the component of antiphase ^{15}N magnetization ($2I_zS_y$) that cross-relaxes to in-phase (S_y) magnetization during a relaxation delay (τ), whereas the other spectrum of each pair detects the component that remains antiphase.[69,70] $\{^1H\}-^{15}N$ NOEs are measured using pairs of spectra recorded in the presence and in the absence of ^{1}H saturation; it is advisable to collect at least two pairs of NOE spectra. The precision of calculated dynamics parameters depends critically on the quality of the primary relaxation data. Therefore, considerable care should be taken to maximize the signal-to-noise ratios of these spectra. Unfortunately, this has often required long data collection times, although this problem is being alleviated by the increasing availability of cryogenically cooled, high-sensitivity NMR probes.

As discussed in section 4, many of the most interesting studies of protein dynamics involve comparison between two or more forms of the same protein. Because the dynamics of a protein can be sensitively dependent on sample conditions (temperature, pH, ionic strength, viscosity, etc.), it is essential to carefully control these factors. We recommend calibrating the probe temperature before collection of each data set and using identical buffers and protein concentrations for comparative samples.

(2) Determination of Relaxation Parameters and Uncertainties. Relaxation parameters and their uncertainties are obtained from the variations of peak intensities (heights or volumes) in the various spectra discussed above. Viles et al. have compared several alternative methods for the determination of peak intensities and the influence of this choice of the precision and accuracy of relaxation parameters.[71] For R_1, R_2, and η_{xy} data, the peak intensities are fit to the functions listed in Table 6. Considering that the precision of the peak intensities varies throughout a series of spectra, it is preferable to weight the data points in these fits according to the inverse squares of the uncertainties in the peak heights. Peak height uncertainties are determined most reliably by recording duplicate spectra at particular τ time points. For a duplicate pair of spectra, the pairwise differences in peak intensities are measured for a representative set of peaks, and the standard deviation of these differences is divided by $\sqrt{2}$ to yield a reasonable estimate of the absolute uncertainty in peak intensities for all peaks in the spectra acquired at that time point. For time points not acquired in duplicate, the absolute uncertainty in peak intensities is determined by linear interpolation between duplicated time points. Uncertainties in relaxation rate constants are determined as the standard errors of the fitted R_1, R_2, and η_{xy} values.

Steady-state $\{^1H\}-^{15}N$ NOEs are determined as the ratios of cross-peak intensities in spectra recorded in the presence ($I_{sat.}$) and in the absence (I_{unsat}) of ^{1}H saturation [NOE = $I_{sat.}/I_{unsat}$]. Uncertainties in NOE measurements can be determined by various methods.[7] In one approach, the uncertainties in $I_{sat.}$ and I_{unsat} are first estimated then propagated through to the NOE values.[7] If only a single pair of NOE spectra has been recorded, the uncertainties in $I_{sat.}$ and I_{unsat} are assumed to be equal to the root-mean-square noise in the spectra, which may underestimate the errors. Therefore, it is preferable to estimate these uncertainties by comparison of replicate spectra. An alternative approach[72] is to first calculate the NOE values independently for each pair of spectra and then to estimate the uncertainty in the NOE values by comparison of the replicate NOE determinations. In this case, the absolute uncertainty in the NOE is the same for all residues.[72]

(3) Identification of Residues Affected by Extensive Disorder on a Picosecond Time Scale or Chemical Exchange on a Microsecond−Millisecond Time Scale. As discussed below, to obtain a reliable estimate of the overall rotational diffusion tensor of a protein, it is necessary to analyze the relaxation parameters for residues having internal motions that are very fast ($\tau_e \ll \tau_m$) and for which there is no significant contribution to R_2 from conformational exchange. Thus, it is important to first identify residues that do not satisfy these criteria and to exclude them from the diffusion tensor determination. Residues that do not satisfy the first criterion are typically identified by their low R_2/R_1 ratios[47,60] or their low NOE values[73] (see Figure 4f,g), although the precise cutoff values used vary between different studies. Residues experiencing conformational exchange on a slow (from microsecond to millisecond) time scale can be identified by their elevated R_2/R_1 ratios,[47,74] by comparing R_2 values measured at different magnetic field strengths, by comparing R_2 (or $R_{1\rho}$) values measured using different spin−echo delays (or spin-locking field strengths) in the pulse sequence, or from measurements of cross-correlated relaxation rate constants. These techniques have been reviewed recently.[75−77] As an example, if the transverse cross-correlated relaxation rate constant has been measured, residues having R_2/η_{xy} ratios that exceed the average by more than one standard deviation may be deemed to have slow conformational exchange.[72]

(4) Determination of the Molecular Rotational Diffusion Tensor. Having excluded residues according to the above criteria, the rotational diffusion tensor of the protein is most commonly obtained by analysis of the R_2/R_1 ratios for the remaining residues. It is reasonable to assume that the dynamics of these residues can be adequately described by the simplified model-free formalism. The spectral density

Table 7. Five Common Mathematical Models Used for Optimization of Dynamics Parameters According to the Lipari−Szabo Model-free Formalism

model	model	spectral density function for isotropic tumbling	parameters optimized[a,b]	assumptions
1	simplified model-free formalism	Table 2, eq 8	S^2	$\tau_e \ll \tau_m$ $R_{ex} \approx 0$
2	original model-free formalism	Table 2, eq 7	S^2, τ_e	$\tau_e < 500$ ps $R_{ex} \approx 0$
3	simplified model-free formalism plus conformational exchange term	Table 2, eq 8	S^2, R_{ex}	$\tau_e \ll \tau_m$
4	original model-free formalism plus conformational exchange term	Table 2, eq 7	S^2, R_{ex}, τ_e	$\tau_e < 500$ ps
5	extended model-free formalism	Table 2, eq 9	S_s^2, S_f^2, τ_s	$\tau_f \ll \tau_m$ $\tau_s \geq 500$ ps $R_{ex} \approx 0$

[a] Parameters are defined in the footnotes to Table 2 and are discussed in the text. [b] Parameters are optimized so as to minimize the χ^2 function: $\chi^2 = \sum_{i=1}^{N} \Gamma_i = \sum_{i=1}^{N} \sum_{j=1}^{M_i} [(R_{ij} - \hat{R}_{ij})^2/\sigma_{ij}^2]$, in which N is the total number of spins. For the ith spin, Γ_i is the sum-squared error, M_i is the number of experimental relaxation parameters, R_{ij} is the jth experimental relaxation parameter, $\hat{R}_{ij}$ is the jth theoretical relaxation parameter calculated from putative values of the dynamics parameters, and σ_{ij} is the experimental uncertainty in the jth relaxation parameter.[62]

function for this formalism (eq 8) does not contain a τ_e term and is directly proportional to the value of S^2. Therefore, both R_2 and R_1 values are directly proportional to S^2 and the ratio R_2/R_1 becomes independent of both S^2 and τ_e, that is, dependent only on the global tumbling parameters and the angle(s) relating the global diffusion axes to the bond vector of interest.

In the case of isotropic molecular tumbling, there is a simple relationship between the molecular rotational correlation time (τ_m) and the R_2/R_1 ratios.[47] Consequently, the R_2/R_1 ratios for individual bond vectors can be used to calculate apparent τ_m values for individual residues.[78,79] The average and standard deviation of these apparent τ_m values provide reasonable estimates of the actual τ_m value and its uncertainty, respectively. If the rotational diffusion of the molecule is significantly anisotropic, the apparent τ_m values determined by this method would be expected to vary systematically according to the orientations of the associated bond vectors in the molecule. The assumption of a single τ_m value would then introduce systematic errors into the internal dynamics parameters. Consequently, rather than assuming an isotropic diffusion tensor, it is advisable to independently determine isotropic, axially symmetric, and fully anisotropic rotational diffusion tensors and then to analyze the fitting statistics to decide on the most appropriate diffusion tensor to use for analysis of internal dynamics. In this approach, the one, four, or six parameters defining a putative diffusion tensor are used to calculate the R_2/R_1 ratios for all bond vectors in the protein; the calculations for axially symmetric and fully anisotropic diffusion tensors take into account the orientations of the bond vectors relative to the principal axes of the diffusion tensor, so a structure must be available. The optimal diffusion tensor is then obtaining by systematic variation of the diffusion tensor parameters so as to minimize the differences between observed and predicted R_2/R_1 ratios.[73] For the axially symmetric case, the optimization function typically has two minima, one for oblate and one for prolate diffusion tensors,[80] so it is necessary to determine both of these minima and select the one with the lowest χ^2 goodness-of-fit parameter. The χ^2 values for the three different models are expected to decrease as the number of fitted parameters increases, from isotropic to axially symmetric to fully anisotropic models. Selection of the most appropriate diffusion tensor model can be readily accomplished using F-statistical comparisons. Programs such as "quadric_diffusion" (A. G. Palmer III, Columbia University) give optimized diffusion tensor parameters along with both χ^2 and F statistics, allowing straightforward selection of the best model by comparison with statistical tables. For example, for one data set of 46 residues from our laboratory, quadric diffusion reported a lower χ^2 for the axial oblate model relative to the axial prolate model, indicating that the former model is preferable. The F statistics reported were 3.43 (isotropic versus axial oblate) and 0.28 (axial oblate versus anisotropic). These compare with tabulated critical values [$F_{0.05}(\nu_1,\nu_2)$] of $F_{0.05}(3,42) = 2.84$ and $F_{0.05}(2,40) = 3.23$, respectively, in which ν_1 is the difference between the number of fitted parameters in the two models and ν_2 is the number of data points minus the number of fitted parameters in the more complex model. The more complex model is chosen only if the F statistic exceeds the critical value. Thus, in this example, the axial oblate diffusion tensor is preferred.

Although the above method is by far the most commonly used, we note that additional approaches for determination of the rotational diffusion tensor from spin relaxation data have also been developed.[59,79,81−84] These relaxation-based methods, as well as experimental approaches based upon measurement of residual dipolar coupling constants and theoretical approaches, have been thoroughly reviewed by Fushman et al.[85]

(5) Model-free Fitting and Selection of the Best Formalism for Internal Dynamics. After the optimum molecular rotational diffusion tensor has been determined, measured NMR relaxation data can be analyzed in the context of the selected diffusion tensor using any of the five versions of the model-free formalism listed in Table 7. These five approaches are commonly referred to as "models" 1−5, but it should be noted that they are merely mathematical models that incorporate certain assumptions about the time scales of internal motions or presence of conformational exchange; they do not presuppose any particular mechanism of internal dynamics, so the resulting parameters are still considered to be "model-free". Typically, relaxation data for each residue are fit independently to each mathematical model to yield the corresponding internal dynamics parameters (Table 7). Fitting can be performed using standard nonlinear optimization programs such as Matlab, although for standard applications it is convenient to utilize a program such as ModelFree (A. G. Palmer III, Columbia University), which was written specifically for model-free analysis and is freely available. Models 1 and 2 represent the simplified and original model-free formalisms, respectively. Models 3 and 4 represent the same two formalisms with the addition of an R_{ex} term to account for conformational exchange broadening. Finally, model 5 represents the extended model-free formal-

ism with two time scales of internal motion. The quality of the fits between the experimental data and each model are calculated as χ^2 statistics, and the different models are then compared to each other using F statistics. Model selection based upon these two statistics can be performed according to the flowchart outlined by Mandel et al.[62] Scripts available with the ModelFree program perform the model selection in a streamlined manner. Limitations of this model selection technique and possible systematic errors resulting from erroneous model selection have been discussed.[86,87]

Uncertainties in calculated dynamics parameters are most commonly determined using Monte Carlo simulations.[74] In this approach, each relaxation parameter and its uncertainty are considered to be the mean and standard deviation, respectively, of a Gaussian distribution, and several hundred sets of relaxation parameters are generated randomly from these distributions. Each set of relaxation data is analyzed using model-free analysis to yield dynamics parameters from which averages and standard deviations are calculated. Standard deviations of simulated dynamics parameters are used as uncertainty values for the model-free dynamics parameters. Although this process is relatively straightforward, the distributions of simulated dynamics parameters may be highly non-Gaussian due to the nonlinear relationship between relaxation and dynamics parameters. Consequently, alternative graphical techniques and Bayesian statistical methods have been developed in an attempt to obtain dynamics parameters and uncertainties that are not biased by the incorrect assumption of Gaussian distributions.[88,89] Although these methods may be more rigorously correct, they have not been used as widely as the Monte Carlo methods, presumably for reasons of convenience. Finally, we note that these methods for estimation of uncertainties take into account only random errors in the data. In addition to these, there may be systematic errors in the dynamics parameters resulting from such sources as[90] systematic errors in the relaxation parameters themselves (e.g., due to nonexponential decay), the existence of alternative relaxation pathways not considered above, incorrect estimation of the X−H bond length or the chemical shift anisotropy, errors in the structural coordinates, and possible coupling between internal and overall motion.

3.6. Specific Motional Models

The major disadvantage of the model-free approach is that it is indeed model-free; that is, it does not provide a detailed physical picture of the internal motions that can then be related to the chemical mechanism, binding interactions, or other physical or spectroscopic properties of the protein. As an alternative approach, it would be attractive to define specific models to describe the details of the internal motions and then to fit each model to the relaxation data so as to determine the most appropriate description of the motions. Daragan and Mayo have written a very detailed review describing a variety of reasonable motional models that can be used to fit relaxation data.[5] Considering that the mathematics of these models is often extremely complicated (by the standards of most physical biochemists), here we provide a brief description of the general approach and then discuss the relationship of some simple motional models to the model-free parameters.

There are two general approaches to fitting relaxation data to specific motional models. In one approach, a series of parameters are defined to describe the internal motions according to the model selected, and a separate set of parameters is used to define the overall rotational diffusion of the protein. The spectral density function is derived in terms of these internal and global parameters. For any given values of the parameters it is then possible to evaluate $J(\omega)$ at the five critical frequencies and hence to calculate values for the relaxation parameters. Iterative adjustment of the motional parameters is used to optimize their agreement with experimental data. The alternative approach is to first analyze the data using the model-free approach and then to optimize the parameters for a specific motion model such that they agree most closely with the model-free parameters. A significant advantage of this latter approach is that the model-free method is quite effective at defining the overall rotational motions of the protein so these are factored out in the analysis, leaving only internal motions to be analyzed on a model-specific basis. However, the caveat of this method is that this approach already imposes a specific functional form on the internal correlation function, and this may not be strictly consistent with a particular motional model. Nevertheless, considering the popularity of the model-free formalism and the mathematical complexity of the alternative approach, this latter approach has been applied more often than the former.

Relating the model-free order parameter to the parameters defining a specific motional model can be achieved because the S^2 is related to the equilibrium distribution of bond vector orientations according to equation

$$S^2 = \int \int \mathrm{d}\Omega_1 \, \mathrm{d}\Omega_2 p_{\mathrm{eq}}(\Omega_1) P_2(\cos\theta_{12}) p_{\mathrm{eq}}(\Omega_2) \quad (33)$$

in which Ω_1 and Ω_1 represent two different orientations of the bond vector, $p_{\mathrm{eq}}(\Omega)$ is the equilibrium probability of orientation Ω, θ_{12} is the angle between the two orientations, $P_2(x)$ is the second Legendre polynomial [$P_2(x) = (3x^2 - 1)/2$], and the integral extends over all initial and final orientations that are accessible within the model. Depending on the motional model of interest, the order parameter can be either evaluated numerically or defined explicitly. However, for any arbitrary model, a single value for the order parameter may not uniquely define the motional parameters. Nevertheless, for some simple models there is a one-to-one correspondence so that an important motional parameter can be obtained from the model-free order parameter.

The specific motional model used most frequently to interpret model-free order parameters is the diffusion-in-a-cone model. In this model, the bond vector is assumed to diffuse freely within a cone defined by semiangle θ, but never to move outside of this cone (Figure 5a). For this model, the order parameter is related to the cone semiangle by equation 34 (Table 8).[45] Thus, as θ decreases from 90° to 0°, S^2 increases from 0 to 1.0 (Figure 5d).

An alternative model is the two-site jump model, in which the bond vector is assumed to alternate (i.e., jump) between two fixed orientations, referred to as states i and j, separated by an angle φ (Figure 5b). For this model, the order parameter is given by eq 35 (Table 8).[60,61] For the simple case in which both orientations are equally populated, the order parameter is related to the separation angle as shown in eq 36 (Table 8) and Figure 5b.

Finally, for bond vectors for which the relaxation is best fit using the extended model-free formalism, Clore et al. have proposed using a combination of diffusion-in-a-cone and two-site jump models (Figure 5c) to represent the internal

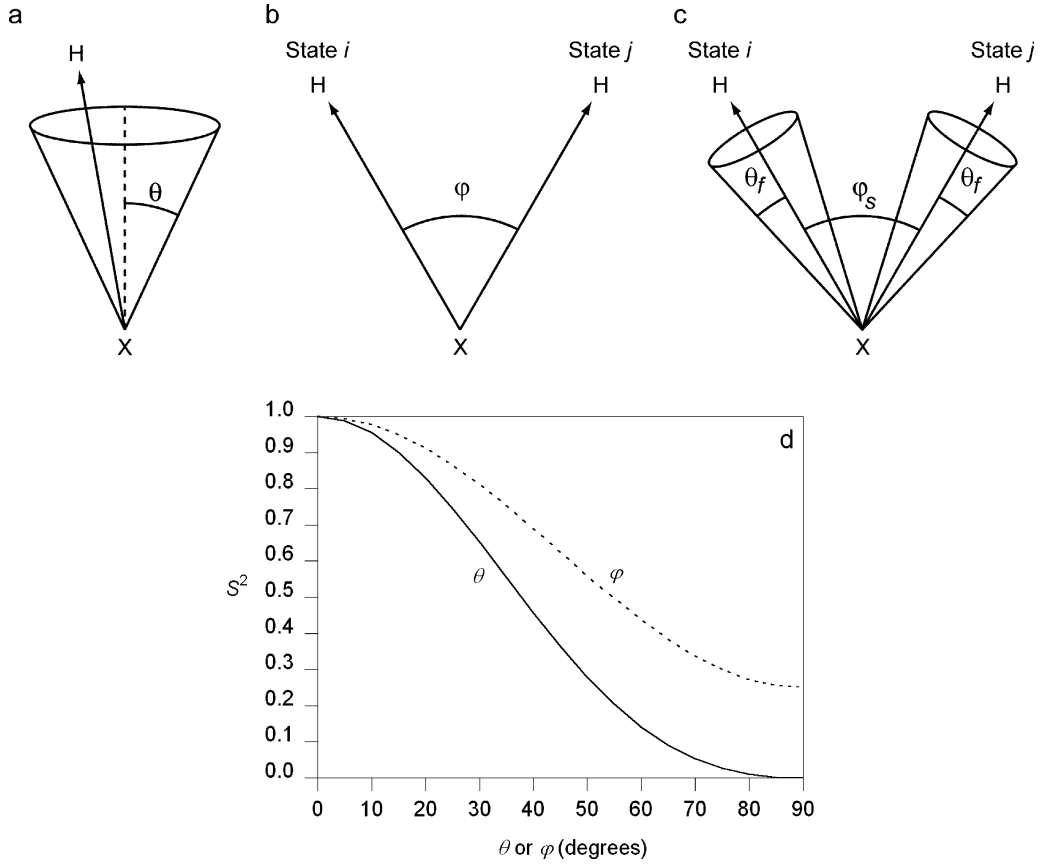

Figure 5. Specific motional models for interpretation of model-free order parameters: (a) diffusion-in-a-cone motional model (the X−H bond vector is assumed to diffuse freely within a cone defined by semiangle θ); (b) two-site jump motional model (the X−H bond vector is assumed to alternate between two states *i* and *j*, separated by an angle φ); (c) combined diffusion-in-a-cone and two-site jump models for internal bond vector motions [the X−H bond vector is assumed to alternate between two equally sized cones (on the slower time scale) or freely diffuse within each cone (on the faster time scale); θ_f is the cone semiangle and φ_s is the angle between the two cones]; (d) relationships of the model-free order parameter (S^2) to the cone semiangle (θ) and the two-site jump angle (φ), as defined by eqs 34 and 36, respectively.

Table 8. Specific Motional Models for Interpretation of Model-free Order Parameters

motional model	interpretation of order parameter in context of motional model	eq
diffusion-in-a-cone[a]	$S^2 = [^1/_2 \cos\theta(1 + \cos\theta)]^2$	34
two-site jump[b]	$S^2 = \sum_i \sum_j p_{eq}(i)p_{eq}(j)P_2(\cos\varphi_{ij})$	35
two-site jump with equal populations[c]	$S^2 = (1 + 3\cos^2\varphi)/4$	36

[a] The X−H bond vector is assumed to diffuse freely within a cone defined by semiangle θ, but never to move outside this cone.[45] [b] The X−H bond vector is assumed to alternate between states *i* and *j*, in which $p_{eq}(i)$ and $p_{eq}(j)$ are the probabilities for residency in states *i* and *j*, with $p_{eq}(i) + p_{eq}(j) = 1$; φ is the angle between the bond vector in states *i* and *j* and $P_2(x) = (3x^2 - 1)/2$.[60,61] [c] This is a special case of the two-site jump model in which $p_{eq}(i) = p_{eq}(j) = 0.5$.

motions.[60,61] In this model, the bond vector can jump between two equally sized cones (on the slower time scale) or freely diffuse within each cone (on the faster time scale), as indicated in Figure 5c. In analogy to the above two models, the order parameter for fast time scale motions (S_f^2) is related to the cone semiangle, whereas the order parameter for slower time scale motions (S_s^2) is related to the jump angle, φ_s.

3.7. Relationship of Model-free Parameters to Conformational Entropy

In section 2 we discussed the importance of relating changes in NMR-derived dynamics parameters to changes in conformational entropy. Three groups have independently developed methods for accomplishing this goal.[91−93] All three methods follow a similar logic. The Lipari−Szabo order parameter for a bond vector is related to the probability distribution of orientations for that bond vector. The probability distribution is then equated with the partition function, which in turn is related to the apparent entropy of bond vector reorientation. The primary difference between the three methods is the definition used for the partition function. Akke et al.[91] derived a relationship between changes in order parameters and changes in conformational entropy that is approximately consistent with a diffusion-in-a-cone motional model, an axially symmetric parabolic potential function, or a maximum entropy potential function as long as the squared order parameter remains >0.5. Li et al. used a partition function corresponding to a simple one-dimensional harmonic oscillator to derive an entropy relationship that takes into account both the spatial (S^2) and temporal (τ_e) motional properties of the bond vector.[92] Finally, Yang and Kay

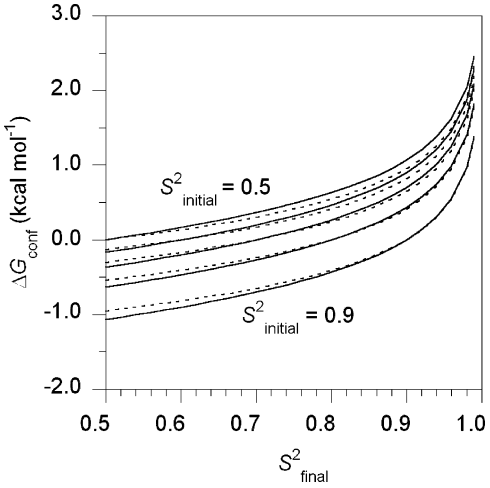

Figure 6. Simulations showing the relationship between changes in conformational free energy (ΔG_{conf}) and changes in model-free order parameters. ΔG_{conf} values were calculated using the Yang and Kay diffusion-in-a-cone relationship, eq 37 (solid lines), and the approximate relationship of Akke et al., eq 38 (dashed lines), at a temperature of 25 °C. $S^2_{initial}$ values are 0.5 (top), 0.6, 0.7, 0.8, and 0.9 (bottom). Note that the range of S^2 values shown is that in which both relationships are valid.

Table 9. Relationships between Order Parameter Changes and Conformational Entropy Changes

citation	change in conformational entropy	eq
Yang and Kay[a,b]	$\Delta S_{conf} = k\sum_{j=1}^{N} \ln\left\{\frac{3-(1+8S_{j,final})^{1/2}}{3-(1+8S_{j,initial})^{1/2}}\right\}$	37
Akke et al.[a,c]	$\Delta S_{conf} = k\sum_{j=1}^{N} \ln\left\{\frac{1-S^2_{j,final}}{1-S^2_{j,initial}}\right\}$	38

[a] ΔS_{conf} is the change in conformational free energy between two states, denoted initial and final, such that $\Delta S_{conf} = S_{conf,final} - S_{conf,initial}$; N is the number of bond vectors. [b] $S = \sqrt{S^2}$.[93] [c] $S^2_{j,initial}$, $S^2_{j,final} > 0.5$.[91]

reported calculations for 10 different probability distributions for bond vector orientations, observing, not surprisingly, that calculated entropy values can be sensitive to the choice of probability function.[93] In particular, as the complexity of the model (i.e., the number of degrees of freedom in the model) increased, the absolute value of the entropy change correspondingly increased for a given change in order parameter. To better understand which motional model best described the motions of protein vectors, Yang and Kay calculated an "entropy versus order parameter" profile from a 1.12 ns molecular dynamics trajectory for *Escherichia coli* ribonuclease HI. This profile was in good agreement with the relationship predicted from the diffusion-in-a-cone model. Thus, the diffusion-in-a-cone relationship has become the most frequently employed method of calculating conformational entropy values from NMR-derived order parameters. Figure 6 illustrates that the Yang and Kay diffusion-in-a-cone relationship (eq 37, Table 9)[93] and the approximate relationship of Akke et al. (eq 38, Table 9) correspond closely to each other for squared order parameters in the range of 0.5−1.[91] Throughout most of this range, an increase in S^2 of 0.1 for a single bond vector corresponds to an increase in conformational free energy of ∼0.15−0.45 kcal mol^{-1}. Thus, similar changes for several bond vectors could potentially have a substantial effect on the stability of the protein.

Collectively, these approaches have numerous caveats.[7,12,14,23,94,95] First, NMR relaxation measurements are limited to a subset of bond vectors within the protein (e.g., specific backbone bond vectors only). Second, the three NMR relaxation parameters, R_1, R_2 and NOE, from which the order parameter is calculated, are generally not sensitive to rotational motions slower than molecular diffusion (a few nanoseconds); although R_2 can be influenced by microsecond to millisecond time scale conformational exchange, the order parameter does not reflect these motions. Third, the NMR relaxation parameters are not sensitive to translational motions. Fourth, relaxation measurements are insensitive to rotations about the heteronuclear bond vector. Finally, all three methods for estimation of conformational entropy strictly apply only to isolated bond vectors. If the total conformational entropy of the system is to be calculated, we are forced to make the assumption that each bond vector moves independently of each other bond vector. As discussed in section 2, it is quite possible that the motions of different groups within a protein are coupled to (or correlated with) each other, which would invalidate this assumption of independence. The first four caveats would tend to result in a reduction of the estimated conformational entropy, whereas the final caveat would result in an increase in the estimated entropy relative to the correct value, so there may be some cancellation between these systematic errors. Moreover, the main application of these conformational entropy estimates is to investigate the *changes* in conformational entropy between different states of the same protein (e.g., free and ligand-bound states), not the *absolute* conformational entropy of the molecule. It would be reasonable to propose that these systematic errors remain quite similar in the different states of a protein, so again they might partially cancel when changes in conformational entropy are considered. On the other hand, a change in, for example, the degree of dynamic coupling could play a role in regulating binding affinity, cooperativity, or catalysis (see section 2.3). To assume that such changes are absent might be to overlook some of the most interesting physical effects underlying the function of the protein.

Despite their limitations, the above methods for relating model-free parameters to entropy have been applied to a wide variety of proteins and their complexes (see section 4).[11,12] In addition, for cases in which dynamics parameters have been obtained at more than one temperature, conformational entropy values have been used to calculate heat capacity changes associated with the changes in the motions of bond vectors. Heat capacity (C_p) is the dependence of enthalpy on temperature (dH/dT) or the dependence of entropy on the natural logarithm of temperature (dS/d ln T). Heat capacity changes are of interest because they control the curvature of free energy versus temperature profiles, thus influencing the stabilities of proteins and their complexes at extreme temperatures.[96] Traditionally, heat capacity changes have been taken to indicate changes in solvent-exposed surface area (the formation or breakage of hydrophobic interactions).[97] However, Freire and colleagues have shown that the intrinsic heat capacity of a protein includes contributions from fluctuating covalent and non-covalent interactions,[98] suggesting that changes in these structural fluctuations (conformational heat capacity changes, $\Delta C_{p,conf}$) could contribute to the overall heat capacity change for a binding or unfolding event. This latter contribution to heat capacity can be estimated from the conformational entropy values calcu-

lated at two or more temperatures ($C_{p,conf} = dS_{conf}/d \ln T$). Conformational heat capacity values determined in this way are subject to the same caveats previously detailed for conformational entropy estimates, as well as the assumption that heat capacity does not vary over the temperature range sampled. Although the latter assumption is not strictly correct,[99] it is a reasonable approximation over the small temperature ranges generally sampled by dynamics studies.[100,101]

As an alternative to the calculation of conformational heat capacity, the temperature dependence of order parameters can be expressed in terms of a characteristic temperature (T^*), which represents the density of thermally accessible conformational energy states for each bond vector.[102] The characteristic temperature of a particular bond vector is calculated from the slope of a linear fit of $(1 - S)$ versus temperature (T) according to the relationship

$$\frac{3}{2T^*} = \frac{d(1 - S)}{dT} \tag{39}$$

For temperatures higher than the characteristic temperature, an increase in temperature allows access to many additional conformational states, whereas for temperatures substantially below the characteristic temperature, an increase in temperature results in access to relatively few additional conformational states. Thus, a low characteristic temperature corresponds qualitatively to a high conformational heat capacity and vice versa.

Recently, Palmer and co-workers have introduced an additional approach to represent the temperature dependence of order parameters,[103,104] defining the parameter Λ, which is related to T^* (see above), as

$$\Lambda = \frac{d \ln(1 - S)}{d \ln T} \tag{40}$$

As for T*, Λ can be readily obtained from the slope of a linear fit of $\ln(1 - S)$ versus $\ln T$. Furthermore, experimentally determined values of Λ (in combination with order parameters) can be used to define the shape of the potential well for orientational fluctuations of NH groups.[103,104]

4. Applications to Specific Proteins and Their Complexes

4.1. Overview

Since Kay et al. first described the application of ^{1}H-detected 2D methods and model-free analysis to probe the fast time scale backbone motions of staphylococcal nuclease,[47] the number of backbone dynamics studies described in the literature increased steadily to about 50 per year in 2001 but subsequently decreased slightly (Figure 7). Table 10 contains a comprehensive list of these studies. Among them, ~77% have exclusively employed the model-free formalism for interpretation of relaxation parameters and ~10% have used only reduced SDM. An additional ~12% have presented data interpreted with both the model-free formalism and either full or reduced SDM and only the remaining <2% have used an alternative method of analysis. A substantial proportion of these past studies have examined the protein of interest under only a single set of physical and chemical conditions, often in conjunction with structural studies performed under the same conditions. However, it has become apparent that in order to gain an understanding of the functional role of fast dynamics, it is necessary to compare the changes in dynamics between different states. Consequently, a number of studies have now investigated the influences of changes in ligand binding,[67,105−142] mutations,[126,143−152] temperature,[72,95,100−103,111,135,153−156] pressure,[157] oxidation state,[158−164] and pH[165,166] on the flexibility of protein backbones. In the following sections we highlight several of these comparative studies that have shed light on the possible contributions of dynamics to protein stability, the thermodynamics of ligand binding, and enzymatic activity.

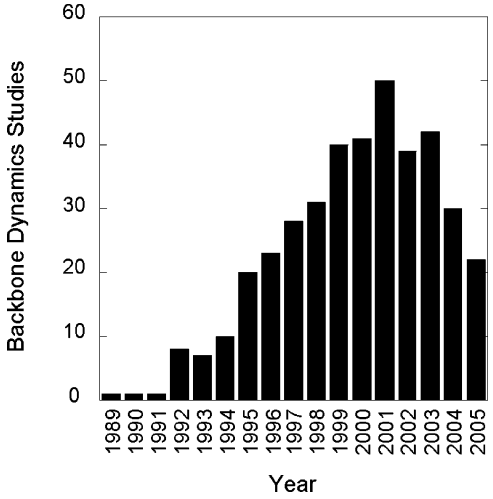

Figure 7. Histogram of number of backbone dynamics studies each year since 1989.

4.2 Effects of Ligand Binding

A substantial number of NMR dynamics studies have examined the effects of binding a ligand (small molecules, metal ions, peptides, nucleic acids, etc.) upon the dynamics of protein backbones. These studies have begun to reveal the role that dynamics can play in regulating the affinity, specificity, and even cooperativity of binding events. Because the effects of ligand binding upon backbone dynamics have been reviewed previously,[12,23,94] the discussion herein focuses primarily on work published within the past five years, with brief mention of some particularly noteworthy earlier studies.

Induced Fit Binding (Reductions in Flexibility). Binding events are characterized by the formation of new interactions (hydrogen bonds, salt bridges, van der Waals and hydrophobic interactions, etc.) that give rise to specific recognition between a protein and its ligand. Although these interactions are thermodynamically favorable, they are offset by the loss of favorable interactions between the binding surfaces and the solvent and the loss of rotational and translational entropy associated with bimolecular association. In general, one might also expect the flexibility of the interacting partners to be reduced in the bimolecular complex so as to optimize the strengths of the new interactions. In this sense the formation of the new interactions and the reduced flexibility of the interacting groups represent a classical case of enthalpy−entropy compensation. In accord with this "induced fit" binding model, backbone dynamics studies examining ligand-binding effects suggest a general trend in which backbone amide bond vectors display decreased flexibility on a fast time scale and thus loss of conformational entropy upon ligand binding. In some cases, a large propor-

Table 10. Published NMR Relaxation Studies of Fast Backbone Dynamics in Proteins[a,b]

protein	form(s)	method of analysis[c]	first author (year)	ref
Small-Molecule-Binding Proteins				
ABC transporter MJ1267	free and bound to ADP-Mg	rSDM	Wang (2004)	204
acyl carrier protein from oxytetracycline polyketide synthase	free	MF	Findlow (2003)	205
acyl-coenzyme A binding protein	free and palmitoyl-coA-bound	none	Rischel (1994)	114
β2-glycoprotein I, phospholipid-binding domain V	intact protein and cleaved (K317−T318 peptide bond) protein	MF	Hoshino (2000)	206
cellular retinol-binding protein I	apo and retinol-bound	MF	Franzoni (2002)	109
cellular retinol-binding protein I	apo and retinol-bound	MF	Lu (2003)	207
cellular retinol-binding protein II	retinol-bound	MF	Lu (2000)	106
cellular retinol-binding protein II	apo and retinol-bound	MF	Lu (2003)	207
cellular retinol-binding protein II	apo	MF	Lu (1999)	208
fatty acid-binding protein (bovine heart)	free	MF	Lucke (1999)	209
fatty acid-binding protein (human epidermal-type)	free	MF	Gutierrez-Gonzalez (2002)	210
fatty acid-binding protein (intestinal)	free and I-FABP-bound	MF	Hodsdon (1997)	112
fatty acid-binding protein (muscle)	free	MF and rSDM	Constantine (1998)	211
FKBP-12	free	MF	Cheng (1993)	212
FKBP-12	FK506-Bound	MF	Cheng (1994)	116
frenolicin acyl carrier protein	holo	MF	Li (2003)	213
ionotropic glutamate receptor GluR2, extracellular ligand-binding (S1S2) core	free	MF	McFeeters (2002)	214
lipid binding protein (porcine ileal)	free	MF	Lucke (1999)	209
lipid-binding protein (adipocyte)	free	MF and rSDM	Constantine (1998)	211
major urinary protein I	free and pheromone-bound	MF	Zidek (1999)	130
major urinary protein I	free and pheromone-bound	rSDM	Krizova (2004)	135
neocarzinostatin	apo	MF	Mispelter (1995)	215
neocarzinostatin	apo	MF	Izadi-Pruneyre (2001)	216
Cytokines, Growth Factors, and Peptide Hormones				
atrial natriuretic peptide	reduced and oxidized	MF and rSDM	Peto (2004)	217
eotaxin	free	MF	Ye (1999)	167
eotaxin	free	MF	Crump (1999)	218
eotaxin-2	free	MF	Mayer (2003)	169
eotaxin-3	free	MF	Ye (2001)	168
fractalkine	free	MF	Mizoue (1999)	219
heregulin-α, EGF-like domain	free	rSDM	Fairbrother (1998)	220
human acidic fibroblast growth factor 1	free and bound to sucrose octasulfate	MF	Chi (2000)	121
human granulocyte colony stimulating factor	free	MF	Zink (1994)	221
human growth hormone	free	MF	Kasimova (2002)	165
human parathyroid hormone (1−34)	micelles	rSDM	Scian (2005)	222
interferon (human, type I) receptor subunit 2, extracellular domain	free	MF	Chill (2004)	223
interleukin-1β	free	MF	Clore (1990)	60
interleukin-3	truncated, multiple substitutions	MF	Feng (1996)	224
interleukin-4	free	MF	Redfield (1992)	225
interleukin-8	free	MF	Grasberger (1993)	226
leukemia inhibitory factor (human-murine chimera)	free	MF	van Heijenoort (2000)	227
leukemia inhibitory factor (murine)	free	MF	Purvis (1997)	228
macrophage inflammatory protein-1β	wild-type and F13A variant	MF	Kim (2001)	229
macrophage migration inhibitory factor	free	MF	Muhlhahn (1996)	230
mature-T-cell proliferation ($p8^{MTCP1}$), C12A mutant	free	rSDM	Barthe (1999)	231
melanoma inhibitory activity protein	free	MF	Stoll (2003)	232
myeloid progenitor inhibitory factor-1	free	MF	Rajarathnam (2001)	233
platelet factor 4, 20-residue peptide	partially folded state	MF	Daragan (1997)	234
prolactin	free	MF	Keeler (2003)	235
transforming growth factor α	free	MF	Li (1995)	236
transforming growth factor β, extracellular domain	free	MF	Deep (2003)	237
viral macrophage-inflammatory protein II	free	MF	Liwang (1999)	238
Extracelluar Matrix, Connective Tissue, and Blood Coagulation Proteins				
CD2 adhesion domain (glycosylated)	free	rSDM	Wyss (1997)	239
collagen, fragment α3-chain type VIC-terminal Kunitz domain	free	MF and rSDM	Sorensen (1997)	240
fibrillin-1, cbEGF12−13 domains	Ca^{2+}-saturated	MF	Smallridge (2003)	241
fibrillin-1, TB6-cbEGF32	wild-type and N2144S (Marfan syndrome) mutant	MF	Yuan (2002)	242
fibrillin-1, calcium-binding epidermal growth factor-like domains 32−33	Ca^{2+}-bound	MF	Werner (2000)	243
fibrillin-1, TGF-β binding protein-like domain	free	MF	Yuan (1998)	244

Table 10 (Continued)

protein	form(s)	method of analysis[c]	first author (year)	ref
Extracelluar Matrix, Connective Tissue, and Blood Coagulation Proteins (Continued)				
fibrinogen γ-chain, 27-residue C-terminal fragment	free	MF	Fan(1995)	245
fibronectin, type 1, fourth and fifth module pair	free	MF	Phan (1996)	246
fibronectin, type III domain	free	MF	Carr (1997)	247
neural cell adhesion molecule, immunoglobulin modules 1−3	free	MF	Thormann (2004)	248
plasminogen kringle 1 domain	free and bound to ϵ-aminocaproic acid	MF	Zajicek (2000)	249
plasminogen kringle 2 domain	bound to antifibrinolytic agent *trans*-(aminomethyl)-cyclohexanecarboxylic acid	MF	Marti (1999)	250
tenascin, fibronection type III domain	free	MF	Carr (1997)	247
tenascin, third fibronectin type III domain	denatured state	rSDM	Meekhof (1999)	251
urokinase-type plasminogen activator, N-terminal fragment	free	MF	Hansen (1994)	252
Antibodies, Antibody-Binding Proteins, and Complement Proteins				
anti-digoxin antibody, VL domain	free	MF	Constantine (1993)	253
catalytic antibody NPN43C9, Fv fragment	free and inhibitor (*p*-nitrophenol)-bound	MF	Kroon (2003)	254
complement receptor type 1 (CR1), 16th complement control protein module	free	MF	O'Leary (2004)	255
heavy chain variable domain H14	antigen-free	MF	Renisio (2002)	256
light chain 1 polypeptide	free	MF	Wu (2003)	257
membrane cofactor protein (MCP), first complement control protein module	free	MF	O'Leary (2004)	255
protein G, B1 domain	free	MF	Barchi (1994)	258
protein G, B1 domain	urea-denatured	MF	Frank (1995)	259
protein G, B1 domain	free	MF	Seewald (2000)	72
protein G, B1 domain	free	MF	Tillett (2000)	260
protein G, B1 domain	3 single-site mutants	MF	Stone (2001)	147
protein G, B1 domain	10 single-site mutants	MF	Mayer (2003)	148
protein G, B1 domain	free	MF and alternative spectral density analysis	Idiyatullin (2003)	156
protein G, B1 domain	free	MF	idiyatullin (2003)	261
protein G, B1 domain	free	MF, alternative spectral density analysis and frequency-dependent approach	Idiyatullin (2003)	156
protein G, B3 domain	free	MF	Hall (2003)	262
protein G, third GA module	free	MF and rSDM	Johansson (2002	263
protein L, B1 domain	free	MF	Wikstrom (1996)	264
Membrane-Associated Proteins				
apolipoprotein CII	SDS micelles	MF	Zdunek (2003)	265
bacterioopsin, residues 1−36 and 1−71	solubilized in a 1:1 chloroform/ethanol mixture	MF	Orekhov (1995)	266
bacterioopsin, residues 1−71	solubilized in a 1:1 chloroform/ethanol mixture	MF	Orekhov (1994)	267
bacterioopsin, residues 1-36	1:1 chloroform/methanol mixture	MF	Orekhov (1999)	268
neuronal glycine receptor α_1 subunit, second transmembrane segment	micelles	MF	Yushmanov (2003)	269
neuronal nicotine acetylcholine receptor, second trans-membrance segment	micelles	MF	Yushmanov (2003)	270
neuropeptide Y	micelle-bound	MF	Bader (2001)	271
neuropeptide Y	wild type and Ala-31, Pro-32 mutant	MF	Bader (2002)	272
opioid peptide E	micelles	MF	Yan(1999)	273
phospholamban	dodecylphophocholine micelles	MF	Metcalfe (2004)	274
Signal Transduction Proteins				
adapter protein drk, N-terminal region, SH3 domain	folded and unfolded equilibrium	MF and rSDM	Farrow (1995)	51
adapter protein drk, N-terminal region, SH3 domain	folded and unfolded	MF and rSDM	Farrow (1997)	275
adapter protein drk, N-terminal region, SH3 domain	folded and unfolded	MF	Yang (1997)	100
adenylate kinase (*E. coli*)	free and inhibitor-bound	MF, SRLS, and GNM	Temiz (2004)	276
adenylate kinase (*E. coli*)	free and inhibitor-bound	MF	Shapiro (2000)	277
adenylate kinase (*E. coli*)	free and inhibitor-bound	SRLS	Shapiro (2002)	278

Table 10 (Continued)

protein	form(s)	method of analysis[c]	first author (year)	ref
	Signal Transduction Proteins (Continued)			
adenylate kinase (*E. coli*)	free	MF and SRLS	Tugarinov (2002)	279
β-adrenergic receptor kinase pleckstrin homology domain	free	MF and rSDM	Pfeiffer (2001)	198
ArcB anaerobic sensor kinase, phosphotransfer domain	free	MF	Ikegami (2001)	280
BAS−like protein tyrosine phosphatase, second PDZ domain	free	MF	Walma (2002)	281
β-platelet-derived growth factor receptor pTyr-1021 site peptide	free and bound to phospholipase C-γ1 C-terminal domain	MF	Finerty (2005)	282
Bruton's tyrosine kinase, SH3 domains	free	MF	Hansson (1998)	283
Cdc42Hs	GDP-bound (inactive) and GMPPCP-bound (active)	MF	Loh (1999)	118
Cdc42Hs	F28L mutant, GDP-bound (inactive)	MF	Adams (2004)	152
Cdc42Hs	GMPPCP-bound, effector (PBD46)-bound	MF	Loh (1999)	118
chemotaxis kinase CheA, CheY-binding domain	free	MF	McEvoy (1996)	284
chemotaxis kinase CheA, phospho-transfer domain	free	MF	Zhou (1995)	285
dynamin, pleckstrin homology domain	free	MF	Fushman (1997)	195
Fyn tyrosine kinase, SH3 domain	wild-type and F20L and F20V hydrophobic core mutants	MF	Mittermaier (2004)	144
hematopoietic cellular kinase, SH2 domains	free and phosphopeptide-bound	MF	Zhang (1998)	105
hematopoietic cellular kinase, SH3 domains	free	MF	Horita (2000)	197
insulin receptor substrate 1, ST domain	free and phosphopeptide-bound	MF	Olejniczak (1997)	117
neurogranin/RC3, calmodulin-binding protein and protein C kinase substrate	free	MF and rSDM	Ran (2003)	286
$p13^{MTCP1}$ oncogenic protein	free	MF and rSDM	Guignard (2000)	287
$p19^{INK4d}$	free	rSDM	Renner (1998)	288
p53, tetrameric oligomerization domain, residues 319−360	tetramer	MF	Clubb (1995)	289
p67phox, C-terminal SH3 domain	free and peptide-bound	MF	Dutta (2004)	290
p85α subunit of phosphoinositide 3-kinase, C-terminal SH2 domain	free and bound to a phospho tyrosine-containing peptide	MF	Kristensen (2000)	291
PBD46	Cdc42Hs-bound	MF	Gizachew (2001)	107
phospholipase Cγ1, C-terminal SH2 domain	free and bound to a phospho-tyrosine-containing peptide	MF	Farrow (1994)	67
postsynaptic density-95 protein, second PDZ domain	free	MF	Tochio (2000)	292
pp60(c-src), SH3 domain	free and bound to proline-rich peptide RLP2	MF	Wang (2001)	125
protein kinase A, dimerization/docking domain	free and bound to kinase anchoring protein Ht31pep	MF	Fayos (2003)	128
protein kinase B, PH domain	free	MF and rSDM	Auguin (2004)	293
protein tyrosine phosphatase, low molecular weight	monomer and dimer	MF	Akerud (2004)	294
protein-tyrosine kinase-6, SH2 domain	free	MF	Hong (2004)	295
sarcoplasmic/endoplasmic reticulum Ca^{2+}-ATPase, nucleotide-binding domain	free and bound to AMP−PNP	MF	Abu-Abed (2004)	296
smooth muscle myosin light chain kinase (MLCK) calmodulin-binding domain peptide	Ca^{2+}-saturated calmodulin-bound	MF	Chen (1993)	297
β-spectrin, pleckstrin homology domain	free and Ins(1,4,5)P_3-bound	MF	Gryk (1998)	298
transcriptional enhancer NtrC	inactive (unphosphorylated), active (phosphorylated), and partially active	MF	Volkman (2001)	299
tyrosine phosphatase 1E (human)	free and peptide-bound	MF	Fuentes (2004)	187
	Metal-Binding Proteins			
α-lactalbumin	chimera with D-helix of lysozyme substituted by fluctuating loop of α-lactalbumin	MF	Tada (2002)	300
azurin	reduced	MF	Kalverda (1999)	301
β-parvalbumin	free and Ca^{2+}-Saturated, wild-type and S55D and G98D mutants	MF	Henzl (2002)	133
calbindin-D_{9k}	$(Ca^{2+})_2$-bound	MF	Kordel (1992)	170
calbindin-D_{9k}	apo and $(Cd^{2+})_1^{II}$-bound	MF	Akke (1993)	136
calbindin-D_{9k}	mutant with engineered EF-hand loop, apo	MF	Malmendal (1998)	302
calbindin-D_{9k}	$(Ca^{2+})_1^{I}$-bound	MF	Maler (2000)	137

Table 10 (Continued)

protein	form(s)	method of analysis[c]	first author (year)	ref
	Metal-Binding Proteins (Continued)			
calcium vector protein, C-terminal domain	C^{2+}-saturated	MF and rSDM	Theret (2001)	303
calcium vector protein, N-terminal domain	free	MF	Theret (2001)	304
calmodulin	Ca^{2+}-saturated	MF	Barbato (1992)	64
calmodulin	apo and $(Ca^{2+})_1$-bound	MF	Malmendal (1999)	305
calmodulin	E140Q mutant	MF	Evenas (1999)	101
calmodulin	Ca^{2+}-saturated, free and peptide (calmodulin-binding domain of the smooth muscle MLCK)-bound	MF	Lee (2000)	306
calmodulin	Ca^{2+}-saturated, peptide (calmodulin-binding domain of the smooth muscle MLCK)-bound, at five temperatures (22−73 °C)	MF	Lee (2002)	155
calmodulin	Ca^{2+}-saturated, free and bound to MLCK peptide	MF	Wang (2005)	307
calmodulin	dimer bound to dimeric bHLH transcription factor SEF2-1/E2-2	MF	Larsson (2005)	308
calsensin	Ca^{2+}-saturated	MF	Venkitara-mani (2005)	309
cystein-rich protein 2	free	MF	Konrat (1998)	310
cystein-rich protein 2	R122A mutant	rSDM	Kloiber (1999)	65
Fe_4S_4 HiPIP protein (*Chromatium vinosum*)	free	MF	Bertini (2000)	311
Fe_7S_8 protein (*Bacillus schlegelii*)	free	MF	Bertini (2000)	311
metal-responsive element binding transcription factor-1 (MTF-1)	Zn^{2+}-bound	rSDM	Potter (2005)	312
metallothionein-3	free	MF	Oz (2001)	313
parvalbumin	F102W mutant	MF	Moncrieffe (2000)	314
S100B	apo, homodimeric	MF	Inman (2001)	315
sarcoplasmic calcium binding protein (*Nereis diversicolor*)	Ca^{2+}-saturated	MF	Rabah (2005)	316
troponin C, C-domain (chicken skeletal)	Ca^{2+}-saturated, free and bound to regulatory peptide (troponin I 1−40)	MF	Mercier (2001)	108
troponin C, regulatory domain (chicken skeletal)	apo	MF	Gagne (1998)	317
troponin C, regulatory domain (human cardiac)	apo and Ca^{2+}-saturated	MF	Spyracopoulos (1998)	138
troponin C, regulatory domain (human cardiac)	Ca^{2+}-saturated	MF	Paakkonen (1998)	318
troponin C, regulatory domain (human cardiac)	calcium-free	MF	Spyracopoulos (2001)	153
troponin C, regulatory domain (trout)	$(Ca^{2+})_1$	MF	Blumenschein (2004)	319
	Redox Regulatory, Electron Transfer, and Heme-Binding Proteins			
apocytochrome b_5	free	MF and rSDM	Bhattacharya (1999)	320
apomyoglobin	unfolded (8 M urea, pH 2.3)	rSDM	Schwarzinger (2002)	321
apomyoglobin	partially folded state	rSDM	Eliezer (2000)	66
apomyoglobin	unfolded state	rSDM	Yao (2001)	322
Cu(I) pseudoazurin	free	MF	Thompson (2000)	323
cytochrome b_5	oxidized	MF and rSDM	Kelly (1997)	324
cytochrome b_5	reduced and oxidized	MF	Dangi (1998)	161
cytochrome b_5	both equilibrium forms of reduced state	MF	Dangi (1998)	325
cytochrome *c* (*Bacillus pasteurii*)	reduced	MF	Bartalesi (2003)	326
cytochrome *c′* (*Rhodobacter capsulatus*)	carbon monoxide-bound	MF	Tsan (2000)	327
cytochrome c_2 (*Rhodobacter capsulatus*)	free	MF	Cordier (1998)	328
cytochrome c_{552}, functional domain (*Paracoccus denitrificans*)	reduced and oxidized	MF	Reincke (2001)	329
ferricytochrome b_{562}	reduced, oxidized, and oxidized R98C variant	MF and rSDM	Assfalg (2001)	330
ferricytochrome c_{551} *Pseudomonas aeruginosa*)	free	MF	Russell (2003)	331
ferrocytochrome c_2 (*R. capsulatus*)	free	MF	Flynn (2001)	332
flavodoxin (*Cyanobacterium anabaena*)	oxidized, C55A mutant	MF	Liu (2001)	333
flavodoxin (*Desulfovibrio vulgaris*)	reduced and oxidized	MF	Hrovat (1997)	159
flavodoxin from *Anacystis nidulans*	bound to FMN	MF and rSDM	Zhang (1997)	334
glutaredoxin-1	reduced and oxidized	MF	Kelley (1997)	160
Glycera dibranchiata monomeric hemoglobin 4	ferrous CO-ligated	MF	Volkman (1998)	335
iso-1-cytochrome *c* (S*accharomyces cerevisiae*)	reduced and oxidized	MF	Fetrow (1999)	163
plastocyanin	reduced	MF	Ma (2003)	336
plastocyanin	reduced and oxidized	MF	Bertini (2001)	164
plastocyanin (apo)	unfolded	rSDM	Bai (2001)	337

Table 10 (Continued)

protein	form(s)	method of analysis[c]	first author (year)	ref
Redox Regulatory, Electron Transfer, and Heme-Binding Proteins (Continued)				
PsaE subunit of photosystem I	free	MF and rSDM	Barth (2002)	338
putidaredoxin (Pdx)	reduced and oxidized	MF	Sari (1999)	162
rubredoxin	free	MF	Lamosa (2003)	339
rusticyanin (Rc, *Thiobacillus ferrooxidans*)	reduced	MF	Jimenez (2003)	340
thioredoxin (*Alicyclobacillus acidocaldarius*) K18G/R82E mutant	free	MF	Leone (2004)	341
thioredoxin (*E. coli*)	reduced and oxidized	MF	Stone (1993)	158
thioredoxin (*E. coli*)	L78K core-packing mutant	MF	de Lorimier (1996)	143
thioredoxin (*E. Coli*)	partially folded fragment	rSDM	Daughdrill (2004)	342
thioredoxin chimera (*E. coli*, human)	oxidized	MF	Dangi (2002)	343
Regulators of Protein Translation, Folding, and Degradation				
DnaJ chaperone protein	DnaJ(1−78) and DnaJ(1−104)	MF	Huang (1999)	344
peptide from heat shock protein 10	free	rSDM	Landry (1997)	345
ribosome recycling factor	free	MF	Yoshida (2003)	346
translation initiation factor (eIF4E)	free, in micelles, and two nucleotide complexes in micelles	rSDM	McGuire (1998)	347
ubiquitin	free	MF	Schneider (1992)	348
ubiquitin	partially folded A state	MF	Brutscher (1997)	349
ubiquitin	free	MF and Gaussian axial fluctuation model	Lienin (1998)	86
ubiquitin	free	MF	Lee (1999)	59
ubiquitin	free	MF	Wang (2003)	95
ubiquitin	free	MF	Chang (2005)	350
ubiquitin	free	MF	Kitahara (2005)	351
Proteases				
α-lytic protease	free and inhibitor-bound	rSDM	Davis (1998)	142
hepatitis C virus NS3 protease	cofactor (NS4A)-bound	MF	Mccoy (2001)	352
HIV-1 protease	free and inhibitor-bound	MF	Nicholson (1995)	353
HIV-1 protease	inhibitor-bound	MF	Freedberg (1998)	354
HIV protease	free	MF	Freedberg (2002)	355
HIV protease, inactive D25N mutant	bound to substrate	MF	Katoh (2003)	356
matrix metalloproteinase 2, catalytic domain	inhibitor-bound	MF	Feng (2002)	357
matrix metalloproteinase 2, second type II module	free	MF	Briknarova (1999)	358
savinase	free	MF	Remerowski (1996)	359
stromelysin, catalytic domain	inhibitor-bound (3 forms)	MF	Yuan (1999)	124
subtilisin, pro-peptide	natively unfolded	MF	Buevich (2001)	360
subtilisin, pro-peptide	unfolded state	Cole−Cole distribution and MF	Buevich (1999)	361
thioesterase/protease I (TEP-I)	free	MF	Huang (2001)	362
Protease Inhibitors				
bovine pancreatic trypsin inhibitor	analogue with disulfide bond between Cys30 and Cys51 only	MF	van Mierlo (1993)	363
bovine pancreatic trypsin inhibitor	free	MF	Smith (1995)	364
bovine pancreatic trypsin inhibitor	wild-type and Y35G mutant	MF	Beeser (1997)	145
bovine pancreatic trypsin inhibitor	wild-type form with reduced and methylated C14−C38 disulfide bond and reduced Y35G mutant	MF	Beeser (1998)	365
bovine pancreatic trypsin inhibitor	single disulfide variant in partially folded state	MF and rSDM	Barbar (1998)	366
bovine pancreatic trypsin inhibitor	free	MF	Sareth (2000)	157
bovine pancreatic trypsin inhibitor	multiple core mutants	MF and rSDM	Hanson (2003)	146
chymotrypsin inhibitor 2 and complex formed by fragments of residues 20−59 and 60−83	intact and complex formed by two fragments (residues 20−59 and 60−83)	MF	Shaw (1995)	367
Cucurbita maxima trypsin inhibitor-V	free	MF	Liu (1996)	368
Cucurbita maxima trypsin inhibitor-V	free	MF	Cai (1996)	369
Cucurbita maxima trypsin inhibitor-V	wild-type and R50A and R52A mutants	MF	Cai (2002)	151
eglin C	free	MF and fSDM	Peng (1992)	50
eglin C	free	fSDM and rSDM	Peng (1995)	55
eglin C	free	MF	Hu (2003)	166
ovumucoid, third domain (Indian peafowl)	uncleaved and cleaved	MF	Song (2003)	370
ovumucoid, third domain (turkey)	uncleaved and cleaved	MF	Song (2003)	370
potato carboxypeptidase inhibitor	free	MF	Gonzalez (2003)	371
Schistocerca gregaria chymotrypsin inhibitor	monomer and dimeric precursor	MF	Szenthe (2004)	372
Schistocerca gregaria trypsin inhibitor	monomer and dimeric precursor	MF	Szenthe (2004)	372
stefin A	monomer and domain-swapped dimer	MF	Japelj (2004)	185

Table 10 (Continued)

protein	form(s)	method of analysis[c]	first author (year)	ref
	Protease Inhibitors (Continued)			
tissue inhibitor of metalloproteinases-1, N-terminal fragment	free	MF and rSDM	Gao (2000)	373
tissue inhibitor of metalloproteinases 1	free and protein-bound	MF	Arumugam (2003)	134
	Nucleases			
α-sarcin ribonuclease	free	MF and rSDM	Perez-Canadillas (2002)	374
barnase	free and inhibitor-bound	MF	Sahu (2000)	122
binase	free	MF	Pang (2002)	375
binase	free	MF	Wang (2003)	95
ribonuclease A	Free	MF	Cole (2002)	376
ribonuclease A	free and inhibitor-bound	MF	Kovrigin (2003)	111
ribonuclease A (S peptide)	free and S protein-bound	MF	Alexandrescu (1998)	377
ribonuclease H Domain (*HIV-1*)	free	MF	Powers (1992)	378
ribonuclease H Domain (*HIV-1*)	free	MF	Mueller (2004)	379
ribonuclease HI (*E. coli*)	free	MF	Yamasaki (1995)	380
ribonuclease HI (*E. coli*)	free	MF	Mandel (1995)	62
ribonuclease HI (*E. coli*)	free	MF	Yang (1996)	93
ribonuclease HI (*E. coli*)	free	MF and rSDM	Mandel (1996)	102
ribonuclease HI (*E. coli*)	free	MF and rSDM	Butterwick (2004)	381
ribonuclease Sa	free	MF	Laurents (2001)	382
ribonuclease T1	free and inhibitor-bound	MF	Fushman (1994)	383
ribonuclease T1	free and inhibitor-bound	MF	Fushman (1994)	115
ribonuclease T1	free	MF and fSDM	Engelke (1997)	384
staphylococcal nuclease	free	MF	Kay (1989)	47
staphylococcal nuclease	disordered 131 residue fragment	MF	Alexandrescu (1994)	385
staphylococcal nuclease	free, Ca^{2+}:inhibitor-bound, "OB-fold" subdomain, denatured 131 residue fragment	MF	Alexandrescu (1996)	386
staphylococcal nuclease	folded and unfolded	MF	Yang (1997)	100
staphylococcal nuclease	denatured 101 residue fragment	MF	Sinclair (1999)	387
	Other Nucleic Acid-Binding Proteins			
434 repressor, DNA-binding domain	free	MF	Luginbuhl (1997)	388
Ada DNA methyl phosphotriester repair domain	free	MF and rSDM	Habazettl (1996)	389
bacteriophage Pf3	free and complexed with $d(A)_6$	rSDM	Folmer (1997)	390
c-Jun, coiled-coil leucine zipper domain	free	MF	Mackay (1996)	391
c-Myb, DNA-binding domain	free and complexed with DNA	MF	Sasaki (2000)	113
cold shock protein A	free	MF	Feng (1998)	392
core binding factor a, runt domain	DNA-bound and CBFb-DNA-bound	MF	Yan (2004)	393
λ-Cro repressor	free	MF	Matsuo (1996)	394
enhancer-binding domain of Mu phage transposase	free	MF	Clubb (1996)	395
estrogen receptor DNA-binding domain	free	MF	Wikstrom (1999)	396
fructose repressor, DNA-binding domain	free	rSDM	van Heijenoort (1998)	397
FUSE-binding protein, KH domains 3 and 4	complex between two domains	MF	Braddock (2002)	398
GCN4, basic region leucine zipper domain	free	rSDM	Bracken (1999)	399
genesis, winged helix DNA-binding domain	free	MF	Jin (1998)	400
glutocorticoid receptor DNA-binding domain	free	MF	Berglund (1992)	401
glutocorticoid receptor DNA-binding domain	free	MF	Wikstrom (1999)	396
heat shock factor, DNA-binding domain	free	MF	Damberger (1995)	402
heterogeneous nuclear ribonucleoprotein D0	free and complexed with DNA and RNA	MF	Katahira (2001)	403
heterogeneous nuclear ribonucleoprotein K, C-terminal KH domain	free wild type, free mutant, and mutant bound to ssDNA	MF	Baber (2000)	404
HMG-1, A domain	free	MF	Broadhurst (1995)	405
HMG box 1 of human upsteam binding factor	free	rSDM	Zhang (2005)	406
Mason−Pfizer monkey virus nucleocapsid protein	free	MF and rSDM	Gao (1998)	407
Mbp1 transcription factor, winged helix−turn−helix domain	free and complexed with DNA	MF and rSDM	McIntosh (2000)	141
Mrf-2, AT-rich interaction domain	free and complexed with DNA	MF	Zhu (2001)	131
Musashi, RNA-binding domains 1 and 2	free	MF	Miyanoiri (2003)	408
nucleocapsid protein NCp7 of HIV-1	free and DNA-bound	rSDM	Ramboarina (2002)	110
Pho4, basic helix-loop-helix domain	free, nonspecifically complexed with DNA, and complexed with cognate DNA	MF and rSDM	Cave (2000)	140
protein HU	free and complexed with DNA	MF and rSDM	Vis (1998)	56
RNA polymerase σ^{70} subunit, region 4	free	rSDM	Poznanski (2003)	409
Sac7d chromatin protein	free	MF	Kahsai (2005)	410
single-stranded DNA-binding (SSB) domain RPA70A from SSB replication protein A	free and DNA-bound	MF and rSDM	Bhattacharya (2002)	411
Sox-5 (SRY-related HMG box)	free	MF	Cary (2001)	412

Table 10 (Continued)

protein	form(s)	method of analysis[c]	first author (year)	ref
Other Nucleic Acid-Binding Proteins (Continued)				
Sao10a, chromatim regulation and DNA packaging protein (*Sulfolobus solfataricus*)	free	MF	Kahsai (2005)	413
Sso10b2 chromatin organization and RNA metabolism protein (*Sulfolobus solfataricus*)	free	MF	Biyani (2005)	414
STAR/GSG quaking protein (pXqua), KH-QUA2 region	free	MF and rSDM	Maguire (2005)	415
topoisomerase 1, C-terminal DNA-binding domain	free and complexed with ssDNA	MF	Yu (1996)	129
transcription factor GAL4, residues 1−65	free	rSDM	Lefevre (1996)	54
transcription factor IIIA, first three zinc-finger domains	free	MF	Bruschweiler (1995)	81
transcription factor Pu.1, ETS domain	free	MF	Jia (1999)	416
transcription factor v-Myc, basic helix−loop−helix, leucine zipper domain	free	rSDM	Fieber (2001)	417
transcriptional activator PUT3, residues 31−100	free	rSDM	Walters (1997)	418
Trp repressor	free	MF	Zheng (1995)	419
U1A, RBD1	free, biomolecular complex between U1A with RNA, trimolecular complex between two U1A proteins and polyadenylation inhibition element	MF	Mittermaier (1999)	139
U1A, RBD1	G53A and G53V mutants	MF	Showalter (2004)	150
U1A, RBD1	Y13F, Q54E, F56Y and Y13F, F56Y mutants	MF	Kranz (1999)	149
U1A, RBD1 and RBD2	free	MF	Lu (1997)	420
Vnd/NK-2 homeodomain	wild-type and H52R/T56W double mutant, free and complexed with DNA	MF	Fausti (2001)	421
Wilms' tumor suppressor protein (WT1)	free and bound to DNA	rSDM	Laity (2000)	422
Xfin-31 zinc finger	free	MF	Palmer (1991)	74
XPA, central domain	free	MF	Ikegami (1999)	423
XPA, minimal DNA binding domain	free and complexed with DNA containing dhT or 64TC lesions	MF	Buchko (1999)	424
Y-box protein 1 (human), cold shock domain	folded and partially unfolded states	rSDM	Kloks (2004)	425
Other Enzymes				
4-oxalocrontonate tautomerase	free and inhibitor-bound	MF	Stivers (1996)	123
arsenate reductase (*Bacillus subtilis*)	reduced and oxidized	MF	Guo (2005)	426
biotin carboxyl carrier protein of acetyl-CoA carboxylase	apo- and holo-	MF	Yao (1999)	119
chorismate mutase (*Bacillus subtilis*)	apo- and transition state analogue-bound	MF	Eletsky (2005)	427
copper/zinc superoxide dismutase	reduced, dimeric wild-type and monomeric mutant (F50E/G51E/E133Q)	MF	Banci (2000)	428
cutinase	inhibitor (phosphonate)-bound	MF	Prompers (1999)	429
Δ^5-3-ketosteroid isomerase	free and steroid-bound	MF	Zhao (1996)	430
Δ^5-3-ketosteroid isomerase	free and steroid-bound	MF	Yun (2001)	132
Δ^5-3-ketosteroid isomerase	in presence and absence of 5% trifluoroethanol	MF	Yun (2002)	431
dihydrofolate reductase	folate-bound	MF	Epstein (1995)	432
dihydrofolate reductase	folate-bound, folate:DHNADPH-bound, folate:NADP(+)-bound	MF	Osborne (2001)	180
dihydrofolate reductase (type II R67)	free and NADP(+)-bound	MF	Pitcher (2003)	433
DNA ligase IIIα, BRCT domain	free	MF and rSDM	Krishnan (2001)	434
DNA polymerase β, N-terminal domain	free and complexed with ssDNA	MF and rSDM	Maciejewski (2000)	435
glucose permease IIA domain	free	MF	Stone (1992)	63
glutathione *S*-transferase, human class Mu (GSTM2-2)	free and bound to substrate, product, or inhibitor	MF	McCallum (2000)	436
hepatitis C virus N53 protein, helicase subdomain 2	free	MF	Liu (2001)	437
lipoate-dependent H protein of glycine decarboxylase complex	methylamine-loaded, oxidized and apoprotein	MF	Guilhaudis (1999)	438
lysozyme (equine)	chimera with D-helix of lysozyme substituted by fluctuating loop of α-lactalbumin	MF	Tada (2002)	300
lysozyme (hen)	wild-type and R14, H15 deletion mutant, free and ligand-bound	MF	Mine (1999)	126
lysozyme (hen)	free	MF	Buck (1995)	439
lysozyme (hen)	partially folded form	MF and rSDM	Buck (1996)	440
lysozyme (human)	free and $(NAG)_3$-bound	MF	Mine (2000)	127
lysozyme, T70N (human)	free	MF	Johnson (2005)	441
lysozyme (T4)	wild-type and L99A core cavity mutant	MF	Mulder (2000)	173
metallo-β-lactamase	free and inhibitor-bound	MF	Huntley (2000)	120
onconase	M1, Q1, M23L mutant and E1S mutant	MF	Gorbatyuk (2004)	442

Table 10 (Continued)

protein	form(s)	method of analysis[c]	first author (year)	ref
	Other Enzymes (Continued)			
orotidine 5′-monophosphate synthase	free	MF	Wang (1999)	443
phosphoglycerate mutase	free	MF	Uhrinova (2001)	444
$\gamma\delta$-resolvase, catalytic domain	free	rSDM	Pan (2001)	445
superoxide dismutase	monomeric, copper-free	MF	Banci (2002)	446
superoxide dismutase (copper−zinc), G93A mutant	free	MF	Shipp (2003)	447
thiopurine methyltransferase, N-terminal deletion mutant	free and bound to an *S*-adenosyl-methionine analogue	MF	Scheuermann (2004)	448
xylanase	native and catalytically competent covalent glycosyl-enzyme intermediate states	MF	Connelly (2000)	449
	Other Proteins			
α_2D, de novo designed dimeric four-helix bundle	free	MF and rSDM	Hill (2000)	450
α_3D, de novo designed three-helix bundle	free	MF	Walsh (2001)	451
actin severing and bundling protein villin, domain 14T	free	MF and rSDM	Markus (1996)	452
AFP1, anti-fungal chitin-binding protein	free	MF	Campos-Olivas (2001)	453
albumin-binding partner PAB, second GA module	free	MF and rSDM	Johansson (2002)	263
α-helical peptide	free	MF and anisotropic diffusion model	Idiyatullin (2000)	454
α-helical peptide	free	MF, SDM, and other models	Mayo (2000)	455
antifreeze glycoprotein fractions 1−5	free	MF	Lane (2000)	456
antifreeze protein	free	MF	Daley (2002)	457
antifreeze protein from spruce budworm	free, at 30 and 5 °C	rSDM	Graether (2003)	458
apolipoprotein E, residues 126−183	in trifluoroethanol	rSDM	Raussens (2002)	459
barstar	C40/82A mutant	MF and rSDM	Wong (1997)	460
barstar	free	MF and rSDM	Sahu (2000)	461
β-hairpin peptide	free	specific motional models	Ramirez-Alvarado (1998)	462
cardiotoxin II from Taiwan cobra	free	MF	Lee (1998)	463
catabolite repression HPr-like protein Crh (*Bacillus subtilis*)	free	MF	Favier (2002)	464
CBFβ/PEP2β (Runx protein partner)	free	MF	Wolf-Watz (2001)	465
chemotaxis protein CheW	free	MF	Griswold (2002)	466
colicin E9 protein toxin (intact)	free	rSDM	MacDonald (2004)	467
colicin E9 (residues 1−61)-E9 DNase fusion protein	free	MF and rSDM	MacDonald (2004)	467
Ω-conotoxin MVIIA precursor	free	MF	Goldenberg (2001)	468
dynein light chain DLC8	free and bound to peptide Bim_L	MF	Fan (2002)	469
dynein light chain km23	homodimeric	MF	Ilangovan (2005)	470
green fluorescent protein	free	rSDM	Seifert (2003)	471
hemolymph protein from mealworm beetle	free	MF	Rothemund (1997)	472
HIV-1 gp41 envelope glycoprotein, N-terminal domain	micelles	MF	Jaroniec (2005)	473
human T-cell leukemia virus type-I capsid protein, N-terminal domain	free	MF	Cornilescu (2003)	474
human T-cell leukemia virus type-I capsid protein, N-terminal domain	D54A mutant	MF	Bouamr (2005)	475
LDL receptor, fifth and sixth A-module repeats (LR5, LR6)	individual modules LR5 and LR6 and the module pair LR5-6	rSDM	Beglova (2001)	476
low-density lipoprotein receptor	containing EGF-A or EGF-AB	MF	Kurniawan (2001)	477
major coat protein (gVIIIp) of filamentous bacteriophage M13	solubilized in detergent micelles	MF and rSDM	Papavoine (1997)	478
major coat protein from filamentous bacteriophage IKe	micelles	MF	Williams (1996)	479
mature T-cell proliferation factor-1, C12A mutant	C12A mutant	rSDM	Barthe (1999)	480
melittin	random coil monomer, helical monomer, tetramer	MF	Kemple (1997)	481
monellin, single-chain variant	double mutant	MF	Sung (2001)	482
olfactory marker protein	free	MF	Gitti (2005)	483
outer surface protein A	free	MF	Pawley (2002)	154
PAK pilin peptide	free	MF and rSDM	Campbell (2000)	484
PAK pilin peptide	free and bound to antibody Fab fragment	MF and rSDM	Campbell (2003)	485
pilin N-terminally truncated monomer	free	MF	Suh (2001)	486
polyomavirus T antigens, J domain	free	MF	Berjanskii (2002)	487
prion protein (PrP), residues 29−231	free	MF	Viles (2001)	488
prion protein (PrP), residues 90−231	free	MF	Viles (2001)	488

Table 10 (Continued)

protein	form(s)	method of analysis[c]	first author (year)	ref
	Other Proteins (Continued)			
rous sarcoma virus, retroviral M Domain	free	MF	McDonnell (1998)	489
SopE2 guanine nucleotide exchange factor (residues 69−240) (*Salmonella*)	free	MF	Williams (2004)	490
sporulation protein Spo0F	free	MF	Feher (1997)	491
thermostable protein Sso7d	free	MF	Allard (1997)	492
thrombomodulin, fourth and fifth epidermal growth factor-like domains	free	rSDM	Prieto (2005)	493
toxin α	free	MF	Guenneugues (1999)	494
transcription elongation factor elongin C (*Saccharomyces cerevisiae*)	bound to peptide	MF and rSDM	Botuyan (2001)	495
villin headpiece domain, helical subdomain HP36	free	MF	Vugmeyster (2002)	103
villin headpiece domain, helical subdomain HP67	wild type and H41Y mutant	MF	Grey (2006)	496
zervamicin IIB, channel-forming peptide antibiotic	free	MF	Korzhnev (2001)	497

[a] This table includes studies in which backbone (NH or $C_\alpha H$) dynamical parameters have been calculated from relaxation data, but does not include studies in which one or more relaxation parameter(s) has/have been reported without the subsequent calculation of dynamics parameters. [b] Although we have endeavored to make this table comprehensive up to December 2005, there may be studies that have been accidentally omitted. In such cases, we invite readers to e-mail additional table entries to be published as an addendum. [c] Abbreviations used for methods of analysis: MF, model-free; rSDM, reduced spectral density mapping; fSDM, full spectral density mapping; SRLS, slowly relaxing local structure approach; GNM, Gaussian network model.

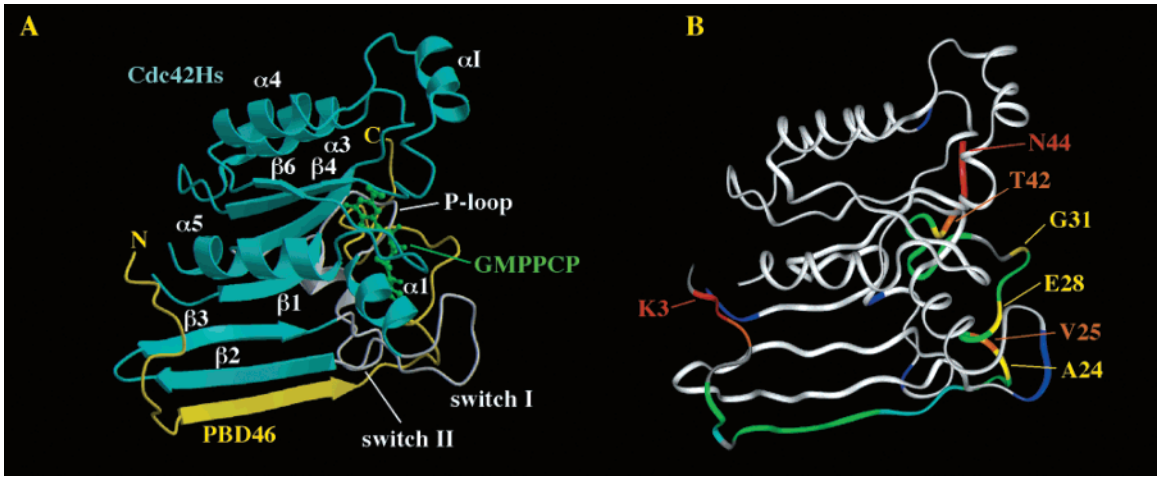

Figure 8. (A) NMR structure of the Cdc42Hs·GMPPCP−PBD46 complex showing the secondary structures of both Cdc42Hs (cyan) and PBD46 (yellow). Switch I, switch II, and the P loop are shown in white, and GMPPCP is shown in green. The regions that appear to undergo mutual induced fit are the β2-strand (cyan ribbon) of Cdc42Hs and the antiparallel β-strand (yellow ribbon) of PBD46, whereas the switch I region (gray unstructured region) and the adjacent region of the peptide (yellow unstructured region) both remain mobile in the complex. Reprinted with permission from ref 107. Copyright 2001 American Chemical Society. (B) Ribbon structure colored according to the order parameters: blue, residues of Cdc42Hs that have S^2 values below 0.8; cyan, residues of PBD46 that have S^2 values above 0.8; green, residues of PBD46 that have S^2 values below 0.8 and above 0.6; yellow, residues of PBD46 that have S^2 values below 0.6 and above 0.4; orange, residues of PBD46 that have S^2 values below 0.4 and above 0.2; red, residues of PBD46 that have S^2 values below 0.2. Residues for which S^2 has not been determined are shown in gray. Reprinted with permission from ref 107. Copyright 2001 American Chemical Society.

tion of the protein undergoes a reduction in flexibility upon binding.[105−111] In other cases, the reduction in dynamics is limited to confined regions of the protein,[112,113] often those surrounding the ligand-binding site.[114−120]

One issue in characterizing induced fit binding is whether one component acts as a template for structural rearrangement of the second component or whether each binding partner becomes substantially more rigid during association, a situation we refer to as "mutual induced fit". One example of the latter that has been characterized using NMR relaxation methods is the interaction between the GTPase Cdc42Hs and an effector peptide (PBD46), derived from the dimerization domain of p21-activated serine/threonine kinase 1.[107,118] Upon binding the peptide, Cdc42Hs exhibited decreased flexibility, specifically in the β2 strand, which comprises part of the PBD46 binding site (Figure 8). During formation of the same interaction the PBD46 peptide also displayed a decrease in flexibility in a region that forms an antiparallel β-sheet with the β2 strand of Cdc42Hs (Figure 8). It is particularly interesting that the switch I region (the loop region between the α1 helix and β2 strand) remains highly flexible upon complex formation and that the segment of the peptide that this loop contacts also maintains high flexibility. These results indicated that there is mutual induced fit between one region of Cdc42Hs and its partner in the PBD46 peptide but that the interactions between another pair of elements are apparently insufficient to limit the flexibility of either partner.

Our comparative dynamics study of the three eotaxin group chemokines has also provided indirect evidence for mutual induced fit with their shared receptor CCR3. The transduction of signals across the cell membrane by chemokine receptors (and also other G protein-coupled receptors) is thought to require a conformational change of the receptor induced by ligand binding. We found that receptor-binding regions of all three chemokines are highly flexible, suggesting that they also undergo induced fit to the receptor during their binding events.[167−169]

Increases in Flexibility Induced by Ligand Binding. Despite the conventional view of binding in terms of induced-fit interactions governed by enthalpy−entropy compensation, several dynamics studies have indicated regions of proteins whose flexibility actually increases upon ligand binding. In some instances significant increases in the flexibility of specific groups were noted despite general reductions in backbone motion.[115,121,122] In other cases, ligand binding appears to induce compensatory changes in backbone flexibility with little change in protein flexibility overall.[67,123−128] Among these studies some have indicated, rather surprisingly, that residues with increased flexibility were located at the ligand binding site. Kay and co-workers investigated the backbone dynamics of the C-terminal SH2 domain of phospholipase Cγ1 and found overall similar trends in order parameters between the free and peptide-bound forms of the protein, yet increased flexibility of residues at the hydrophobic peptide-binding site upon complex formation.[67] Similarly, in a study of the dimerization/docking domain of protein kinase A, Fayos and co-workers observed similar average order parameters between free and peptide-bound forms, but found decreased order parameters for >20 residues upon complex formation, many of which are located in the hydrophobic peptide-binding groove (Figure 9a).[128] In an earlier study of binding between a hydrophobic pheromone and a mouse urinary protein, we also observed increased flexibility of the hydrophobic binding pocket.[130] We speculated that the replacement of ordered water in the binding pocket with the hydrophobic groups from the ligand might reduce the structural constraints in the binding pocket, giving rise to an increase in flexibility and a favorable change in conformational entropy. Because peptide binding by the SH2 domain and the PKA dimerization/docking domain also involve hydrophobic surfaces, the increases in dynamics in these systems could be influenced by a similar mechanism.

A growing number of dynamics studies have noted widespread rather than localized increases in flexibility upon ligand binding.[129−135] In an interesting recent example, Arumugam and colleagues examined the backbone dynamics of the N-terminal domain of tissue inhibitor of metalloproteinases 1 (N-TIMP-1) upon binding stromelysin-1 (MMP-3).[134] Although the interaction occurs with nanomolar affinity, it is enthalpically unfavorable ($\Delta H = 6.5$ kcal/mol) and therefore entropy-driven. The NMR data indicated that binding induces a rigidification of residues within the MMP-binding ridge of N-TIMP-1, but that remote regions within the β-barrel core of N-TIMP-1 become more flexible upon binding of MMP-3 (Figure 9b). The changes in backbone amide bond flexibility contribute an estimated −10.2 kcal mol^{-1} to the change in conformational free energy (entropy) upon ligand binding, a substantial contribution to the binding free energy. Thus, the N-TIMP-1:MMP-3 interaction is a unique example of how a high-affinity interaction between two proteins can be driven by binding-induced, remote increases in backbone flexibility within the core of a protein.

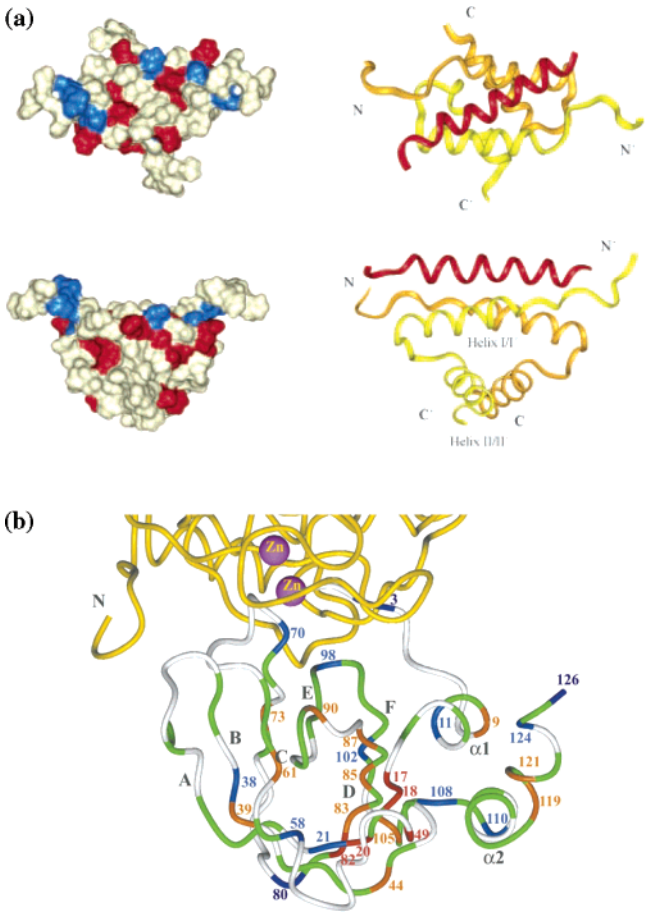

Figure 9. Two proteins in which increases in backbone dynamics occur at a ligand binding site. (a) Space-filling representation (left) and ribbon structure (right) of the dimerization/docking domain of protein kinase A bound to the prototype anchoring protein $HT31_{pep}$. The right panel shows the two monomeric units of the dimerization/docking domain (yellow and orange) and the peptide ($HT31_{pep}$) derived from the human thyroid anchoring protein Ht31 in red. The left panel highlights the residues that undergo increases (red) and decreases (blue) in backbone flexibility upon binding to $HT31_{pep}$. Reprinted with permission from ref 128. Copyright 2003 The American Society for Biochemistry and Molecular Biology. (b) Complex between MMP-3 (yellow) and N-TIMP-1, showing the changes in order parameters of N-TIMP-1 upon binding, color coded as follows (where negative values of ΔS^2 indicate an increase in flexibility upon binding): red, $\Delta S^2 \leq -0.1$; orange, $-0.1 < \Delta S^2 \leq -0.05$; green, $-0.05 < \Delta S^2 < 0.05$; blue, $0.05 \leq \Delta S^2 < 0.1$; dark blue, $\Delta S^2 \geq 0.1$. Reprinted with permission from *Journal of Molecular Biology 237* (3), 719−734 (Arumugam et al., Increased Backbone Mobility in β-Barrel Enhances Entropy Gain Driving Binding of N-TIMP-1 to MMP-3). Copyright 2003 Elsevier.

Relevance of Dynamics to Binding Cooperativity. In certain cases binding of a ligand can induce changes in the flexibility of a protein not only at the binding site but also at more distant positions in the protein structure. Section 5.4 is devoted to a discussion of these long-range effects. One special case is the situation in which the remote site is also a binding site for a second ligand. In this case, the change in dynamics induced by the first ligand could affect the affinity of the protein for the second ligand, that is, the cooperativity of binding. The best characterized case of this phenomenon is that of calbindin D_{9k}, in which binding of one calcium ion reduces the flexibility of both the first and second calcium-binding sites.[136,137,170] This example is dis-

cussed in more detail in the section on long-range effects (section 5.4).

Ligand Specificity and Drug Design. Many protein dynamics studies have found flexible regions close to ligand-binding sites, often leading to the speculation that the flexibility is required for the active site to undergo induced fit to different ligands. In this sense, active site dynamics can relax the ligand specificity of a protein, with important consequences not only for the biological activity of the protein but also for the development of drugs that target the flexible active site. Support for this proposal can be obtained by measuring the dynamics of the protein in the presence of a ligand or, preferably, more than one ligand.

One class of proteins for which dynamics could potentially influence binding specificity is nucleic acid-binding proteins[139−141] because these proteins often bind with measurable affinity even to noncognate nucleic acid sequences. To investigate the importance of dynamics in cognate versus noncognate sequence recognition, Cave and colleagues studied the changes in dynamics of the basic helix−loop−helix domain of the yeast transcription factor Pho4 upon binding to either nonspecific or cognate DNA.[140] Although the DNA-binding basic region of Pho4 is a random coil in the absence of DNA, both cognate and nonspecific DNA induced a transition to a helical structure and resulted in almost identical secondary structure characteristics as well as fast backbone dynamics parameters. On the other hand, the nonspecifically bound Pho4−DNA complex exhibited line-broadening for residues within the basic region, apparently because these residues were sampling multiple base pair environments. The similarities between the sub-nanosecond time scale backbone dynamics of nonspecifically and cognate-bound Pho4−DNA complexes led the authors to conclude that preferential binding to the cognate sequence is not substantially influenced by fast backbone dynamics, although fast side chain motions could still play a role. In light of the above discussion of induced fit binding, it is interesting that the backbone of Pho4 is restricted to a similar extent (on the fast time scale) when binding to both nonspecific and cognate DNA. It appears that the restricted motions of the backbone either are intrinsic to the folded state of the domain or are imposed by interactions with both cognate and noncognate base pairs.

Several groups have addressed the relationship between specificity and backbone dynamics in hydrolytic enzymes. Davis and Agard determined the backbone dynamics of α-lytic protease (αLP) both free and bound to the transition state analogue inhibitor, *N-tert*-butyloxycarbonyl-Ala-Pro-boroVal (Boc-Ala-Pro-BVal).[142] αLP is specific for single, small hydrophobic residues at the cleavage position, but has broad specificity for residues contacting other regions of the binding pocket. Inhibitor binding did not substantially affect the fast time scale motions of αLP but caused a reduction in chemical exchange processes on a slow time scale, particularly in regions of the binding pocket. The results suggested that the enzyme may also undergo induced fit binding to substrates (or even to the transition state during the catalytic mechanism), possibly providing an explanation for the low substrate specificity away from the cleavage position.

Although the αLP study indicated that slow time scale motions are most important in the response of active site dynamics to inhibitor binding, a more recent study of a metallo-β-lactamase from *Bacillus fragilis* has suggested a role for backbone dynamics on the sub-nanosecond time scale. Upon inhibitor binding, amide group order parameters decreased slightly and internal correlation times decreased more dramatically in both the major and minor active-site loops (Figure 10), indicating that these active site elements are less restricted and move at higher frequencies in the bound state. [120] The observed plasticity of the active site led Huntley et al. to propose that the low specificity of this enzyme is related to its ability to mold its active site to a variety of different substrates. Therefore, they suggested that derivatization of β-lactam-based antibiotics is likely to be a relatively ineffective means of fighting antibiotic resistance mediated by metallo-β-lactamases; instead, targeted development of more effective β-lactamase inhibitors may be a more successful approach.

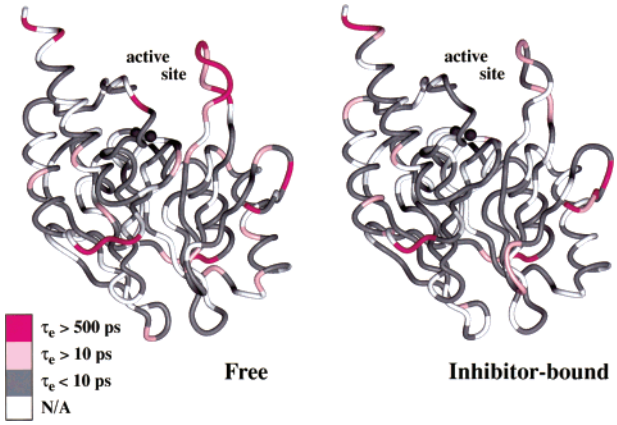

Figure 10. Structures of the free and inhibitor-bound forms of the *B. fragilis* metallo-β-lactamase color-coded according to measured τ_e values as indicated in the color bar. Note the faster motions (less pink color) in the major (right) and minor (left) active site loops upon inhibitor binding. Reprinted with permission from ref 120. Copyright 2000 American Chemical Society.

Another example in which the analysis of fast backbone dynamics has provided information relevant to both binding specificity and drug design is the study of the matrix metalloproteinase (MMP) stromelysin, which degrades protein components of connective tissue. The catalytic domain of stromelysin, in particular, has been used as a target in the design of MMP inhibitors to be used as drugs for treating arthritis, cancer metastasis, connective tissue disorders, and other disease states exhibiting overexpression of MMPs.[171,172] Yuan et al. have examined the backbone dynamics of stromelysin bound to three different inhibitors.[124] One inhibitor binds to the $S_1'-S_3'$ subsites or right side of the enzyme's active site and the other two bind to the S_1-S_3 subsites or left side of the active site. The apo form of stromelysin was not directly accessible, so dynamics parameters measured for residues in the empty side of each inhibitor-bound complex were used to gauge the response of amide group motion to inhibitor binding, under the assumption that the S_1-S_3 and S_1'-S_3' subsites are independent. Inhibitor binding to the S_1-S_3 subsites had relatively little effect upon backbone dynamics; both the free and inhibitor-bound complexes are rigid in this region. However, inhibitor binding to the $S_1'-S_3'$ subsites resulted in a loss of flexibility for active site residues combined with an increase in flexibility of some surface residues. Interestingly, the majority of MMP inhibitors bind to the S_1'-S_3' subsites. Thus, the authors proposed that the ability of the S_1'-S_3' subsites to undergo induced fit binding allows them to accommodate a broader range of inhibitors, whereas the rigidity of the S_1-

S_3 subsites in both the free and bound forms may prevent such accommodation and impose greater binding specificity. Consequently, they suggested that future efforts to design broadly active inhibitors of MMPs should be targeted against the S_1'-S_3' subsites.

4.3 Effects of Mutations

A number of groups have examined the effects of mutation upon protein dynamics in attempts to elucidate the roles of internal motions in regulating the stabilities and/or functions of the proteins. The general approach has been to select mutants that are known to cause changes in stability, binding affinity, or other functional characteristics and then to compare the dynamics of these mutants with those of the wild-type proteins. As discussed below, this approach has provided some interesting insights into the possible significance of fast internal motions. However, a fundamental difficulty with the approach is that it is extremely difficult to introduce mutations that affect the fast time scale dynamics without also changing the average structure, the structural ensemble, and/or the slow conformational dynamics of the protein. Therefore, it is important to carefully select mutants that cause minimal structural perturbations. In addition, it is advantageous to study several mutants and to correlate the dynamics with the stability or function among the group of mutants.

Comparisons of Dynamics with Stability. We first discuss several studies in which the relationships between backbone dynamics and protein stability have been investigated. One group of studies has addressed the influence of destabilizing core mutations on protein flexibility. Not surprisingly, some of these core mutations result in increased flexibility, presumably reflecting the removal of steric constraints when the wild-type core packing is disrupted. For example, de Lorimier and colleagues found that mutating the thioredoxin core residue Leu-78 to Lys reduced the mean S^2 value from 0.86 to 0.81, thus indicating a global increase in backbone flexibility upon disruption of the hydrophobic core.[143] In a more recent study, Mittermaier and Kay measured backbone and side-chain dynamics for wild-type, F20L, and F20V mutants of the SH3 domain from the Fyn tyrosine kinase.[144] They found that both mutations increased protein flexibility and that the magnitude of the increase correlated with the reduction in side-chain volume of the mutated residue, underscoring the influence of steric interactions on the internal dynamics of protein cores. In contrast, the Goldenberg group found a more complex influence of core mutations on dynamics in the bovine pancreatic trypsin inhibitor (BPTI). They studied seven mutants, each with a single mutation at one of five different sites within the core.[145,146] Although these mutations destabilized the protein by approximately 3−8 kcal/mol, they were found to have a negligible effect on the fast time scale dynamics of BPTI. Instead, four of the mutants, representing two positions within the protein, exhibited increased conformational exchange on the slow (microsecond−millisecond) time scale compared with the wild-type protein and the remaining three mutants, suggesting the stability differences might be influenced by a redistribution of conformers within the structural ensemble of the protein. Similarly, Mulder and co-workers found that the cavity-forming mutation L99A in T4 lysozyme also resulted in extensive motion on a microsecond−millisecond time scale, although picosecond−nanosecond time scale motions were unaffected by this mutation.[173]

Considering that core mutations are often disruptive to the structure as well as the dynamics of the protein, it is possible that correlations between dynamics and stability will be easier to observe when mutations are made on the surface of the protein. In this light, we and our colleagues have determined both the backbone and side-chain methyl dynamics of 10 surface mutants of the B1 domain from streptococcal protein G.[147,148,174] These mutants were all identical except for a single residue located on the solvent-exposed surface of a β-sheet, yet they were previously known to vary in stability over a 2.2 kcal/mol range.[175] Although both backbone and side-chain conformational entropy values estimated from NMR-derived order parameters varied substantially among the 10 mutants (ranges of ~4.1 and 4.5 kcal/mol, respectively), these entropy estimates did not correlate with the global stabilities of the mutants. The simplest interpretation of these results is that variations in conformational entropy do make a significant contribution to the relative stabilities of the mutants but that, not surprisingly, the overall stability results from the balance between these changes and other thermodynamic factors (in both the folded and unfolded states).

Comparisons of Dynamics with Function. Several studies have compared the backbone dynamics of wild-type and mutant proteins in which the mutation has an influence on function. In one example, a mutational approach was utilized by the Hall group to better understand the role of backbone dynamics in the RNA-binding affinity and specificity of the N-terminal RNA-binding domain (RBD1) from human U1A protein.[149,150] The study was guided by the observation that mutation of three highly conserved amino acids (Y13, Q54, and F56) affects binding affinity and specificity but that these effects are nonadditive, indicating that the mutated residues interact with each other. The Y13F, F56Y, Y13F/F56Y, and Q45E mutants[149] displayed small increases in flexibility for residues throughout the mutant proteins, the most consistent of which were observed for the RNA-recognition element labeled loop 3 (Figure 11A). The changes in dynamics for the loop 3 region in combination with the measured thermodynamic pairwise coupling energies led the authors to propose that local cooperative interactions between the three highly conserved residues are communicated to the nonconserved loop 3 region, thus affecting RNA binding. In a subsequent study, Hall and colleagues used two additional RBD1 mutants (G53A and G53V) to investigate the hypothesis that the conserved residue G53, located between loop 3 and β-strand 3 (Figure 11A), could provide the necessary flexibility to mediate conformational changes of loop 3 upon RNA binding.[150] Although both mutants displayed reduced RNA-binding affinity, NMR dynamics data indicated no significant differences between the backbone dynamics of the two mutant proteins and the wild-type RBD1. Thus, it appeared that the RNA affinities of these latter mutants were not dominated by dynamic changes.

In a different comparison of dynamics with function, Cai and co-workers have utilized two mutants of the *Cucurbita maxima* (potato family) trypsin inhibitor V (CMTI-V) to investigate the relationship of both backbone and side-chain flexibility to proteolytic stability, a critical determinant of protease inhibitor function.[151] In each CMTI-V mutant, one of two arginine residues, R50 or R52, was mutated to alanine, thereby eliminating hydrogen-bonding interactions that tether the protease-binding loop to the protein scaffold (Figure 11B). Replacement of either arginine residue by alanine

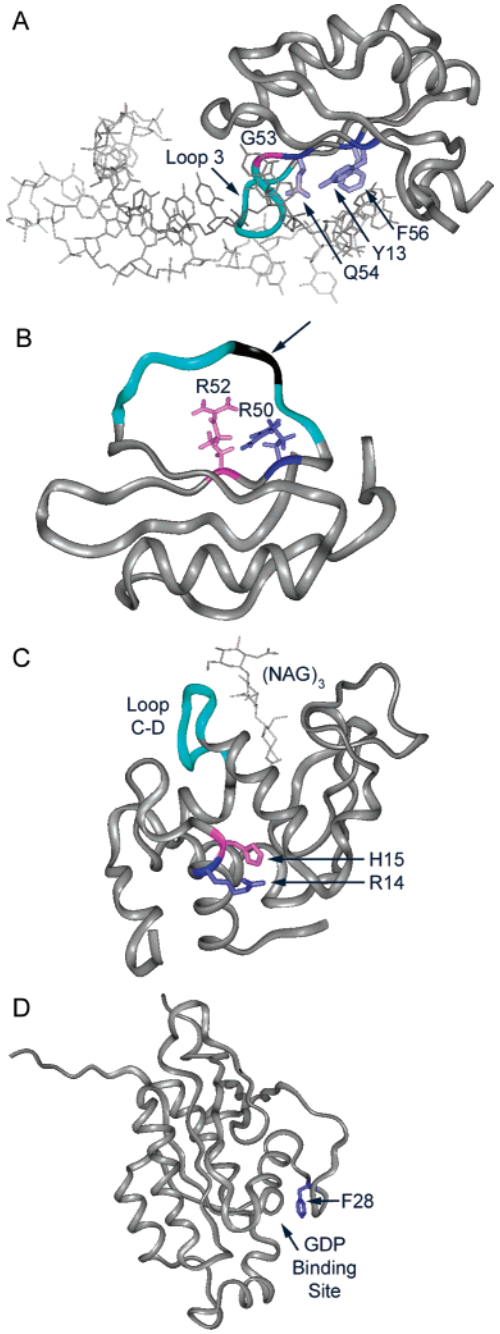

Figure 11. Structures of proteins for which effects of mutations on dynamics and function are discussed. (A) Ribbon structure of the RNA-binding domain 1 (RBD1) of the human UlA protein (PDB file 1URN) complexed with RNA. Residues Y13, Q54, and F56 are blue, and their side chains are displayed in stick representation. Residue G53 is magenta. Loop 3 (residues 46−52) is cyan. RNA is gray and displayed in stick representation. (B) Ribbon diagram of *Curcurbita maxima* trypsin inhibitor V (PDB file 1MIT). Residues R50 and R52 are blue and magenta, respectively, and their side chains are displayed in stick representation. The protease binding loop (residues 39−47) that contains residues that make hydrogen-bonding interactions with R50 and R52 is cyan. The arrow indicates the scissile peptide bond between residues K44 and D45, colored black. (C) Ribbon diagram of hen egg white lysozyme, complexed with tri-*N*-acetyl-chitotrioside [$(NAG)_3$] (PDB file 1HEW). Residues R14 and H15 are blue and magenta, respectively, and their side chains are displayed in stick representation. Loop C−D (residues 100−107) is cyan. $(NAG)_3$ is gray and displayed in stick representation. (D) Ribbon structure of Cdc42Hs·GDP complex (PDB file 1AJE). Residue F28 is blue, and its side chain is displayed in stick representation. The GDP binding site is indicated.

resulted in a decreased stability of CMTI-V toward trypsin proteolysis and hence a reduced inhibitory effect. As anticipated, both mutations caused decreased order parameters and increased flexibility of binding loop residues, reflecting the loss of the anchoring hydrogen bonds. However, the R52A-CMTI-V mutant displayed a slight decrease in the mean S^2 value for the N-terminal portion of the binding loop (residues 39−47), whereas the R50A-CMTI-V mutant exhibited decreases in S^2 value for the entire binding loop, with a dramatic decrease of approximately 0.3 in the mean S^2 values for the C-terminal portion of the loop (residues 45−47). Kinetic data indicated a lower activation free energy barrier of specific hydrolysis for the R50A versus R52A mutant, and thermodynamic studies showed that R50A was destabilized by 1.7 kcal mol^{-1} more than R52A relative to wild-type CMTI-V. Collectively, the dynamics, kinetic, and thermodynamics data led Cai and colleagues to propose that although both arginine residues were required for optimal inhibitory stability and function, mutating R50 not only removes the R50 hydrogen bond but also results in a loss of the R52 hydrogen bond. Thus, the R50 mutation causes a greater increase in flexibility of the binding loop than the R52 mutation, and this increase accounts for the larger decrease of inhibitor stability in the R50 mutant.

In addition to influencing the activity of enzyme inhibitors, dynamics could potentially influence the catalytic activity of enzymes themselves (see section 2.3). Here we discuss two enzymes in which this possibility has been investigated using enzyme mutants, the glycosidase lysozyme and the GTPase Cdc42Hs. For the case of hen lysozyme, the backbone dynamics of a deletion mutant were compared to the dynamics of the wild-type protein in both free and *N*-acetylglucosamine [$(NAG)_3$] substrate analogue-bound forms.[126] The mutant, in which residues R14 and H15 were deleted together (Figure 11C), has a higher activity against glycol chitin and a decreased stability compared with wild-type lysozyme. In the uncomplexed state, backbone dynamics parameters of the wild-type and mutant proteins exhibited no significant differences. However, in complex with the substrate analogue the mutant protein displayed a more significant increase in internal mobility on a fast time scale compared with the wild-type protein. Furthermore, a greater number of residues in the mutant complex exhibited increases in conformational exchange contributions, including residues in the functionally important loop C−D region (Figure 11C). One explanation of the increased conformational exchange terms is that the mutant protein can populate a particular minor conformation to a greater extent than the wild-type protein can populate this conformation. This minor form might represent the catalytic conformation, providing an explanation for the increased catalytic efficiency of the complex. Interestingly, Mine et al. proposed that the increased fast time scale motions of the mutant protein enable the mutant to overcome an enthalpic penalty associated with populating the active conformation. Thus, it is possible that both the fast and slow motions play a role in regulating the enzymatic activity.

An interesting recent study examined the possibility that internal protein motion influences the signaling function of Cdc42Hs, a GTP-binding signal transduction protein and member of the Ras superfamily.[152] Introduction of the F28L mutation into Cdc42Hs (Figure 11D) destabilizes the interaction with guanine nucleotides and increases GTP−GDP exchange leading to cell transformation.[176] Adams and

colleagues measured backbone dynamics parameters for the GDP-bound (inactive) forms of wild-type Cdc42Hs and the F28L mutant.[118,152] The mutant displayed increased flexibility relative to the wild-type protein at residue 28 itself, in addition to increased motion within the loops comprising the nucleotide-binding site. On the whole, however, the order parameter profile remained quite similar between wild-type and mutant proteins, suggesting that increased GDP cycling of the F28L mutant is related, at least in part, to confined dynamic effects and leading the authors to conclude that local changes in flexibility of a ligand-binding region can alter entire signaling processes of a protein. Considering the importance of related GTPases in numerous signaling pathways, this result may have rather widespread significance.

In summary, although the functional role of backbone dynamics remains obscure for many proteins, careful comparisons between the functional and dynamical properties of protein mutants are beginning to reveal influences of dynamics on binding affinity and specificity, protein stability, and catalytic function. These initial results should encourage future investigations in other systems.

4.4 Effects of Temperature and Pressure

Although most previous studies of backbone dynamics have been conducted at a single temperature and pressure, there have now been several investigations into how these physical parameters influence fast protein motions. As discussed in section 3.7, the temperature dependence of order parameters can be interpreted in terms of the conformational heat capacity ($C_{p,\mathrm{conf}}$) of the protein. Both protein unfolding and many binding events are accompanied by substantial changes in the heat capacity of the system. In general, the major contribution to these changes is the hydrophobic effect; burial of hydrophobic surface area releases ordered water from these surfaces, giving rise to negative heat capacity changes. However, changes in the intrinsic motional landscape of the protein could also contribute to heat capacity changes. Studying the temperature dependence of internal dynamics may provide important insights in this regard.

As temperature is increased the internal motions of proteins also increase. The magnitude of this increase can be expressed in terms of either the conformational heat capacity ($C_{p,\mathrm{conf}}$) or a characteristic temperature (T^*), with $C_{p,\mathrm{conf}}$ and T^* being inversely related (see section 3.7). For the sake of consistency, the following discussion is stated in terms of $C_{p,\mathrm{conf}}$, even in cases for which the original analysis was presented with respect to T^* calculations.

Relationship between Conformational Heat Capacity and Protein Stability. The free energy of protein unfolding is related to the unfolding enthalpy (ΔH_{ref}) and entropy (ΔS_{ref}) at some reference temperature (T_{ref}) and the heat capacity of unfolding (ΔC_p, assumed to be independent of temperature) by the equation[96]

$$\Delta G = \Delta H_{\mathrm{ref}} - T\Delta S_{\mathrm{ref}} + \Delta C_p[T - T_{\mathrm{ref}} - T\ln(T/T_{\mathrm{ref}})] \quad (41)$$

The unfolding of proteins is typically accompanied by an increase in heat capacity that is approximately proportional to the nonpolar surface area exposed upon unfolding.[97] Consequently, the unfolding free energy profile has a downward curve as shown in Figure 12. Decreased values of ΔC_p reduce the curvature of the free energy profile, leading to high stability at both high and low temperatures, that is, increased melting temperatures (T_{m}) and decreased cold denaturation temperatures (T_{c}).

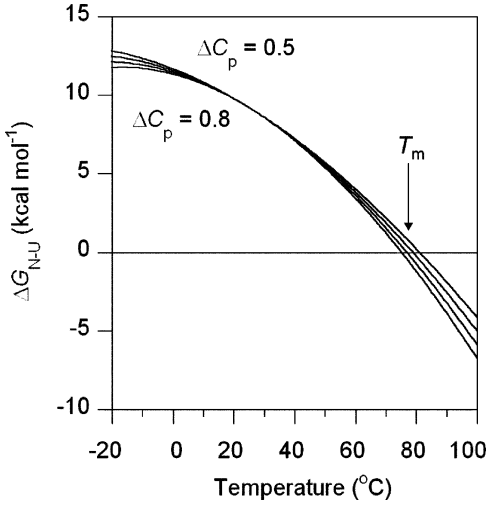

Figure 12. Simulations showing the relationship between $\Delta G_{\mathrm{N-U}}$ and temperature (°C) for varying ΔC_p values. $\Delta G_{\mathrm{N-U}}$ values were simulated using eq 41 and values of $\Delta H = 45$ kcal mol^{-1} and $\Delta S = 120$ cal K^{-1} mol^{-1} at a reference temperature of 25 °C; ΔC_p values are 0.5 (top), 0.6, 0.7, and 0.8 (bottom).

Palmer and colleague's study of the backbone dynamics of *E. coli* ribonuclease H (RNase H) at 12, 27, and 37 °C was the first NMR dynamics study to examine the effects of temperature upon fast protein internal motions.[102] In this study, order parameters and conformational exchange terms both decreased with increasing temperature, whereas internal correlation times remained invariant to changes in temperature. The magnitudes of changes in order parameters were observed to be structure-dependent, with the apparent conformational heat capacities decreasing in the order C terminus > loops > secondary structure. In a subsequent backbone dynamics study of the Ca^{2+}-saturated E140Q mutant of the C-terminal domain of calmodulin, Evenas and colleagues also observed that apparent conformational heat capacities were significantly lower in well-ordered regions and elements of secondary structure elements compared with flexible regions such as the termini and loops.[101] Spyracopoulos et al. have noted similar weak temperature dependencies of order parameters and low heat capacities for regions of secondary structure in the protein troponin C.[153] Two further examples of this trend were observed by Yang and co-workers, who examined the temperature dependence of order parameters for both folded and unfolded states of staphylococcal nuclease (SNase) and the N-terminal SH3 domain from drk (drkN SH3).[100] Both proteins exhibited considerably smaller backbone conformational heat capacities in the folded state compared with unfolded state. All of these studies indicate that the conformational heat capacities of folded proteins are lower than those of the unfolded states. Thus, the increase in conformational heat capacity upon unfolding makes some contribution to the total positive heat capacity change, increasing the curvature of the free energy profile and limiting the stability of the protein at extreme temperatures (Figure 12).

In contrast to the above cases, there have now been several observations of proteins in which the apparent conformational heat capacities of secondary structure regions are comparable to those of loops and termini. Our laboratory analyzed the dynamics of a small (56 residue), thermostable ($T_{\mathrm{m}} \sim 89$

°C) globular protein, the B1 domain of protein G, at six temperatures over the range from 0 to 50 °C.[72] Secondary structure elements as well as loops and termini exhibited heat capacity values similar to those measured in unstructured regions of RNase H, SNase, and drkN SH3. Subsequently, Vugmeyster and co-workers examined the backbone dynamics of the thermostable helical subdomain, HP36, from the F-actin-binding headpiece domain of chicken villin, at five temperatures ranging from 2 to 32 °C, finding that the heat capacity was near maximal in the folded state.[103] Finally, Pawley and colleagues studied the temperature dependence of backbone dynamics in outer surface protein A (OspA) from the Lyme disease bacterium *Borrelia burgdorferi*.[154] Again, they observed high conformational heat capacities in this folded protein, including in the unique single-layer β-sheet structure of OspA. The high conformational heat capacities in the folded states of these three proteins will tend to minimize the ΔC_p values for protein unfolding. Consequently, the stability profiles will have decreased curvature, leading to stabilization of these domains at extreme temperatures. Therefore, one possible strategy to attain high thermal stability is evolution of a structure that has a high intrinsic conformational heat capacity, that is, that can accommodate increased thermal fluctuations without substantial disruption of the native fold. In this situation, increasing the temperature leads to an increase in the conformational entropy of the native state, hence stabilizing the native state relative to a protein with lower conformational heat capacity.

Despite the above suggestions that conformational heat capacity contributes to overall protein stability, it is important to point out that the motions observed in these studies of backbone $^{15}N-^{1}H$ amide bond vectors represent only one aspect of the conformational heat capacity in proteins. For example, in a study of a calmodulin bound to a peptide from myosin light chain kinase over the temperature range of 15−73 °C,[155] Lee and co-workers found that the sensitivity of backbone amide order parameters to temperature was substantially smaller and less variable than the sensitivity of side-chain methyl group order parameters. Furthermore, in a comparison between backbone dynamics as probed through measurements of $^{15}N-^{1}H$ amide and $^{13}CO-^{13}C_\alpha$ bond vector relaxation, Wang and colleagues found that $^{15}N-^{1}H$ vector order parameters decreased by ~2.5% over a temperature range of 5−30 °C, whereas $^{13}CO-^{13}C_\alpha$ vector S^2 values decreased by 10% over the same temperature range.[95] The authors concluded that protein backbone motions activated at room temperature are not always sensed by the amide bond vector, and additional NMR relaxation experiments are necessary for a more complete estimation of protein backbone motions. Clearly, additional temperature variation studies are needed to explore the conformational heat capacities of proteins in more detail.

Activation Energies for Fast Internal Motions. In an interesting recent study, Idiyatullin et al. investigated the temperature dependence of both order parameters and internal correlation times in the B1 domain from protein G in the range of 5−50 °C.[156] An internal motional activation energy, E_i, for each amide bond vector was derived from the temperature dependence of the internal correlation time. Residues with the highest E_i values were all involved in hydrogen bonding and were concentrated in one region of the protein, generally facing toward the hydrophobic core. The conformational heat capacities obtained in this study were slightly higher than those reported previously for the same protein,[72] but discrepancies were attributed to an increase in the number of relaxation parameters acquired and the use of different approaches to analyze relaxation data. Nevertheless, both studies agreed that the heat capacities of secondary structure regions were high in comparison to the early studies discussed above. Interestingly, heat capacity values were found to correlate with amide bond activation energies and both C_p and E_i values correlated with the free energies for transient exposure of NH groups within the folded B1 domain, derived from H−D exchange measurements. These observations suggested that the response of the fast time scale motions to temperature may be related to the mechanism that dictates opening of NH group hydrogen bonds and H−D exchange, even though the latter occur on a much slower macroscopic time scale.

Relationship between Conformational Heat Capacity and Ligand Binding. Although most temperature variation studies of protein dynamics have focused on only one form of the protein, usually the unligated form, two recent studies have investigated whether conformational heat capacity changes upon ligand binding. The potential importance of conformational heat capacity in controlling ligand binding is analogous to its role in dictating protein folding (eq 41 and Figure 12). A decrease in the heat capacity term upon binding would tend to destabilize the complex at extreme temperatures. Kovrigin and co-workers characterized the temperature dependence of the backbone dynamics of bovine pancreatic ribonuclease A (RNase A) in the free form and bound to the inhibitor 5′-phosphothymidine(3′−5′)pyrophosphate adenosine 3′-phosphate (pTppAp).[111] Although both the free and inhibitor-bound RNase A displayed decreased order parameters as the temperature increased from 21 to 38 °C, the temperature dependence of S^2 values for both states indicated no significant contribution to the ΔC_p for the protein−ligand interaction. Nevertheless, changes in the apparent conformational heat capacities were observed for individual residues, indicating that there is a redistribution of backbone energetics upon RNase A binding to pTppAp.

In a contrasting study, Krizova et al. observed a slight decrease in the apparent backbone conformational heat capacity when the mouse major urinary protein-I (MUP-I) binds to a pheromone.[135] This negative contribution to the ΔC_p of binding corresponds with the large, negative overall heat capacity for pheromone binding by MUP-I, although the dominant factor in this overall heat capacity is likely to be hydrophobic association. The latter study utilized a novel approach in which the order parameters and characteristic temperatures were obtained simultaneously through global analysis of the multiple-temperature data.

Much work remains to be done to understand the possible roles of conformational heat capacity in regulating the thermodynamics of protein−ligand binding. As with the above studies of protein stability, this component of binding thermodynamics may be particularly significant in interactions from thermophilic species.

Pressure Dependence of Dynamics. To date, a single study has examined the influence of pressure upon fast time scale internal motions of protein backbones. Sareth and co-workers compared the backbone dynamics of BPTI at 30 and 2000 bar.[157] With the exception of small, isolated changes in R_2 values, no significant changes were observed in relaxation or order parameters with increasing pressure. Initially expecting the compaction of BPTI as a result of increased

pressure[177−179] to cause decreased mobility of amide bond vectors, the authors rationalized their results as follows. Both ^{1}H and ^{15}N chemical shifts were observed to change linearly and reversibly with pressure between 1 bar and 2 kbar,[177−179] indicating that no major conformational change, such as protein denaturation, occurs in BPTI structure at 2 kbar, but instead there are very slight changes in the population distribution within the same native ensemble. The authors proposed that the local conformational changes could be approximated as linear functions of pressure, suggesting that the local compressibility and hence the variations in local volume are pressure-independent. The pressure-independent fluctuations in volume are proposed to be the basis for the insensitivity of fast time scale backbone motions to increasing pressure.

4.5. Long-Range Effects and Correlated Motions

In the above sections on the effects of mutations and ligand binding we have noted several cases in which these perturbations have induced changes in the internal dynamics of a protein at positions distant from the mutation site or binding site. These situations deserve special attention because they could provide insights into the underlying networks of interactions that control the energetics of the protein (conformational entropy and fold stability) and the transmission of functional information (allostery).[13] Below we discuss several studies in which long-range dynamical perturbations have been observed, discuss the possible general mechanisms for these effects, and outline some recently developed strategies to elucidate these mechanisms.

Long-Range Effects upon Ligand Binding. Several of the cases in which ligand binding has induced distant dynamical changes have involved the binding of enzymes to substrate or product analogues or to inhibitors. One interesting example is that of dihydrofolate reductase (DHFR), for which Osborne and co-workers have examined three ligand−protein complexes: (1) DHFR and the substrate analogue, folate (E:folate); (2) DHFR, folate, and the cofactor 5,6-dihydroNADPH (E:folate:DHNADPH); and (3) DHFR, folate, and the oxidized cofactor NADP$^+$ (E:folate:NADP$^+$).[180] The backbone dynamics of E:folate and E:folate:DHNADPH, referred to as "occluded" complexes, were essentially the same with the exception of small changes in order parameters for residues near the folate-binding site. On the other hand, the "closed" E:folate:NADP$^+$ complex exhibited significant changes in dynamics compared with the occluded complexes (Figure 13). In most cases, changes in dynamics parameters, such as those observed in the Met20 and F−G loops, could be rationalized in terms of conformational changes between complexes. However, the adenosine binding loop, which is >18 Å away from regions of conformational change, displayed slower subnanosecond motion (τ_e terms needed to fit the relaxation data for a larger number of residues) in the E:folate:NADP$^+$ complex. The authors noted that motional coupling between residues of the adenosine-binding site and regions surrounding the substrate-binding site has been observed in molecular dynamics simulations as well as ensemble-based computer modeling studies of DHFR,[181,182] thus providing additional support for a long-range network of interactions between the adenosine-binding loop and the active site. A recent review by Schnell et al. summarizes the dynamics of DHFR on a variety of time scales.[183]

Another dynamics study probing the long-range effects of substrate binding is the investigation of human lysozyme

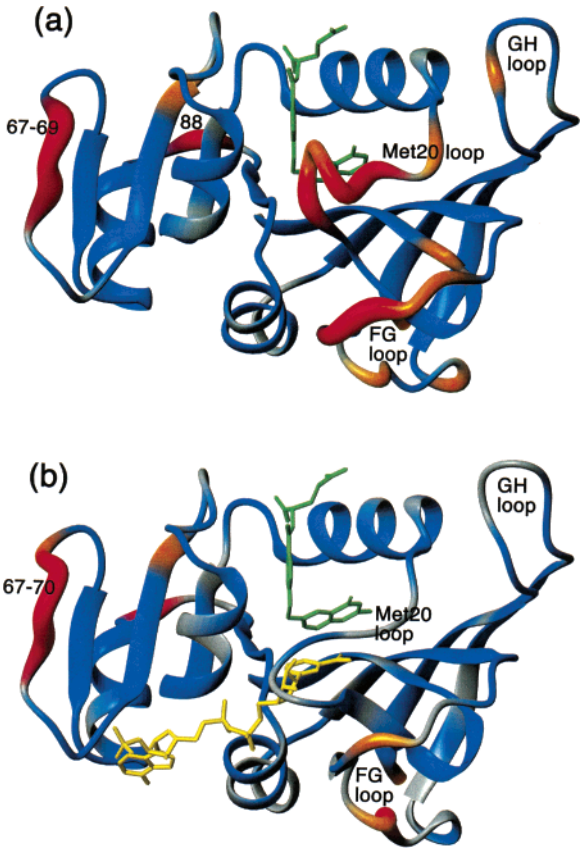

Figure 13. Ribbon diagram of dihydrofolate reductase showing the location of regions in which there are enhanced motions on the picosecond/nanosecond time scale in (a) the occluded E:folate binary complex and (b) the closed E:folate:NADP$^+$ complex. The ribbon is color coded to indicate S^2 value: blue, $S^2 > 0.8$; orange, $0.71 < S^2 < 0.8$; red, $S^2 < 0.70$. The radius of the ribbon is also increased to reflect the decrease in S^2 values. Bound folic acid and NADP$^+$ are green and yellow, respectively, and displayed in stick representation. Reprinted with permission from ref 180. Copyright 2001 American Chemical Society.

binding to the substrate analogue, tri-*N*-acetyl-chitotrioside [$(NAG)_3$] by Mine and colleagues.[127] In this study, residues remote from the active site at the C-terminal region of the enzyme displayed both significantly increased and decreased order parameters, suggesting to the authors that the internal motions of the enzyme are closely linked to substrate binding.

Several examples have been described in which binding of inhibitors to enzyme active sites induced changes in the dynamics distant from the active site. Upon binding of the competitive inhibitor *cis*,*cis*-muconate to the enzyme 4-oxalocrotonate tautomerase (4-OT), residues in direct contact with the inhibitor as well as numerous residues outside the active site exhibited both increases and decreases in order parameters.[123] Of the nonactive site residues, six showed decreased flexibility and two showed increased flexibility. In particular, significant changes in order parameters upon inhibitor binding were observed in the distant β1-strand, which forms part of the 4-OT dimer interface. Here a pattern of increases and decreases in order parameters was observed in which backbone amide groups participating in intersubunit hydrogen bonds showed decreased order parameters (increased mobility) and amides participating in intrasubunit hydrogen bonds showed increased order parameters (decreased mobility), suggesting to the authors that inhibitor binding tightened intrasubunit interactions at the expense of remote intersubunit interactions. Yun and colleagues obtained similar results from

their study of the backbone dynamics of free and steroid inhibitor-bound Δ^5-3-ketosteroid isomerase (KSI).[132] Upon binding 19-nortestosterone hemisuccinate (19-NTHS) residues in the β4-strand exhibited decreased flexibility in contrast to the remaining β-sheet strands (β3, β5, and β6), which all increased in mobility. Whereas some regions of the β4−β6 β-sheet come in direct contact with 19-NTHS, other regions of the sheet are rather remote from the steroid inhibitor, suggesting some long-range transmission of dynamics changes. Yun and co-workers have likened the contrasting increases and decreases in β-strand order parameters of KSI to those changes observed in 4-OT upon inhibitor binding; proposing that binding of 19-NTHS causes increased mobility in the intersubunit region of KSI. A third enzyme−inhibitor study is the reduced spectral density mapping analysis by Davis and Agard of α-lytic protease (αLP) binding to the competitive inhibitor *N-tert*-butyloxycarbonyl-Ala-Pro-boroVal.[142] Residue I172, which is >10 Å away from the inhibitor, displayed significant changes in $J(0)$ upon inhibitor binding. Interestingly, this residue was implicated by a previous scanning alanine mutagenesis study as a distant, but key, modulator of αLP activity,[184] leading Davis and Agard to propose that I172 could be dynamically coupled as well as functionally coupled to the substrate binding pocket of αLP. Finally, Sahu and colleagues have examined the backbone dynamics of the ribonuclease barnase, both free and in complex with the protein inhibitor barstar. They observed an overall increase in average order parameters upon inhibitor binding but noted significant decreases in order parameters of five residues.[122] Of these, four are located at or near the binding interface, but one residue, D22, which displayed a decrease in order parameter between the free and bound forms, is located on the face of the protein opposite that of the ligand-binding site.

In addition to the above enzyme−ligand complexes, ligand binding to noncatalytic proteins can also induce distant changes in protein dynamics. For example, Olejniczak and colleagues have observed changes in backbone dynamics of the phosphotyrosine-binding domain of the insulin receptor substrate 1 when complexed with a tyrosine−phosphorylated peptide derived from the interleukin 4 (IL-4) receptor.[117] Upon binding the peptide, several residues that are not in direct contact with the peptide became more motionally restricted. In particular, residues in the loop between β3 and β4, located on the opposite side of the protein from the peptide-binding site, exhibited increases in order parameters and internal correlation times, leading Olejniczak and coworkers to propose that reductions in mobility were a result of indirect contacts with the IL-4 peptide mediated by adjacent loops and β-strands.

Finally, metal ion-binding can also cause long-range changes in protein backbone dynamics. Probably the best characterized case is that of the calcium-binding protein, calbindin D_{9k} (Figure 14).[136,137,170] Calbindin D_{9k} is a small protein that contains a pair of calcium-binding EF-hand motifs and is involved in the intracellular buffering of calcium ions. The Chazin group has analyzed the differences between the apo form, the half-saturated form in which a cadmium ion is bound in site II [$(Cd^{2+})_1$], and the calcium-saturated state [$(Ca^{2+})_2$]. Four residues in calcium-binding loop II displayed increased order parameters upon cadmium binding to site II and calcium binding to sites I and II. Binding of a Cd^{2+} ion to site II also caused a slight reduction in flexibility in the remote site I. In addition, two residues

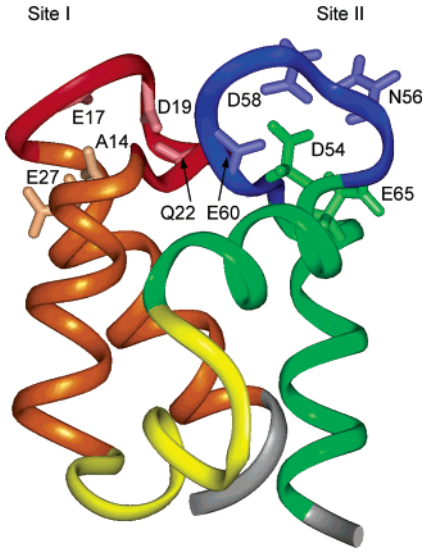

Figure 14. Ribbon diagram of calbindin D_{9k} (PDB file 2BCA). The N-terminal (left) and C-terminal (right) EF-hand motifs are orange and green, respectively, with the calcium-binding loops within these motifs red and blue, respectively. Atoms involved in calcium coordination are shown in stick representation. For residues A14, E17, D19, and Q22 (site I) and E60 (site II), coordination occurs through backbone carbonyl groups, whereas for residues E27 (site I) and D54, N56, D58, and E65 (site II), coordination utilizes side-chain functional groups. The linker between the two EF-hand motifs is yellow.

in the C-terminal region of the protein demonstrated decreased flexibility in the $(Cd^{2+})_1$ and $(Ca^{2+})_2$ states as compared with the apo state, despite the lengthy distance from either binding sites I or II.[136,170] In a more recent study, the same group examined the dynamics of the site I half-saturated [$(Ca^{2+})_1$] form of a N56A calbindin mutant.[137] They observed that Ca^{2+}-binding to site I in the N56A mutant reduces the mobility of both Ca^{2+}-binding motifs (i.e. site I and II) compared with the apo state, and that the reduction of flexibility at the remote site II is very dramatic. If these changes are analyzed in terms of contributions to backbone conformational entropies, it becomes apparent that over half of the total conformational entropy change for site II occurs upon occupation of the first binding site, i.e., prior to Ca^{2+}-binding to site II itself. Chazin and colleagues have hypothesized that the long-range structural and dynamic changes induced by binding of the first Ca^{2+} ion lowers the free energy cost for subsequent structural reorganization during the second binding step, hence providing a mechanistic explanation of the observed cooperativity of calcium binding. Similar results were demonstrated in a dynamics study of the EF-hand containing regulatory domain of human cardiac troponin C (cTnC) in the apo and Ca^{2+}-saturated states.[138] Spyracopoulus and co-workers observed that upon Ca^{2+}-binding to the functional site II, flexibility decreases to a similar extent in both site II and the nonfunctional site I. Despite the fact that only site II is functional and thus a cooperative Ca^{2+}-binding mechanism between sites I and II is not observed, the finding that both sites of cTnC are dynamically coupled is consistent with the observed long-range, site−site dynamic communication effects observed in calbindin D_{9k}. Together, such results suggest that changes in dynamics may be a conserved mechanism for regulating cooperative Ca^{2+}-binding in EF-hand proteins. A recent review by Kern and Zuiderweg discusses the roles of both fast and slow time scale motions in allosteric binding.[13]

Long-Range Effects upon Domain-Swapping. 3D domain swapping of proteins involves the interconversion between monomeric and twofold symmetrical dimeric forms of a protein. The monomer is defined to consist of two "domains" (a "domain" can mean any individual structural element or group of elements) that are packed against each other. In the dimer, the first structural element of one monomer packs against the second structural element of the other monomer and vice versa, such that each half of the dimer has a structure almost identical to that of the monomer alone; the only difference is typically in the linker between the two domains. Therefore, the observation that dynamics of the monomer and the dimer are different in a region distant from the linker can be viewed as the transmission of dynamic information from the linker to the remote region. Precisely this type of effect has been observed by Japelj and co-workers for the cysteine protease inhibitor, stefin A (Figure 15).[185] Under native conditions stefin A forms a monomer. Under destabilizing conditions (high temperature, low pH, chemical denaturant), however, stefin A forms a domain-swapped dimer in which one domain consists of βA, α-helix, and βB of one subunit and βC, βD, and βE of the other subunit. Upon dimer formation, residues remote from the domain linker exhibited changes in dynamics (Figure 15). In particular, residues in the first half of the second binding loop (between βD and βE) as well as the last residue in the second half of the loop and the first residue in βE all displayed decreased order parameters relative to the monomeric state. Notably, in the dimeric state β-strands D and E comprise one subunit and do not appear to undergo the conformational change experienced by elements of the protein at the domain-swapping interface (near the linker).

Possible Mechanisms of Long-Range Dynamic Effects. All of the above examples beg the following question: how does the perturbation (ligand binding or domain swapping) give rise to changes in dynamics at remote positions in the protein? There are several possible mechanisms. First, the perturbation could induce a conformational change of the protein, including the remote region, so the dynamical change could merely reflect this structural difference. In this case, it is difficult to attribute any functional outcome to the dynamical change as opposed to the change in average conformation. A second possibility is that the perturbation induces a conformational change of residues located at and/or near the site of perturbation, leading to a modification of the strength of their interactions with residues located between the perturbation site and the remote residues ("intervening" residues). This change in the environment of the intervening residues could thus change the energy landscape and structural restraints of the remote residues, resulting in changes in their dynamic properties. Finally, it is possible that the perturbation does not induce any change in the average structure of the protein but instead affects the dynamics of residues both at the perturbation site and at the remote site. The intervening residues would be expected to undergo changes in their interactions with both the perturbed and remote residues and possibly changes in their own dynamic properties. Separating these possible mechanisms is extremely difficult and will require careful comparisons of both the structures and dynamics of several forms of the same protein, preferably without large conformational changes between the different forms. Below we highlight two recently developed approaches for probing the mechanism of dynamical communication across protein domains.

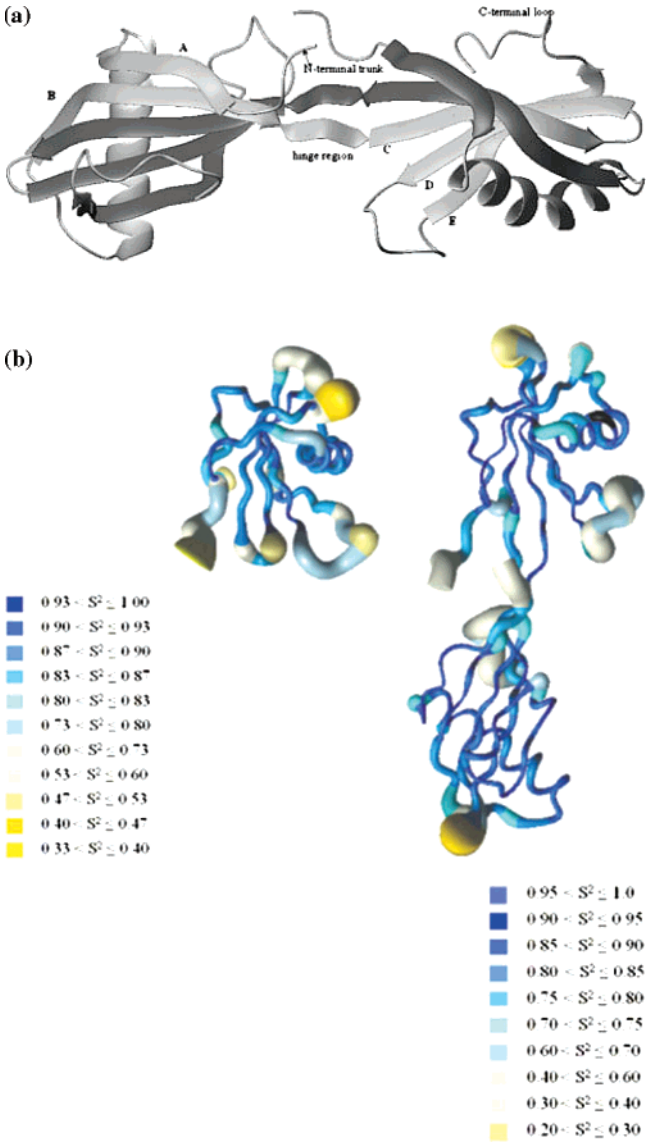

Figure 15. (a) Tertiary structure of stefin A dimer. Homodimer consists of two symmetrical subunits depicted in different shades, which are connected with a short linker region. One domain consists of strand A, α-helix, and strand B of one subunit and strands C, D, and E of the other subunit. (b) Worm structures for the stefin A monomer (left) and the stefin A dimer (right). The worms are color-coded according to measured S^2 values as indicated in the figure. The widths of the worms are proportional to $(1 - S^2)$. Reprinted with permission from *Comparison of Backbone Dynamics of Monomeric and Domain-Swapped Stefin A*, Japelj et al. Copyright 2004 Wiley-Liss.

Comparison of Dynamical Changes to Statistical Coupling Energies. Fuentes and co-workers have investigated the effect of peptide binding upon the dynamics of a PDZ (postsynaptic density-95/discs large/zonula occludens-1) domain and compared their results to statistical coupling energies obtained by analysis of the PDZ domain sequence database; the coupling energies are essentially a measure of the degree to which pairs of residues have covaried throughout the evolution of the domain family.[186] Peptide binding to the second PDZ domain (PDZ2) of human protein tyrosine phosphatase 1E (hPTP1E) caused small structural changes and only small changes in the fast time scale backbone dynamics. However, substantial changes were observed in the fast dynamics of side-chain methyl groups and in slow time scale backbone dynamics.[187] The residues with altered

dynamical properties were located in two distinct regions of the domain, each forming a continuous van der Waals surface and each at least 9 Å away from the nearest residue in the peptide ligand. Similarly, mapping the statistical coupling energies onto a representative member of the PDZ domain family indicated that residues with large coupling energies form a continuous pathway of van der Waals interactions linking distant regions of the domain to the peptide-binding face. The correspondence between those residues undergoing changes in dynamics upon peptide binding with those residues exhibiting energetic couplings led Fuentes and coworkers to propose that changes in protein dynamics upon ligand binding may serve to identify long-range effects that are of significance in terms of protein evolution and hence function. Additionally, the authors proposed that fast time scale dynamics may serve as a mechanism for the propagation of long-range energetic signals in the PDZ domain as well as other protein folds. Although the results of this study were of most interest with regard to side-chain dynamics, the novel approach of combining NMR-derived dynamics data and statistical coupling analysis can also be applied to backbone data and so has implications for understanding the long-range propagation of backbone motions discussed above.

Covariation of Internal Protein Dynamics. We have recently proposed an alternative experimental approach for mapping the pathways of dynamical communication in proteins.[148,174] The method involves analyzing the covariation of dynamics for each pair of bond vectors among several different perturbed states of a protein, for example, different ligand complexes, different mutants, or different chemical or physical conditions. Consider two bond vectors in the protein having motions that are coupled to each other; one bond vector might directly sense the motions of the other, or they might both be coupled to the dynamical, structural, or energetic properties of the same intervening residues. In any of these cases, a perturbation that affects the motion of one bond vector might be expected to also affect the motion of the second bond vector. Among the several perturbed states, one might therefore expect to observe a statistical correlation between the dynamical properties of the two bond vectors, indicating that they are coupled to each other. There are two important criteria for the success of this approach. The perturbations must be sufficiently severe to cause measurable changes in the dynamics parameters, but they must not be so strong as to disrupt the coupling mechanisms between different pairs of bond vectors. Application of this approach to 10 mutants of the B1 domain of protein G revealed a slightly higher level of covariation of backbone amide S^2 and τ_e values than would be randomly expected, thus supporting the existence of a network of coupled motions within this domain (Figure 16).[148] Side-chain methyl group motions were even more weakly correlated,[174] indicating that the coupling might be mediated through the protein backbone.

The results of the covariation method have potential implications for the estimation of residual entropy in proteins. If the motions of two bond vectors are truly correlated (synchronized), as discussed in section 5.5, one would expect to see significant covariation of the dynamics parameters for these two bond vectors in response to a series of protein perturbations, as long as the perturbations are strong enough to influence the dynamics of each bond vector. Therefore, a significant change in dynamics of one vector and a lack of covariation with the dynamics of a second bond vector would indicate the absence of strongly correlated motions between these two vectors. In this sense, the observation that there is only very weak covariation of dynamics in the B1 domain

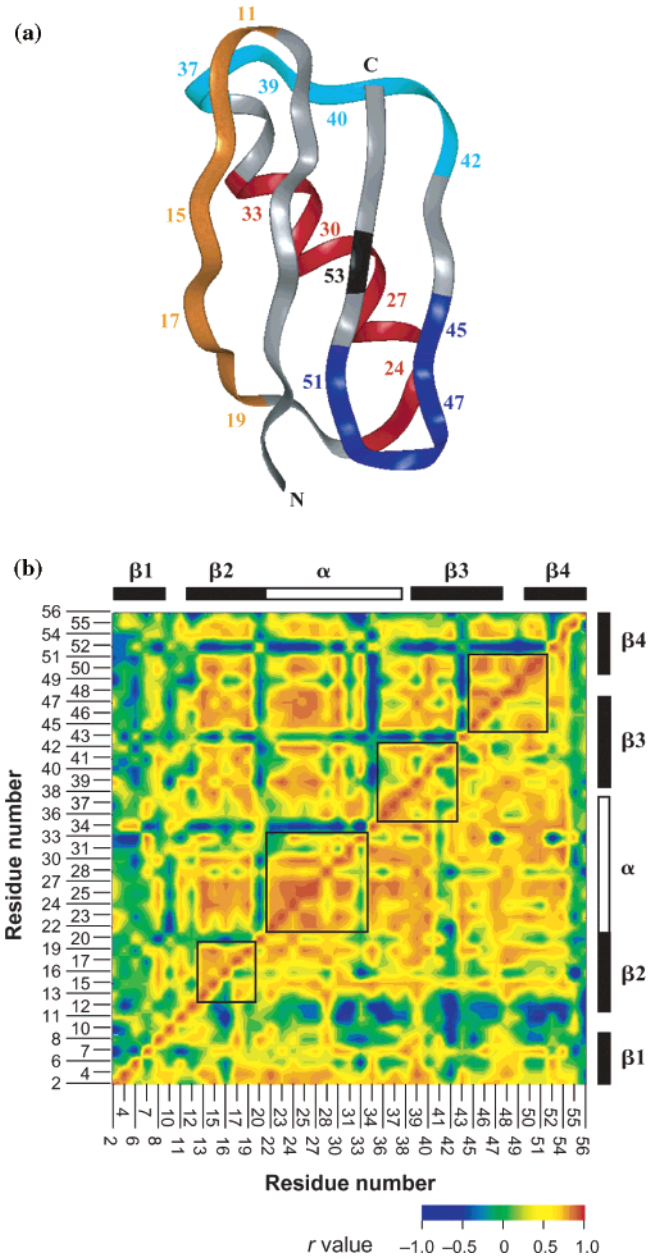

Figure 16. Covariation of backbone dynamics in 10 mutants of the B1 domain from protein G. (A) Ribbon diagram of the B1 domain of protein G. Regions with the highest prevalence of correlated dynamics are shown in orange, β2-strand; red, α-helix; cyan, extended loop; and blue, β3−β4 turn. The guest position (residue 53) is black. (B) Structural distributions of dynamical covariations. The color map shows the strengths of the observed correlations (r values) for each pair of residues. Data for S^2 covariations are above the diagonal, whereas those for τ_e correlations are below the diagonal. Black boxes indicate positions of the structural elements for which correlated changes in dynamics are most prevalent: the second β-strand (residues 11−19), the first ~3 turns of the α-helix (residues 22−33), the extended loop (residues 36−42), and the β3−β4 hairpin turn (residues 45−51). The positions of secondary structure elements are indicated at the top and on the right as solid or open bars (β-strands and α-helix, respectively). Reprinted with permission from *Nature* (http://www.nature.com), ref 148. Copyright 2003 Nature Publishing Group.

suggests that the motions of most bond vectors are predominantly independent of rather than correlated with the motions of other bond vectors. This provides increased confidence in the estimation of conformational entropy from order parameters.

5. Summary and Future Directions

Over the past 15 years, there has been a dramatic increase in our knowledge of the internal motions of proteins, primarily driven by the availability of ^{1}H-detected NMR methods for the detection of ^{15}N and ^{13}C relaxation in proteins. Many studies of backbone dynamics have been performed as extensions of NMR-based structure determinations, allowing a more complete picture of the proteins' structural ensembles. In addition, there has been increasing interest in understanding the roles that the internal motions play in determining the stabilities and activities of proteins. In the following sections, we briefly summarize the past achievements and discuss possible directions for future studies that will shed light on the functional consequences of protein dynamics.

5.1. Role of Dynamics in the Thermodynamics of Ligand Binding

Perhaps the most consistent theme to emerge from the many past studies is that *the fast backbone dynamics of a protein almost always change upon binding to a ligand*. Binding of a ligand often reduces the mobility of backbone groups in or near the binding site. This is consistent with the classical "induced fit" binding model and indicates that there is an entropic cost associated with formation of the optimal binding interactions. In contrast, binding of ligands can sometimes increase the mobility of backbone groups. When these groups are outside the primary binding site, the increased flexibility may compensate for entropic losses of other groups at the binding site. Alternatively, in a few cases involving predominantly hydrophobic binding sites, the binding site itself has been found to become more flexible, suggesting that binding is driven in part by enhanced conformational entropy. A corollary of the proposal that changes in dynamics can influence affinity for a particular ligand is that changes in dynamics upon binding to different ligands can affect the relative affinities and hence the binding specificity of the protein. Although the evidence for a relationship between specificity and dynamics is more limited, it has been proposed that low specificity can be a consequence of a protein maintaining binding site flexibility even in the bound state[120] or of a protein undergoing induced fit binding to more than one ligand.[124]

Although there is now little doubt that dynamics can influence binding affinity, the magnitude of the effect remains a matter of debate. Calculation of conformational entropy under the assumption that all measured bond vectors are completely independent[91−93] can yield estimates in excess of 10 kcal mol^{-1},[134] enough to change the binding constant by >7 orders of magnitude. Correlation of motions between the measured bond vectors will decrease the conformational entropy of each state and hence will also decrease the entropy difference between the two states. Moreover, the degree to which motions of different bond vectors are correlated could change upon binding, causing a possible increase or decrease in the entropy difference. In addition, it is important to recognize that the measured bond vectors are usually a small fraction of all the bond vectors in the molecule, so the reported entropy changes disregard the motions of the additional bond vectors and any correlations between them or between the measured and nonmeasured vectors. Added to the facts that order parameters are insensitive to translational motions, rotational motions slower than about a nanosecond or rotations around the measured bond vector, and that the physical details of the motions are not revealed by the NMR data, the cumulative uncertainties in reported conformational entropies are enormous. Nevertheless, the current data suggest that changes in conformational entropy upon binding may well be large enough to influence binding constants and to make the difference between high and low binding affinity. *We are left with the dilemma that theoretical estimation of binding affinities without taking conformational entropy into account is almost certain to yield incorrect answers, yet currently we do not know how to obtain confident estimates of conformational entropy.*

The above considerations highlight one of the most important questions for future dynamics investigations: *How can one obtain a more accurate determination of the change in conformational entropy when a protein binds to a ligand?* One obvious step is to measure the dynamics of more bond vectors throughout both the backbone and side chains of the protein (in free and bound states). An additional experimental approach, pioneered by Zuiderweg and colleagues,[188−190] is to measure the relaxation of multiple bond vectors that are affected by rotations around different but overlapping groups of axes. For example, motions of N−H and C_α−CO bond vectors are both influenced by rotation around the intervening peptide bond, but each is also influenced by rotation around the other bond vector but not around itself. Combined analysis of the relaxation data can provide an improved physical description of anisotropic bond vector motions,[189,190] which could assist in the selection of appropriate relationships between order parameters and entropy. Although extension of this approach to characterizing additional backbone and side-chain motions is technically achievable, it would require a large amount of primary data for each form of the protein studied. Consequently, the data collection time required for a thorough dynamics analysis of this type may not be much different from the typical data collection time for a complete structure determination. Moreover, even if such extensive data were available, accurate determination of conformational entropy would not be straightforward. One would still require information about the extent and nature of motional correlations, both between adjacent groups and across longer distances. As discussed below, we imagine that theoretical approaches such as molecular dynamics will play a leading role in providing such information.

5.2. Role of Dynamics in the Thermodynamics of Protein Folding

In addition to influencing the stability of protein−ligand complexes, there is increasing evidence that *changes in fast backbone dynamics can affect the stability of the folded state of a protein*. In particular, mutations in the core or on the surface of a protein can give rise to measurable changes in the dynamics of the folded state, and the associated changes in conformational entropy could have a measurable effect on the folding stability of the protein. As in the case of ligand binding, the accurate quantification of conformational entropy is problematic, and the approaches discussed above may improve this situation. However, understanding the influence

of dynamics on folding free energy also requires information about the dynamics of the unfolded state. Unfortunately, the model-free approach is not applicable to unfolded proteins because the overall and local motions are not well separated and definition of global motions is not possible.[191−193] Furthermore, the degree of motional correlation is likely to change dramatically upon folding, presumably in the direction of increased motional coupling in the folded state. Thus, there is a need for new methods for characterizing motions of unfolded proteins, identifying motional correlations that may exist in the unfolded state, and estimating the entropic value of unfolded state motions.

The motions of a protein can influence stability not only through their effects on conformational entropy but also by affecting the heat capacity of the protein. As expected, the motions of protein backbones increase with increasing temperature. However, a more surprising observation is that the magnitude of the change (i.e., the conformational heat capacity) can vary both between different structural elements within a protein and between different proteins. These variations suggest a minor but possibly measurable influence of conformational heat capacity on the thermal stability of protein structures. However, there is currently little understanding of the features that control these variations in temperature sensitivity. In addition, there is very little current information about whether conformational heat capacity can be substantially influenced by ligand binding and hence affect the thermal stability of the resulting complex. Future experimental and theoretical studies are needed in these areas.

5.3. Role of Dynamics in the Catalytic Activity of Enzymes

One of the most intriguing and widely discussed aspects of protein dynamics is that it could potentially affect the catalytic efficiency of enzymes. However, despite the substantial number of enzymes now studied by NMR relaxation methods (see Table 10), progress toward establishing a clear relationship between dynamics and activity has been slow. In a few cases, mutations that influence catalytic activity of enzymes also affect the dynamics of the enzyme structure,[126,142] suggesting that dynamics may play a functional role. However, a major problem in interpreting results of this type is that the mutations almost always affect the average structure of the enzyme as well as its dynamics, so the functional differences may be more a consequence of the change in structure. Even when a change in average structure occurs, there may still be changes in dynamics (either coupled to or independent of the structural changes) that influence catalytic function. Indeed, at some level, distinguishing between changes in structure and dynamics becomes meaningless because structures are merely approximations of complex dynamical systems.

Notwithstanding the aforementioned philosophical quandary, to firmly establish a causal relationship between dynamics and catalytic activity, it will be necessary first to identify enzyme mutations (or other modifications) that do not measurably affect the average structure of the active site but do affect both active site dynamics and enzymatic activity (turnover rate, Michaelis constant, product dissociation rate, etc.). Next, one would need to modify the system (additional or alternative mutations, substrate modifications, variations in pH, temperature, etc.) and to observe a statistical correlation between dynamics and activity, again ideally without affecting the average structure. Identifying such a system

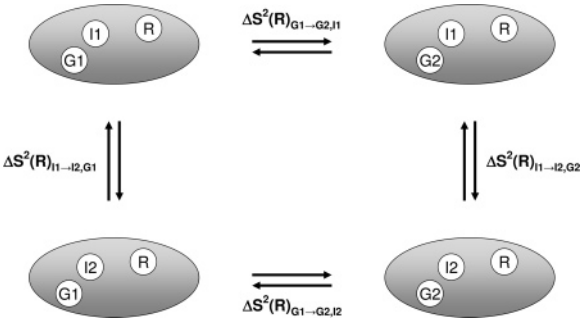

Figure 17. Schematic illustration of the double-mutant approach for probing pathways of dynamic communication in proteins, as discussed in the text.

and picking the right mutations is very difficult, not least because many enzymes are relatively large compared to typical targets for high-resolution NMR relaxation studies. One approach is to initially study an enzyme in the absence and presence of an active site ligand (e.g., transition state analogue) and to look for elements of the structure removed from the active site that undergo changes in dynamics, suggesting that they are energetically coupled to the active site. Subsequent mutations at those remote sites might be expected to influence the energetics of the active site through the same coupling mechanism, so one could screen for remote mutants that influence activity and then a subset of those having active site structures that are the same as those of the wild-type enzyme. In this light, the apparent dynamical coupling between the adenosine-binding site and the substrate-binding site of dihydrofolate reductase makes this enzyme particularly promising for uncovering a functional role for dynamics in enzyme activity.

5.4. Mechanisms of Dynamical Changes and Long-Range Effects

Although there is now ample evidence that mutations and ligand binding can alter the backbone dynamics of a protein, the precise changes observed have not generally been predicted or even successfully rationalized. Thus, we currently have little understanding of how a particular modification gives rise to the measured changes in order parameters or correlation times. This is particularly evident for systems in which changes in flexibility are observed at positions distant from the binding site or mutation site.[117,122,123,127,132,137,138,142,180,185,187] As the functional roles of protein motions become better established there will be an increasing need to uncover these mechanisms. One obvious approach is to again compare a series of mutants or ligands and to monitor the influence of each on the resulting protein dynamics. One potential difficulty in the case of long-range effects is that there may be several alternative pathways connecting the mutation or binding site to the remote site for which the dynamics are observed to change. The dynamics of the intervening residues might not be directly affected by the mutation or the ligand, so modification of these factors would not indicate the mechanism by which distant residues are coupled to each other.

To investigate the mechanism by which a mutation induces changes in dynamics at a distant position in the protein, it would be possible to utilize the double-mutant strategy outlined in Figure 17. In this approach, one hypothesizes that an initial mutation at a position designated the guest position (G) affects the dynamics at a remote site (R) by a

mechanism involving the side chain of an intervening residue (I). Dynamics parameters for the remote residue would be measured in four proteins containing either of two amino acids [G1 (left structures) and G2 (right structures)] in position G and two amino acids [I1 (top structures) and I2 (bottom structures)] in position I. If the side chain of amino acid I influences the communication between positions G and R, then the change in order parameter of R when amino acid G1 is substituted by G2 with amino acid I1 at the intervening position [$\Delta S^2(R)_{G1 \rightarrow G2,I1}$; top horizontal transition] should be different from the corresponding change when amino acid I2 is located at the intervening position [$\Delta S^2(R)_{G1 \rightarrow G2,I2}$; bottom horizontal transition]. Otherwise, they should be identical (within error). A particular strength of this approach is that, for each mutant, the dynamics of many remote positions would be determined. Thus, the double-mutant experiments would allow one to determine the role of a particular intervening residue on dynamic communication between the guest position and each of the remote positions. An analogous thermodynamic cycle could be used to analyze the mechanisms by which ligand binding induces remote changes in dynamics. As with all mutational studies, this approach will not reveal information about the role of backbone groups in transmission of dynamic effects.

5.5. Energetic Coupling and Correlated Dynamics

A recurring theme in much of the above discussion is that the dynamics at different positions in a protein may be coupled to each other, potentially influencing the conformational entropy of the protein, the transmission of changes in motion across a domain, and the mechanisms of enzymatic activity. Consequently, there is widespread interest in identifying correlated dynamics between groups spread throughout a domain. As discussed in section 4.5, the comparison of dynamics changes with statistical coupling energies,[187] and the analysis of dynamic covariation among mutants[148,174] are starting to provide some insights into possible dynamical coupling pathways. The application of thermodynamic cycles as proposed above could also benefit efforts in this area. However, none of these approaches directly reveals whether the motions of two groups are truly correlated (i.e., the groups are moving in synchrony) as opposed to one group affecting the amplitude or frequency of the other group's motion without the motions on the two groups being synchronous.

There are currently no experimental approaches that unequivocally identify synchronous motions for groups that are not directly adjacent to each other. On the other hand, simulated molecular dynamics (MD) trajectories contain all of the spatial detail required for mechanistic interpretation, so they can be interpreted to reveal the motional covariation between each pair of bond vectors in a protein, irrespective of their proximity to each other.[181] Importantly, such analyses of MD data can be applied to all bond vectors in a molecule, not only those that are easily observable by NMR. In addition, the motions in the MD simulation could be partitioned into translational and rotational components, allowing an assessment of the entropy related to each type of motion and also allowing the MD parameters describing rotational motions to be compared to NMR-derived dynamics data. Thus, it appears that analysis of MD data is the preferred approach for the identification and quantification of motional correlations in proteins.

Although MD simulations are extremely powerful, it remains disconcerting that NMR-derived and MD-derived order parameters often do not agree at a detailed level. For example, the agreement between NMR and MD tends to be quite good for the more rigid regions of proteins but not in flexible elements such as loops.[1,90,194−198] As discussed in an excellent review by Case,[90] part of the discrepancy is attributable to the random and systematic errors that can occur in the interpretation of the NMR data.[90,199] However, the MD-derived order parameters may also contain both random and systematic errors related to the limited duration of the trajectory, the choice of starting structures, and the force field itself.[1,90,195,197−201] Consequently, there is a need to carefully validate the fast time scale dynamic information provided by MD simulations and possibly to develop more accurate MD methods. NMR relaxation data should be considered the benchmark for validating and calibrating such improved methods, but this comparison should be performed with full awareness of the limitation of both methods. To improve confidence in the MD results, it may be beneficial to compare MD trajectories for several forms (e.g., mutants) of the same protein with experimental NMR dynamics data for the same species. Although these studies may be labor-intensive, they could have far-reaching consequences for understanding the functional roles of protein motions.

6. Acknowledgments

We thank Dr. Jeff Peng for helpful discussions, Dr. Arthur G. Palmer III for providing updates to Table 10, and Drs. Jane Dyson, Patricia Jennings, Roman Jerala, Robert Oswald, Steven VanDoren, and Peter Wright for permission to use figures from their previous publications. This work was supported by a grant awarded to M.J.S. from the National Science Foundation (MCB-0212746).

7. References

(1) Palmer, A. G. *Annu. Rev. Biophys. Biomol. Struct.* **2001**, *30*, 129−155.
(2) Palmer, A. G., III. *Curr. Opin. Biotechnol.* **1993**, *4*, 385−391.
(3) Peng, J. W.; Wagner, G. *Methods Enzymol.* **1994**, *239*, 563−596.
(4) Dayie, K. T.; Wagner, G.; Lefevre, J. F. *Annu. Rev. Phys. Chem.* **1996**, *47*, 243−282.
(5) Daragan, V. A.; Mayo, K. H. *Prog. Nucl. Magn. Reson. Spectrosc.* **1997**, *31*, 63−105.
(6) Palmer, A. G. *Curr. Opin. Struct. Biol.* **1997**, *7*, 732−737.
(7) Fischer, M. W. F.; Majumdar, A.; Zuiderweg, E. R. P. *Prog. Nucl. Magn. Reson. Spectrosc.* **1998**, *33*, 207−272.
(8) Kay, L. E. *Nat. Struct. Biol.* **1998**, *5*, 513−517.
(9) Kay, L. E. *Biochem. Cell Biol.* **1998**, *76*, 145−152.
(10) Ishima, R.; Torchia, D. A. *Nat. Struct. Biol.* **2000**, *7*, 740−743.
(11) Spyracopoulos, L.; Sykes, B. D. *Curr. Opin. Struct. Biol.* **2001**, *11*, 555−559.
(12) Stone, M. J. *Acc. Chem. Res.* **2001**, *34*, 379−388.
(13) Kern, D.; Zuiderweg, E. R. *Curr. Opin. Struct. Biol.* **2003**, *13*, 748−757.
(14) Palmer, A. G., III. *Chem. Rev.* **2004**, *104*, 3623−3640.
(15) Fischer, E. *Ber. Dtsch. Chem. Ges.* **1894**, *27*, 2985−2993.
(16) Lemieux, R. U.; Spohr, U. *Adv. Carbohydr. Chem. Biochem.* **1994**, *50*, 1−20.
(17) Creighton, T. E. *Proteins: Structures and Molecular Properties*; W. H. Freeman: New York, 1993; pp 139−169.
(18) Fersht, A. *Structure and Mechanism in Protein Science*; W. H. Freeman: New York, 1999; pp 324−348.
(19) Luque, I.; Freire, E. *Methods Enzymol.* **1998**, *295*, 100−127.
(20) Freire, E. *Methods Mol. Biol.* **2001**, *168*, 37−68.
(21) Williams, D. H.; Cox, J. P. L.; Doig, A. J.; Gardner, M.; Gerhard, U.; Kaye, P. T.; Lal, A. R.; Nicholls, I. A.; Salter, C. J.; Mitchell, R. C. *J. Am. Chem. Soc.* **1991**, *113*, 7020−7030.
(22) Searle, M. S.; Williams, D. H. *J. Am. Chem. Soc.* **1992**, *114*, 10690−10697.
(23) Forman-Kay, J. D. *Nat. Struct. Biol.* **1999**, *6*, 1086−1087.
(24) Creighton, T. E. *Proteins: Structures and Molecular Properties*; W. H. Freeman: New York, 1993; p 291.

(25) Fersht, A. *Structure and Mechanism in Protein Science*; W. H. Freeman: New York, 1999; p 509.
(26) Shortle, D.; Ackerman, M. S. *Science* **2001**, *293*, 487−489.
(27) Shi, Z.; Olson, C. A.; Rose, G. D.; Baldwin, R. L.; Kallenbach, N. R. *Proc. Natl. Acad. Sci. U.S.A.* **2002**, *99*, 9190−9195.
(28) Fitzkee, N. C.; Rose, G. D. *Proc. Natl. Acad. Sci. U.S.A.* **2004**, *101*, 12497−12502.
(29) Kohn, J. E.; Millett, I. S.; Jacob, J.; Zagrovic, B.; Dillon, T. M.; Cingel, N.; Dothager, R. S.; Seifert, S.; Thiyagarajan, P.; Sosnick, T. R.; Hasan, M. Z.; Pande, V. S.; Ruczinski, I.; Doniach, S.; Plaxco, K. W. *Proc. Natl. Acad. Sci. U.S.A.* **2004**, *101*, 12491−12496.
(30) Karush, F. *J. Am. Chem. Soc.* **1950**, *72*, 2705−2713.
(31) Koshland, D. E. *Proc. Natl. Acad. Sci. U.S.A.* **1950**, *44*, 98−104.
(32) van Holde, K. E.; Johnson, W. C.; Ho, P. S. *Principles of Physical Biochemistry*; Prentice Hall: Englewood Cliffs, NJ, 1998; pp 613−621.
(33) Cooper, A.; Dryden, D. T. *Eur. Biophys. J.* **1984**, *11*, 103−109.
(34) Bruice, T. C.; Benkovic, S. J. *Biochemistry* **2000**, *39*, 6267−6274.
(35) Wand, A. J. *Science* **2001**, *293*, U1.
(36) Wand, A. J. *Nat. Struct. Biol.* **2001**, *8*, 926−931.
(37) Bruice, T. C. *Acc. Chem. Res.* **2002**, *35*, 139−148.
(38) Knapp, M. J.; Klinman, J. P. *Eur. J. Biochem.* **2002**, *269*, 3113−3121.
(39) Kohen, A.; Klinman, J. P. *Chem. Biol.* **1999**, *6*, R191−R198.
(40) Kohen, A.; Cannio, R.; Bartolucci, S.; Klinman, J. P. *Nature* **1999**, *399*, 496−499.
(41) Kohen, A.; Jonsson, T.; Klinman, J. P. *Biochemistry* **1997**, *36*, 2603−2611.
(42) Antoniou, D.; Schwartz, S. D. *J. Phys. Chem. B* **2001**, *105*, 5553−5558.
(43) Knapp, M. J.; Rickert, K.; Klinman, J. P. *J. Am. Chem. Soc.* **2002**, *124*, 3865−3874.
(44) Balabin, I. A.; Onuchic, J. N. *Science* **2000**, *290*, 114−117.
(45) Lipari, G.; Szabo, A. *J. Am. Chem. Soc.* **1982**, *104*, 4546−4559.
(46) Lipari, G.; Szabo, A. *J. Am. Chem. Soc.* **1982**, *104*, 4559−4570.
(47) Kay, L. E.; Torchia, D. A.; Bax, A. *Biochemistry* **1989**, *28*, 8972−8979.
(48) Cavanagh, J.; Fairbrother, W. J.; Palmer, A. G., III; Skelton, N. J. *Protein NMR Spectroscopy Principles and Practice*; Academic Press: San Diego, CA, 1996.
(49) Peng, J. W.; Wagner, G. *J. Magn. Reson.* **1992**, *98*, 308−332.
(50) Peng, J. W.; Wagner, G. *Biochemistry* **1992**, *31*, 8571−8586.
(51) Farrow, N. A.; Zhang, O.; Forman-Kay, J. D.; Kay, L. E. *Biochemistry* **1995**, *34*, 868−878.
(52) Farrow, N. A.; Zhang, O.; Szabo, A.; Torchia, D. A.; Kay, L. E. *J. Biomol. NMR* **1995**, *6*, 153−162.
(53) Ishima, R.; Nagayama, K. *J. Magn. Reson. Ser. B* **1995**, *108*, 73−76.
(54) Lefevre, J. F.; Dayie, K. T.; Peng, J. W.; Wagner, G. *Biochemistry* **1996**, *35*, 2674−2686.
(55) Peng, J. W.; Wagner, G. *Biochemistry* **1995**, *34*, 16733−16752.
(56) Vis, H.; Vorgias, C. E.; Wilson, K. S.; Kaptein, R.; Boelens, R. *J. Biomol. NMR* **1998**, *11*, 265−277.
(57) Tugarinov, V.; Liang, Z.; Shapiro, Y. E.; Freed, J. H.; Meirovitch, E. *J. Am. Chem. Soc.* **2001**, *123*, 3055−3063.
(58) Jin, D.; Andrec, M.; Montelione, G. T.; Levy, R. M. *J. Biomol. NMR* **1998**, *12*, 471−492.
(59) Lee, A. L.; Wand, A. J. *J. Biomol. NMR* **1999**, *13*, 101−112.
(60) Clore, G. M.; Driscoll, P. C.; Wingfield, P. T.; Gronenborn, A. M. *Biochemistry* **1990**, *29*, 7387−7401.
(61) Clore, G. M.; Szabo, A.; Bax, A.; Kay, L. E.; Driscoll, P. C.; Gronenborn, A. M. *J. Am. Chem. Soc.* **1990**, *112*, 4989−4991.
(62) Mandel, A. M.; Akke, M.; Palmer, A. G., III. *J. Mol. Biol.* **1995**, *246*, 144−163.
(63) Stone, M. J.; Fairbrother, W. J.; Palmer, A. G., III; Reizer, J.; Saier, M. H., Jr.; Wright, P. E. *Biochemistry* **1992**, *31*, 4394−4406.
(64) Barbato, G.; Ikura, M.; Kay, L. E.; Pastor, R. W.; Bax, A. *Biochemistry* **1992**, *31*, 5269−5278.
(65) Kloiber, K.; Weiskirchen, R.; Krautler, B.; Bister, K.; Konrat, R. *J. Mol. Biol.* **1999**, *292*, 893−908.
(66) Eliezer, D.; Chung, J.; Dyson, H. J.; Wright, P. E. *Biochemistry* **2000**, *39*, 2894−2901.
(67) Farrow, N. A.; Muhandiram, R.; Singer, A. U.; Pascal, S. M.; Kay, C. M.; Gish, G.; Shoelson, S. E.; Pawson, T.; Forman-Kay, J. D.; Kay, L. E. *Biochemistry* **1994**, *33*, 5984−6003.
(68) Kay, L. E. *Prog. Biophys. Mol. Biol.* **1995**, *63*, 277−299.
(69) Tjandra, N.; Szabo, A.; Bax, A. *J. Am. Chem. Soc.* **1996**, *118*, 6986−6991.
(70) Kroenke, C. D.; Loria, J. P.; Lee, L. K.; Rance, M.; Palmer, A. G. *J. Am. Chem. Soc.* **1998**, *120*, 7905−7915.
(71) Viles, J. H.; Duggan, B. M.; Zaborowski, E.; Schwarzinger, S.; Huntley, J. J.; Kroon, G. J.; Dyson, H. J.; Wright, P. E. *J. Biomol. NMR* **2001**, *21*, 1−9.
(72) Seewald, M. J.; Pichumani, K.; Stowell, C.; Tibbals, B. V.; Regan, L.; Stone, M. J. *Protein Sci.* **2000**, *9*, 1177−1193.
(73) Tjandra, N.; Feller, S. E.; Pastor, R. W.; Bax, A. *J. Am. Chem. Soc.* **1995**, *117*, 12562−12566.
(74) Palmer, A. G.; Rance, M.; Wright, P. E. *J. Am. Chem. Soc.* **1991**, *113*, 4371−4380.
(75) Palmer, A. G.; Kroenke, C. D.; Loria, J. P. *Methods Enzymol.* **2001**, *339*, 204−238.
(76) Akke, M. *Curr. Opin. Struct. Biol.* **2002**, *12*, 642−647.
(77) Wang, C. Y.; Palmer, A. G. *Magn. Reson. Chem.* **2003**, *41*, 866−876.
(78) Schurr, J. M.; Babcock, H. P.; Fujimoto, B. S. *J. Magn. Reson. Ser. B* **1994**, *105*, 211−224.
(79) Lee, L. K.; Rance, M.; Chazin, W. J.; Palmer, A. G. *J. Biomol. NMR* **1997**, *9*, 287−298.
(80) Blackledge, M.; Cordier, F.; Dosset, P.; Marion, D. *J. Am. Chem. Soc.* **1998**, *120*, 4538−4539.
(81) Bruschweiler, R.; Liao, X. B.; Wright, P. E. *Science* **1995**, *268*, 886−889.
(82) Fushman, D.; Xu, R.; Cowburn, D. *Biochemistry* **1999**, *38*, 10225−10230.
(83) Dosset, P.; Hus, J. C.; Blackledge, M.; Marion, D. *J. Biomol. NMR* **2000**, *16*, 23−28.
(84) Walker, O.; Varadan, R.; Fushman, D. *J. Magn. Reson.* **2004**, *168*, 336−345.
(85) Fushman, D.; Varadan, R.; Assfalg, M.; Walker, O. *Prog. Nucl. Magn. Reson. Spec.* **2004**, *44*, 189−214.
(86) Osborne, M. J.; Wright, P. E. *J. Biomol. NMR* **2001**, *19*, 209−230.
(87) d'Auvergne, E. J.; Gooley, P. R. *J. Biomol. NMR* **2003**, *25*, 25−39.
(88) Jin, D. Q.; Figueirido, F.; Montelione, G. T.; Levy, R. M. *J. Am. Chem. Soc.* **1997**, *119*, 6923−6924.
(89) Andrec, M.; Montelione, G. T.; Levy, R. M. *J. Magn. Reson.* **1999**, *139*, 408−421.
(90) Case, D. A. *Acc. Chem. Res.* **2002**, *35*, 325−331.
(91) Akke, M.; Bruschweiler, R.; Palmer, A. G. *J. Am. Chem. Soc.* **1993**, *115*, 9832−9833.
(92) Li, Z.; Raychaudhuri, S.; Wand, A. J. *Protein Sci.* **1996**, *5*, 2647−2650.
(93) Yang, D.; Kay, L. E. *J. Mol. Biol.* **1996**, *263*, 369−382.
(94) Cavanagh, J.; Akke, M. *Nat. Struct. Biol.* **2000**, *7*, 11−13.
(95) Wang, T.; Cai, S.; Zuiderweg, E. R. *J. Am. Chem. Soc.* **2003**, *125*, 8639−8643.
(96) Creighton, T. E. *Proteins: Structures and Molecular Properties*; W. H. Freeman: New York, 1993; pp 296−303.
(97) Spolar, R. S.; Record, M. T. *Science* **1994**, *263*, 777−784.
(98) Gomez, J.; Hilser, V. J.; Xie, D.; Freire, E. *Proteins* **1995**, *22*, 404−412.
(99) Privalov, P. L.; Makhatadze, G. I. *J. Mol. Biol.* **1990**, *213*, 385−391.
(100) Yang, D.; Mok, Y. K.; Forman-Kay, J. D.; Farrow, N. A.; Kay, L. E. *J. Mol. Biol.* **1997**, *272*, 790−804.
(101) Evenas, J.; Forsen, S.; Malmendal, A.; Akke, M. *J. Mol. Biol.* **1999**, *289*, 603−617.
(102) Mandel, A. M.; Akke, M.; Palmer, A. G., III. *Biochemistry* **1996**, *35*, 16009−16023.
(103) Vugmeyster, L.; Trott, O.; McKnight, C. J.; Raleigh, D. P.; Palmer, A. G., III. *J. Mol. Biol.* **2002**, *320*, 841−854.
(104) Massi, F.; Palmer, A. G. *J. Am. Chem. Soc.* **2003**, *125*, 11158−11159.
(105) Zhang, W. X.; Smithgall, T. E.; Gmeiner, W. H. *Biochemistry* **1998**, *37*, 7119−7126.
(106) Lu, J.; Lin, C. L.; Tang, C.; Ponder, J. W.; Kao, J. L.; Cistola, D. P.; Li, E. *J. Mol. Biol.* **2000**, *300*, 619−632.
(107) Gizachew, D.; Oswald, R. E. *Biochemistry* **2001**, *40*, 14368−14375.
(108) Mercier, P.; Spyracopoulos, L.; Sykes, B. D. *Biochemistry* **2001**, *40*, 10063−10077.
(109) Franzoni, L.; Lucke, C.; Perez, C.; Cavazzini, D.; Rademacher, M.; Ludwig, C.; Spisni, A.; Rossi, G. L.; Ruterjans, H. *J. Biol. Chem.* **2002**, *277*, 21983-21997.
(110) Ramboarina, S.; Srividya, N.; Atkinson, R. A.; Morellet, N.; Roques, B. P.; Lefevre, J. F.; Mely, Y.; Kieffer, B. *J. Mol. Biol.* **2002**, *316*, 611−627.
(111) Kovrigin, E. L.; Cole, R.; Loria, J. P. *Biochemistry* **2003**, *42*, 5279−5291.
(112) Hodsdon, M. E.; Cistola, D. P. *Biochemistry* **1997**, *36*, 2278−2290.
(113) Sasaki, M.; Ogata, K.; Hatanaka, H.; Nishimura, Y. *J. Biochem. (Tokyo)* **2000**, *127*, 945−953.
(114) Rischel, C.; Madsen, J. C.; Andersen, K. V.; Poulsen, F. M. *Biochemistry* **1994**, *33*, 13997−14002.
(115) Fushman, D.; Weisemann, R.; Thuring, H.; Ruterjans, H. *J. Biomol. NMR* **1994**, *4*, 61−78.
(116) Cheng, J. W.; Lepre, C. A.; Moore, J. M. *Biochemistry* **1994**, *33*, 4093−4100.

(117) Olejniczak, E. T.; Zhou, M. M.; Fesik, S. W. *Biochemistry* **1997**, *36*, 4118−4124.
(118) Loh, A. P.; Guo, W.; Nicholson, L. K.; Oswald, R. E. *Biochemistry* **1999**, *38*, 12547−12557.
(119) Yao, X.; Soden, C.; Summers, M. F.; Beckett, D. *Protein Sci.* **1999**, *8*, 307−317.
(120) Huntley, J. J. A.; Scrofani, S. D. B.; Osborne, M. J.; Wright, P. E.; Dyson, H. J. *Biochemistry* **2000**, *39*, 13356−13364.
(121) Chi, Y.; Kumar, T. K.; Chiu, I. M.; Yu, C. *J. Biol. Chem.* **2000**, *275*, 39444−39450.
(122) Sahu, S. C.; Bhuyan, A. K.; Udgaonkar, J. B.; Hosur, R. V. *J. Biomol. NMR* **2000**, *18*, 107−118.
(123) Stivers, J. T.; Abeygunawardana, C.; Mildvan, A. S. *Biochemistry* **1996**, *35*, 16036−16047.
(124) Yuan, P.; Marshall, V. P.; Petzold, G. L.; Poorman, R. A.; Stockman, B. J. *J. Biomol. NMR* **1999**, *15*, 55−64.
(125) Wang, C.; Pawley, N. H.; Nicholson, L. K. *J. Mol. Biol.* **2001**, *313*, 873−887.
(126) Mine, S.; Tate, S.; Ueda, T.; Kainosho, M.; Imoto, T. *J. Mol. Biol.* **1999**, *286*, 1547−1565.
(127) Mine, S.; Ueda, T.; Hashimoto, Y.; Imoto, T. *Protein Sci.* **2000**, *9*, 1669−1684.
(128) Fayos, R.; Melacini, G.; Newlon, M. G.; Burns, L.; Scott, J. D.; Jennings, P. A. *J. Biol. Chem.* **2003**, *278*, 18581−18587.
(129) Yu, L.; Zhu, C. X.; Tse-Dinh, Y. C.; Fesik, S. W. *Biochemistry* **1996**, *35*, 9661−9666.
(130) Zidek, L.; Novotny, M. V.; Stone, M. J. *Nat. Struct. Biol.* **1999**, *6*, 1118−1121.
(131) Zhu, L.; Hu, J.; Lin, D.; Whitson, R.; Itakura, K.; Chen, Y. *Biochemistry* **2001**, *40*, 9142−9150.
(132) Yun, S. G.; Jang, D. S.; Kim, D. H.; Choi, K. Y.; Lee, H. C. *Biochemistry* **2001**, *40*, 3967−3973.
(133) Henzl, M. T.; Wycoff, W. G.; Larson, J. D.; Likos, J. J. *Protein Sci.* **2002**, *11*, 158−173.
(134) Arumugam, S.; Gao, G. H.; Patton, B. L.; Semenchenko, V.; Brew, K.; Van Doren, S. R. *J. Mol. Biol.* **2003**, *327*, 719−734.
(135) Krizova, H.; Zidek, L.; Stone, M. J.; Novotny, M. V.; Sklenar, V. *J. Biomol. NMR* **2004**, *28*, 369−384.
(136) Akke, M.; Skelton, N. J.; Kordel, J.; Palmer, A. G., III; Chazin, W. J. *Biochemistry* **1993**, *32*, 9832−9844.
(137) Maler, L.; Blankenship, J.; Rance, M.; Chazin, W. J. *Nat. Struct. Biol.* **2000**, *7*, 245−250.
(138) Spyracopoulos, L.; Gagne, S. M.; Li, M. X.; Sykes, B. D. *Biochemistry* **1998**, *37*, 18032−18044.
(139) Mittermaier, A.; Varani, L.; Muhandiram, D. R.; Kay, L. E.; Varani, G. *J. Mol. Biol.* **1999**, *294*, 967−979.
(140) Cave, J. W.; Kremer, W.; Wemmer, D. E. *Protein Sci.* **2000**, *9*, 2354−2365.
(141) McIntosh, P. B.; Taylor, I. A.; Frenkiel, T. A.; Smerdon, S. J.; Lane, A. N. *J. Biomol. NMR* **2000**, *16*, 183−196.
(142) Davis, J. H.; Agard, D. A. *Biochemistry* **1998**, *37*, 7696−7707.
(143) de Lorimier, R.; Hellinga, H. W.; Spicer, L. D. *Protein Sci.* **1996**, *5*, 2552−2565.
(144) Mittermaier, A.; Kay, L. E. *Protein Sci.* **2004**, *13*, 1088−1099.
(145) Beeser, S. A.; Goldenberg, D. P.; Oas, T. G. *J. Mol. Biol.* **1997**, *269*, 154−164.
(146) Hanson, W. M.; Beeser, S. A.; Oas, T. G.; Goldenberg, D. P. *J. Mol. Biol.* **2003**, *333*, 425−441.
(147) Stone, M. J.; Gupta, S.; Snyder, N.; Regan, L. *J. Am. Chem. Soc.* **2001**, *123*, 185−186.
(148) Mayer, K. L.; Earley, M. R.; Gupta, S.; Pichumani, K.; Regan, L.; Stone, M. J. *Nat. Struct. Biol.* **2003**, *10*, 962−965.
(149) Kranz, J. K.; Hall, K. B. *J. Mol. Biol.* **1999**, *285*, 215−231.
(150) Showalter, S. A.; Hall, K. B. *J. Mol. Biol.* **2004**, *335*, 465−480.
(151) Cai, M. L.; Gong, Y. X.; Wen, L.; Krishnamoorthi, R. *Biochemistry* **2002**, *41*, 9572−9579.
(152) Adams, P. D.; Loh, A. P.; Oswald, R. E. *Biochemistry* **2004**, *43*, 9968−9977.
(153) Spyracopoulos, L.; Lavigne, P.; Crump, M. P.; Gagne, S. M.; Kay, C. M.; Sykes, B. D. *Biochemistry* **2001**, *40*, 12541−12551.
(154) Pawley, N. H.; Koide, S.; Nicholson, L. K. *J. Mol. Biol.* **2002**, *324*, 991−1002.
(155) Lee, A. L.; Sharp, K. A.; Kranz, J. K.; Song, X. J.; Wand, A. J. *Biochemistry* **2002**, *41*, 13814−13825.
(156) Idiyatullin, D.; Nesmelova, I.; Daragan, V. A.; Mayo, K. H. *J. Mol. Biol.* **2003**, *325*, 149−162.
(157) Sareth, S.; Li, H.; Yamada, H.; Woodward, G. K.; Akasaka, K. *FEBS Lett.* **2000**, *470*, 11−14.
(158) Stone, M. J.; Chandrasekhar, K.; Holmgren, A.; Wright, P. E.; Dyson, H. J. *Biochemistry* **1993**, *32*, 426−435.
(159) Hrovat, A.; Blumel, M.; Lohr, F.; Mayhew, S. G.; Ruterjans, H. *J. Biomol. NMR* **1997**, *10*, 53−62.
(160) Kelley, J. J., III; Caputo, T. M.; Eaton, S. F.; Laue, T. M.; Bushweller, J. H. *Biochemistry* **1997**, *36*, 5029−5044.
(161) Dangi, B.; Blankman, J. I.; Miller, C. J.; Volkman, B. F.; Guiles, R. D. *J. Phys. Chem. B* **1998**, *102*, 8201−8208.
(162) Sari, N.; Holden, M. J.; Mayhew, M. P.; Vilker, V. L.; Coxon, B. *Biochemistry* **1999**, *38*, 9862−9871.
(163) Fetrow, J. S.; Baxter, S. M. *Biochemistry* **1999**, *38*, 4480−4492.
(164) Bertini, I.; Bryant, D. A.; Ciurli, S.; Dikiy, A.; Fernandez, C. O.; Luchinat, C.; Safarov, N.; Vila, A. J.; Zhao, J. *J. Biol. Chem.* **2001**, *276*, 47217−47226.
(165) Kasimova, M. R.; Kristensen, S. M.; Howe, P. W.; Christensen, T.; Matthiesen, F.; Petersen, J.; Sorensen, H. H.; Led, J. J. *J. Mol. Biol.* **2002**, *318*, 679−695.
(166) Hu, H.; Clarkson, M. W.; Hermans, J.; Lee, A. L. *Biochemistry* **2003**, *42*, 13856−13868.
(167) Ye, J. Q.; Mayer, K. L.; Stone, M. J. *J. Biomol. NMR* **1999**, *15*, 115−124.
(168) Ye, J.; Mayer, K. L.; Mayer, M. R.; Stone, M. J. *Biochemistry* **2001**, *40*, 7820−7831.
(169) Mayer, K. L.; Stone, M. J. *Proteins* **2003**, *50*, 184−191.
(170) Kordel, J.; Skelton, N. J.; Akke, M.; Palmer, A. G., III; Chazin, W. J. *Biochemistry* **1992**, *31*, 4856−4866.
(171) MacDougall, J. R.; Matrisian, L. M. *Cancer Metastasis Rev.* **1995**, *14*, 351−362.
(172) Cawston, T. E. *Pharmacol. Ther.* **1996**, *70*, 163−182.
(173) Mulder, F. A. A.; Hon, B.; Muhandiram, D. R.; Dahlquist, F. W.; Kay, L. E. *Biochemistry* **2000**, *39*, 12614−12622.
(174) Goehlert, V. A.; Krupinska, E.; Regan, L.; Stone, M. J. *Protein Sci.* **2004**, *13*, 3322−3330.
(175) Smith, C. K.; Withka, J. M.; Regan, L. *Biochemistry* **1994**, *33*, 5510−5517.
(176) Lin, R.; Bagrodia, S.; Cerione, R.; Manor, D. *Curr. Biol.* **1997**, *7*, 794−797.
(177) Li, H.; Yamada, H.; Akasaka, K. *Biochemistry* **1998**, *37*, 1167−1173.
(178) Li, H.; Yamada, H.; Akasaka, K. *Biophys. J.* **1999**, *77*, 2801−2812.
(179) Akasaka, K.; Li, H.; Yamada, H.; Li, R. H.; Thoresen, T.; Woodward, C. K. *Protein Sci.* **1999**, *8*, 1946−1953.
(180) Osborne, M. J.; Schnell, J.; Benkovic, S. J.; Dyson, H. J.; Wright, P. E. *Biochemistry* **2001**, *40*, 9846−9859.
(181) Radkiewicz, J. L.; Brooks, C. L. *J. Am. Chem. Soc.* **2000**, *122*, 225−231.
(182) Pan, H.; Lee, J. C.; Hilser, V. J. *Proc. Natl. Acad. Sci. U.S.A.* **2000**, *97*, 12020−12025.
(183) Schnell, J. R.; Dyson, H. J.; Wright, P. E. *Annu. Rev. Biophys. Biomol. Struct.* **2004**, *33*, 119−140.
(184) Mace, J. E.; Wilk, B. J.; Agard, D. A. *J. Mol. Biol.* **1995**, *251*, 116−134.
(185) Japelj, B.; Waltho, J. P.; Jerala, R. *Proteins* **2004**, *54*, 500−512.
(186) Lockless, S. W.; Ranganathan, R. *Science* **1999**, *286*, 295−299.
(187) Fuentes, E. J.; Der, C. J.; Lee, A. L. *J. Mol. Biol.* **2004**, *335*, 1105−1115.
(188) Zeng, L.; Fischer, M. W. F.; Zuiderweg, E. R. P. *J. Biomol. NMR* **1996**, *7*, 157−162.
(189) Fischer, M. W. F.; Zeng, L.; Pang, Y. X.; Hu, W. D.; Majumdar, A.; Zuiderweg, E. R. P. *J. Am. Chem. Soc.* **1997**, *119*, 12629−12642.
(190) Fischer, M. W.; Zeng, L.; Majumdar, A.; Zuiderweg, E. R. *Proc. Natl. Acad. Sci. U.S.A.* **1998**, *95*, 8016−8019.
(191) Dyson, H. J.; Wright, P. E. *Annu. Rev. Phys. Chem.* **1996**, *47*, 369−395.
(192) Dyson, H. J.; Wright, P. E. *Methods Enzymol.* **2001**, *339*, 258−270.
(193) Dyson, H. J.; Wright, P. E. *Adv. Protein Chem.* **2002**, *62*, 311−340.
(194) Philippopoulos, M.; Lim, C. *J. Mol. Biol.* **1995**, *254*, 771−792.
(195) Fushman, D.; Cahill, S.; Cowburn, D. *J. Mol. Biol.* **1997**, *266*, 173−194.
(196) Chatfield, D. C.; Szabo, A.; Brooks, B. R. *J. Am. Chem. Soc.* **1998**, *120*, 5301−5311.
(197) Horita, D. A.; Zhang, W. X.; Smithgall, T. E.; Gmeiner, W. H.; Byrd, R. A. *Protein Sci.* **2000**, *9*, 95−103.
(198) Pfeiffer, S.; Fushman, D.; Cowburn, D. *J. Am. Chem. Soc.* **2001**, *123*, 3021−3036.
(199) Philippopoulos, M.; Mandel, A. M.; Palmer, A. G., III; Lim, C. *Proteins* **1997**, *28*, 481−493.
(200) Smith, L. J.; Mark, A. E.; Dobson, C. M.; Vangunsteren, W. F. *Biochemistry* **1995**, *34*, 10918−10931.
(201) Stocker, U.; van Gunsteren, W. F. *Proteins* **2000**, *40*, 145−153.
(202) Abragam, A. *Principles of Nuclear Magnetism*; Clarendon Press: Oxford, U.K., 1961.
(203) Sklenar, V.; Torchia, D.; Bax, A. *J. Magn. Reson.* **1987**, *73*, 375−379.
(204) Wang, C.; Karpowich, N.; Hunt, J. F.; Rance, M.; Palmer, A. G. *J. Mol. Biol.* **2004**, *342*, 525−537.

(205) Findlow, S. C.; Winsor, C.; Simpson, T. J.; Crosby, J.; Crump, M. P. *Biochemistry* **2003**, *42*, 8423−8433.
(206) Hoshino, M.; Hagihara, Y.; Nishii, I.; Yamazaki, T.; Kato, H.; Goto, Y. *J. Mol. Biol.* **2000**, *304*, 927−939.
(207) Lu, J.; Cistola, D. P.; Li, E. *J. Mol. Biol.* **2003**, *330*, 799−812.
(208) Lu, J.; Lin, C. L.; Tang, C.; Ponder, J. W.; Kao, J. L.; Cistola, D. P.; Li, E. *J. Mol. Biol.* **1999**, *286*, 1179−1195.
(209) Lucke, C.; Fushman, D.; Ludwig, C.; Hamilton, J. A.; Sacchettini, J. C.; Ruterjans, H. *Mol. Cell. Biochem.* **1999**, *192*, 109−121.
(210) Gutierrez-Gonzalez, L. H.; Ludwig, C.; Hohoff, C.; Rademacher, M.; Hanhoff, T.; Ruterjans, H.; Spener, F.; Lucke, C. *Biochem. J.* **2002**, *364*, 725−737.
(211) Constantine, K. L.; Friedrichs, M. S.; Wittekind, M.; Jamil, H.; Chu, C. H.; Parker, R. A.; Goldfarb, V.; Mueller, L.; Farmer, B. T. *Biochemistry* **1998**, *37*, 7965−7980.
(212) Cheng, J. W.; Lepre, C. A.; Chambers, S. P.; Fulghum, J. R.; Thomson, J. A.; Moore, J. M. *Biochemistry* **1993**, *32*, 9000−9010.
(213) Li, Q.; Khosla, C.; Puglisi, J. D.; Liu, C. W. *Biochemistry* **2003**, *42*, 4648−4657.
(214) McFeeters, R. L.; Oswald, R. E. *Biochemistry* **2002**, *41*, 10472−10481.
(215) Mispelter, J.; Lefevre, C.; Adjadj, E.; Quiniou, E.; Favaudon, V. *J. Biomol. NMR* **1995**, *5*, 233−244.
(216) Izadi-Pruneyre, N.; Quiniou, E.; Blouquit, Y.; Perez, J.; Minard, P.; Desmadril, M.; Mispelter, J.; Adjadj, E. *Protein Sci.* **2001**, *10*, 2228−2240.
(217) Peto, H.; Stott, K.; Sunde, M.; Broadhurst, R. W. *J. Struct. Biol.* **2004**, *148*, 214−225.
(218) Crump, M. P.; Spyracopoulos, L.; Lavigne, P.; Kim, K. S.; Clark-Lewis, I.; Sykes, B. D. *Protein Sci.* **1999**, *8*, 2041−2054.
(219) Mizoue, L. S.; Bazan, J. F.; Johnson, E. C.; Handel, T. M. *Biochemistry* **1999**, *38*, 1402−1414.
(220) Fairbrother, W. J.; Liu, J.; Pisacane, P. I.; Sliwkowski, M. X.; Palmer, A. G. *J. Mol. Biol.* **1998**, *279*, 1149−1161.
(221) Zink, T.; Ross, A.; Luers, K.; Cieslar, C.; Rudolph, R.; Holak, T. A. *Biochemistry* **1994**, *33*, 8453−8463.
(222) Scian, M.; Marin, M.; Bellanda, M.; Tou, L.; Alexander, J. M.; Rosenblatt, M.; Chorev, M.; Peggion, E.; Mammi, S. *Biopolymers* **2005**.
(223) Chill, J. H.; Quadt, S. R.; Anglister, J. *Biochemistry* **2004**, *43*, 10127−10137.
(224) Feng, Y.; Klein, B. K.; McWherter, C. A. *J. Mol. Biol.* **1996**, *259*, 524−541.
(225) Redfield, C.; Boyd, J.; Smith, L. J.; Smith, R. A.; Dobson, C. M. *Biochemistry* **1992**, *31*, 10431−10437.
(226) Grasberger, B. L.; Gronenborn, A. M.; Clore, G. M. *J. Mol. Biol.* **1993**, *230*, 364−372.
(227) Yao, S.; Smith, D. K.; Hinds, M. G.; Zhang, J. G.; Nicola, N. A.; Norton, R. S. *Protein Sci.* **2000**, *9*, 671−682.
(228) Purvis, D. H.; Mabbutt, B. C. *Biochemistry* **1997**, *36*, 10146−10154.
(229) Kim, S.; Jao, S.; Laurence, J. S.; Liwang, P. J. *Biochemistry* **2001**, *40*, 10782−10791.
(230) Muhlhahn, P.; Bernhagen, J.; Czisch, M.; Georgescu, J.; Renner, C.; Ross, A.; Bucala, R.; Holak, T. A. *Protein Sci.* **1996**, *5*, 2095−2103.
(231) Barthe, P.; Chiche, L.; Declerck, N.; Delsuc, M. A.; Lefevre, J. F.; Malliavin, T.; Mispelter, J.; Stern, M. H.; Lhoste, J. M.; Roumestand, C. *J. Biomol. NMR* **1999**, *15*, 271−288.
(232) Stoll, R.; Renner, C.; Buettner, R.; Voelter, W.; Bosserhoff, A. K.; Holak, T. A. *Protein Sci.* **2003**, *12*, 510−519.
(233) Rajarathnam, K.; Li, Y. L.; Rohrer, T.; Gentz, R. *J. Biol. Chem.* **2001**, *276*, 4909−4916.
(234) Daragan, V. A.; Ilyina, E. E.; Fields, C. G.; Fields, G. B.; Mayo, K. H. *Protein Sci.* **1997**, *6*, 355−363.
(235) Keeler, C.; Dannies, P. S.; Hodsdon, M. E. *J. Mol. Biol.* **2003**, *328*, 1105−1121.
(236) Li, Y. C.; Montelione, G. T. *Biochemistry* **1995**, *34*, 2408−2423.
(237) Deep, S.; Walker, K. P., III; Shu, Z.; Hinck, A. P. *Biochemistry* **2003**, *42*, 10126−10139.
(238) Liwang, A. C.; Cao, J. J.; Zheng, H.; Lu, Z. H.; Peiper, S. C.; Liwang, P. J. *Biochemistry* **1999**, *38*, 442−453.
(239) Wyss, D. F.; Dayie, K. T.; Wagner, G. *Protein Sci.* **1997**, *6*, 534−542.
(240) Sorensen, M. D.; Bjorn, S.; Norris, K.; Olsen, O.; Petersen, L.; James, T. L.; Led, J. J. *Biochemistry* **1997**, *36*, 10439−10450.
(241) Smallridge, R. S.; Whiteman, P.; Werner, J. M.; Campbell, I. D.; Handford, P. A.; Downing, A. K. *J. Biol. Chem.* **2003**, *278*, 12199−12206.
(242) Yuan, X.; Werner, J. M.; Lack, J.; Knott, V.; Handford, P. A.; Campbell, I. D.; Downing, A. K. *J. Mol. Biol.* **2002**, *316*, 113−125.
(243) Werner, J. M.; Knott, V.; Handford, P. A.; Campbell, I. D.; Downing, A. K. *J. Mol. Biol.* **2000**, *296*, 1065−1078.
(244) Yuan, X.; Werner, J. M.; Knott, V.; Handford, P. A.; Campbell, I. D.; Downing, K. *Protein Sci.* **1998**, *7*, 2127−2135.
(245) Fan, F.; Mayo, K. H. *J. Biol. Chem.* **1995**, *270*, 24693−24701.
(246) Phan, I. Q. H.; Boyd, J.; Campbell, I. D. *J. Biomol. NMR* **1996**, *8*, 369−378.
(247) Carr, P. A.; Erickson, H. P.; Palmer, A. G., III. *Structure* **1997**, *5*, 949−959.
(248) Thormann, T.; Soroka, V.; Nielbo, S.; Berezin, V.; Bock, E.; Poulsen, F. M. *Biochemistry* **2004**, *43*, 10364−10369.
(249) Zajicek, J.; Chang, Y.; Castellino, F. J. *J. Mol. Biol.* **2000**, *301*, 333−347.
(250) Marti, D. N.; Schaller, J.; Llinas, M. *Biochemistry* **1999**, *38*, 15741−15755.
(251) Meekhof, A. E.; Freund, S. M. V. *J. Mol. Biol.* **1999**, *286*, 579−592.
(252) Hansen, A. P.; Petros, A. M.; Meadows, R. P.; Fesik, S. W. *Biochemistry* **1994**, *33*, 15418−15424.
(253) Constantine, K. L.; Friedrichs, M. S.; Goldfarb, V.; Jeffrey, P. D.; Sheriff, S.; Mueller, L. *Proteins* **1993**, *15*, 290−311.
(254) Kroon, G. J.; Mo, H.; Martinez-Yamout, M. A.; Dyson, H. J.; Wright, P. E. *Protein Sci.* **2003**, *12*, 1386-1394.
(255) O'Leary, J. M.; Bromek, K.; Black, G. M.; Uhrinova, S.; Schmitz, C.; Wang, X.; Krych, M.; Atkinson, J. P.; Uhrin, D.; Barlow, P. N. *Protein Sci.* **2004**, *13*, 1238−1250.
(256) Renisio, J. G.; Perez, J.; Czisch, M.; Guenneugues, M.; Bornet, O.; Frenken, L.; Cambillau, C.; Darbon, H. *Proteins* **2002**, *47*, 546−555.
(257) Wu, H.; Blackledge, M.; Maciejewski, M. W.; Mullen, G. P.; King, S. M. *Biochemistry* **2003**, *42*, 57−71.
(258) Barchi, J. J., Jr.; Grasberger, B.; Gronenborn, A. M.; Clore, G. M. *Protein Sci.* **1994**, *3*, 15−21.
(259) Frank, M. K.; Clore, G. M.; Gronenborn, A. M. *Protein Sci.* **1995**, *4*, 2605−2615.
(260) Tillett, M. L.; Blackledge, M. J.; Derrick, J. P.; Lian, L. Y.; Norwood, T. J. *Protein Sci.* **2000**, *9*, 1210−1216.
(261) Idiyatullin, D.; Daragan, V. A.; Mayo, K. H. *J. Phys. Chem. B* **2003**, *107*, 2602−2609.
(262) Hall, J. B.; Fushman, D. *J. Biomol. NMR* **2003**, *27*, 261−275.
(263) Johansson, M. U.; Nilsson, H.; Evenas, J.; Forsen, S.; Drakenberg, T.; Bjorck, L.; Wikstrom, M. *J. Mol. Biol.* **2002**, *316*, 1083−1099.
(264) Wikstrom, M.; Forsen, S.; Drakenberg, T. *Eur. J. Biochem.* **1996**, *235*, 543−548.
(265) Zdunek, J.; Martinez, G. V.; Schleucher, J.; Lycksell, P. O.; Yin, Y.; Nilsson, S.; Shen, Y.; Olivecrona, G.; Wijmenga, S. *Biochemistry* **2003**, *42*, 1872−1889.
(266) Orekhov, V. Y.; Pervushin, K. V.; Korzhnev, D. M.; Arseniev, A. S. *J. Biomol. NMR* **1995**, *6*, 113−122.
(267) Orekhov, V. Y.; Pervushin, K. V.; Arseniev, A. S. *Eur. J. Biochem.* **1994**, *219*, 887−896.
(268) Orekhov, V. Y.; Korzhnev, D. M.; Diercks, T.; Kessler, H.; Arseniev, A. S. *J. Biomol. NMR* **1999**, *14*, 345−356.
(269) Yushmanov, V. E.; Mandal, P. K.; Liu, Z.; Tang, P.; Xu, Y. *Biochemistry* **2003**, *42*, 3989−3995.
(270) Yushmanov, V. E.; Xu, Y.; Tang, P. *Biochemistry* **2003**, *42*, 13058−13065.
(271) Bader, R.; Bettio, A.; Beck-Sickinger, A. G.; Zerbe, O. *J. Mol. Biol.* **2001**, *305*, 307−329.
(272) Bader, R.; Rytz, G.; Lerch, M.; Beck-Sickinger, A. G.; Zerbe, O. *Biochemistry* **2002**, *41*, 8031−8042.
(273) Yan, C. H.; Digate, R. J.; Guiles, R. D. *Biopolymers* **1999**, *49*, 55−70.
(274) Metcalfe, E. E.; Zamoon, J.; Thomas, D. D.; Veglia, G. *Biophys. J.* **2004**, *87*, 1205−1214.
(275) Farrow, N. A.; Zhang, O.; Forman-Kay, J. D.; Kay, L. E. *Biochemistry* **1997**, *36*, 2390−2402.
(276) Temiz, N. A.; Meirovitch, E.; Bahar, I. *Proteins* **2004**, *57*, 468−480.
(277) Shapiro, Y. E.; Sinev, M. A.; Sineva, E. V.; Tugarinov, V.; Meirovitch, E. *Biochemistry* **2000**, *39*, 6634−6644.
(278) Shapiro, Y. E.; Kahana, E.; Tugarinov, V.; Liang, Z.; Freed, J. H.; Meirovitch, E. *Biochemistry* **2002**, *41*, 6271−6281.
(279) Tugarinov, V.; Shapiro, Y. E.; Liang, Z. C.; Freed, J. H.; Meirovitch, E. *J. Mol. Biol.* **2002**, *315*, 155−170.
(280) Ikegami, T.; Okada, T.; Ohki, I.; Hirayama, J.; Mizuno, T.; Shirakawa, M. *Biochemistry* **2001**, *40*, 375−386.
(281) Walma, T.; Spronk, C. A.; Tessari, M.; Aelen, J.; Schepens, J.; Hendriks, W.; Vuister, G. W. *J. Mol. Biol.* **2002**, *316*, 1101−1110.
(282) Finerty, P. J., Jr.; Mittermaier, A. K.; Muhandiram, R.; Kay, L. E.; Forman-Kay, J. D. *Biochemistry* **2005**, *44*, 694−703.
(283) Hansson, H.; Mattsson, P. T.; Allard, P.; Haapaniemi, P.; Vihinen, M.; Smith, C. I. E.; Hard, T. *Biochemistry* **1998**, *37*, 2912−2924.
(284) McEvoy, M. M.; Muhandiram, D. R.; Kay, L. E.; Dahlquist, F. W. *Biochemistry* **1996**, *35*, 5633−5640.
(285) Zhou, H.; Lowry, D. F.; Swanson, R. V.; Simon, M. I.; Dahlquist, F. W. *Biochemistry* **1995**, *34*, 13858−13870.

(286) Ran, X.; Miao, H. H.; Sheu, F. S.; Yang, D. *Biochemistry* **2003**, *42*, 5143−5150.
(287) Guignard, L.; Padilla, A.; Mispelter, J.; Yang, Y. S.; Stern, M. H.; Lhoste, J. M.; Roumestand, C. *J. Biomol. NMR* **2000**, *17*, 215−230.
(288) Renner, C.; Baumgartner, R.; Noegel, A. A.; Holak, T. A. *J. Mol. Biol.* **1998**, *283*, 221−229.
(289) Clubb, R. T.; Omichinski, J. G.; Sakaguchi, K.; Appella, E.; Gronenborn, A. M.; Clore, G. M. *Protein Sci.* **1995**, *4*, 855−862.
(290) Dutta, K.; Shi, H.; Cruz-Chu, E. R.; Kami, K.; Ghose, R. *Biochemistry* **2004**, *43*, 8094−8106.
(291) Kristensen, S. M.; Siegal, G.; Sankar, A.; Driscoll, P. C. *J. Mol. Biol.* **2000**, *299*, 771−788.
(292) Tochio, H.; Hung, F.; Li, M.; Bredt, D. S.; Zhang, M. J. *J. Mol. Biol.* **2000**, *295*, 225−237.
(293) Auguin, D.; Barthe, P.; Auge-Senegas, M. T.; Stern, M. H.; Noguchi, M.; Roumestand, C. *J. Biomol. NMR* **2004**, *28*, 137−155.
(294) Akerud, T.; Thulin, E.; Van Etten, R. L.; Akke, M. *J. Mol. Biol.* **2002**, *322*, 137−152.
(295) Hong, E.; Shin, J.; Kim, H. I.; Lee, S. T.; Lee, W. *J. Biol. Chem.* **2004**, *279*, 29700−29708.
(296) Abu-Abed, M.; Millet, O.; MacLennan, D. H.; Ikura, M. *Biochem. J.* **2004**, *379*, 235−242.
(297) Chen, C.; Feng, Y.; Short, J. H.; Wand, A. J. *Arch. Biochem. Biophys.* **1993**, *306*, 510−514.
(298) Gryk, M. R.; Abseher, R.; Simon, B.; Nilges, M.; Oschkinat, H. *J. Mol. Biol.* **1998**, *280*, 879−896.
(299) Volkman, B. F.; Lipson, D.; Wemmer, D. E.; Kern, D. *Science* **2001**, *291*, 2429−2433.
(300) Tada, M.; Kobashigawa, Y.; Mizuguchi, M.; Miura, K.; Kouno, T.; Kumaki, Y.; Demura, M.; Nitta, K.; Kawano, K. *Biochemistry* **2002**, *41*, 13807−13813.
(301) Kalverda, A. P.; Ubbink, M.; Gilardi, G.; Wijmenga, S. S.; Crawford, A.; Jeuken, L. J. C.; Canters, G. W. *Biochemistry* **1999**, *38*, 12690−12697.
(302) Malmendal, A.; Carlstrom, G.; Hambraeus, C.; Drakenberg, T.; Forsen, S.; Akke, M. *Biochemistry* **1998**, *37*, 2586−2595.
(303) Theret, I.; Cox, J. A.; Mispelter, J.; Craescu, C. T. *Protein Sci.* **2001**, *10*, 1393−1402.
(304) Theret, I.; Baladi, S.; Cox, J. A.; Gallay, J.; Sakamoto, H.; Craescu, C. T. *Biochemistry* **2001**, *40*, 13888−13897.
(305) Malmendal, A.; Evenas, J.; Forsen, S.; Akke, M. *J. Mol. Biol.* **1999**, *293*, 883−899.
(306) Lee, A. L.; Kinnear, S. A.; Wand, A. J. *Nat. Struct. Biol.* **2000**, *7*, 72−77.
(307) Wang, T.; Frederick, K. K.; Igumenova, T. I.; Wand, A. J.; Zuiderweg, E. R. *J. Am. Chem. Soc.* **2005**, *127*, 828−829.
(308) Larsson, G.; Schleucher, J.; Onions, J.; Hermann, S.; Grundstrom, T.; Wijmenga, S. S. *Biophys. J.* **2005**, *89*, 1214−1226.
(309) Venkitaramani, D. V.; Fulton, D. B.; Andreotti, A. H.; Johansen, K. M.; Johansen, J. *Protein Sci.* **2005**, *14*, 1894−1901.
(310) Konrat, R.; Krautler, B.; Weiskirchen, R.; Bister, K. *J. Biol. Chem.* **1998**, *273*, 23233−23240.
(311) Bertini, I.; Luchinat, C.; Niikura, Y.; Presenti, C. *Proteins* **2000**, *41*, 75−85.
(312) Potter, B. M.; Feng, L. S.; Parasuram, P.; Matskevich, V. A.; Wilson, J. A.; Andrews, G. K.; Laity, J. H. *J. Biol. Chem.* **2005**, *280*, 28529−28540.
(313) Oz, G.; Zangger, K.; Armitage, I. M. *Biochemistry* **2001**, *40*, 11433−11441.
(314) Moncrieffe, M. C.; Juranic, N.; Kemple, M. D.; Potter, J. D.; Macura, S.; Prendergast, F. G. *J. Mol. Biol.* **2000**, *297*, 147−163.
(315) Inman, K. G.; Baldisseri, D. M.; Miller, K. E.; Weber, D. J. *Biochemistry* **2001**, *40*, 3439−3448.
(316) Rabah, G.; Popescu, R.; Cox, J. A.; Engelborghs, Y.; Craescu, C. T. *FEBS J.* **2005**, *272*, 2022−2036.
(317) Gagne, S. M.; Tsuda, S.; Spyracopoulos, L.; Kay, L. E.; Sykes, B. D. *J. Mol. Biol.* **1998**, *278*, 667−686.
(318) Paakkonen, K.; Annila, A.; Sorsa, T.; Pollesello, P.; Tilgmann, C.; Kilpelainen, I.; Karisola, P.; Ulmanen, I.; Drakenberg, T. *J. Biol. Chem.* **1998**, *273*, 15633−15638.
(319) Blumenschein, T. M.; Gillis, T. E.; Tibbits, G. F.; Sykes, B. D. *Biochemistry* **2004**, *43*, 4955−4963.
(320) Bhattacharya, S.; Falzone, C. J.; Lecomte, J. T. J. *Biochemistry* **1999**, *38*, 2577−2589.
(321) Schwarzinger, S.; Wright, P. E.; Dyson, H. J. *Biochemistry* **2002**, *41*, 12681−12686.
(322) Yao, J.; Chung, J.; Eliezer, D.; Wright, P. E.; Dyson, H. J. *Biochemistry* **2001**, *40*, 3561−3571.
(323) Thompson, G. S.; Leung, Y. C.; Ferguson, S. J.; Radford, S. E.; Redfield, C. *Protein Sci.* **2000**, *9*, 846−858.
(324) Kelly, G. P.; Muskett, F. W.; Whitford, D. *Eur. J. Biochem.* **1997**, *245*, 349−354.
(325) Dangi, B.; Sarma, S.; Yan, C. H.; Banville, D. L.; Guiles, R. D. *Biochemistry* **1998**, *37*, 8289−8302.
(326) Bartalesi, I.; Bertini, I.; Rosato, A. *Biochemistry* **2003**, *42*, 739−745.
(327) Tsan, P.; Hus, J. C.; Caffrey, M.; Marion, D.; Blackledge, M. *J. Am. Chem. Soc.* **2000**, *122*, 5603−5612.
(328) Cordier, F.; Caffrey, M.; Brutscher, B.; Cusanovich, M. A.; Marion, D.; Blackledge, M. *J. Mol. Biol.* **1998**, *281*, 341−361.
(329) Reincke, B.; Perez, C.; Pristovsek, P.; Lucke, C.; Ludwig, C.; Lohr, F.; Rogov, V. V.; Ludwig, B.; Ruterjans, H. *Biochemistry* **2001**, *40*, 12312−12320.
(330) Assfalg, M.; Banci, L.; Bertini, I.; Ciofi-Baffoni, S.; Barker, P. D. *Biochemistry* **2001**, *40*, 12761−12771.
(331) Russell, B. S.; Zhong, L.; Bigotti, M. G.; Cutruzzola, F.; Bren, K. L. *J. Biol. Inorg. Chem.* **2003**, *8*, 156−166.
(332) Flynn, P. F.; Bieber Urbauer, R. J.; Zhang, H.; Lee, A. L.; Wand, A. J. *Biochemistry* **2001**, *40*, 6559−6569.
(333) Liu, W.; Flynn, P. F.; Fuentes, E. J.; Kranz, J. K.; McCormick, M.; Wand, A. J. *Biochemistry* **2001**, *40*, 14744−14753.
(334) Zhang, P.; Dayie, K. T.; Wagner, G. *J. Mol. Biol.* **1997**, *272*, 443−455.
(335) Volkman, B. F.; Alam, S. L.; Satterlee, J. D.; Markley, J. L. *Biochemistry* **1998**, *37*, 10906−10919.
(336) Ma, L.; Hass, M. A.; Vierick, N.; Kristensen, S. M.; Ulstrup, J.; Led, J. J. *Biochemistry* **2003**, *42*, 320−330.
(337) Bai, Y.; Chung, J.; Dyson, H. J.; Wright, P. E. *Protein Sci.* **2001**, *10*, 1056−1066.
(338) Barth, P.; Savarin, P.; Gilquin, B.; Lagoutte, B.; Ochsenbein, F. *Biochemistry* **2002**, *41*, 13902−13914.
(339) Lamosa, P.; Turner, D. L.; Ventura, R.; Maycock, C.; Santos, H. *Eur. J. Biochem.* **2003**, *270*, 4606−4614.
(340) Jimenez, B.; Piccioli, M.; Moratal, J. M.; Donaire, A. *Biochemistry* **2003**, *42*, 10396−10405.
(341) Leone, M.; Di, L. P.; Ohlenschlager, O.; Pedone, E. M.; Bartolucci, S.; Rossi, M.; Di, B. B.; Pedone, C.; Saviano, M.; Isernia, C.; Fattorusso, R. *Biochemistry* **2004**, *43*, 6043−6058.
(342) Daughdrill, G. W.; Vise, P. D.; Zhou, H.; Yang, X.; Yu, W. F.; Tasayco, M. L.; Lowry, D. F. *J. Biomol. Struct. Dyn.* **2004**, *21*, 663−670.
(343) Dangi, B.; Dobrodumov, A. V.; Louis, J. M.; Gronenborn, A. M. *Biochemistry* **2002**, *41*, 9376−9388.
(344) Huang, K.; Ghose, R.; Flanagan, J. M.; Prestegard, J. H. *Biochemistry* **1999**, *38*, 10567−10577.
(345) Landry, S. J.; Steede, N. K.; Maskos, K. *Biochemistry* **1997**, *36*, 10975−10986.
(346) Yoshida, T.; Oka, S.; Uchiyama, S.; Nakano, H.; Kawasaki, T.; Ohkubo, T.; Kobayashi, Y. *Biochemistry* **2003**, *42*, 4101−4107.
(347) McGuire, A. M.; Matsuo, H.; Wagner, G. *J. Biomol. NMR* **1998**, *12*, 73−88.
(348) Schneider, D. M.; Dellwo, M. J.; Wand, A. J. *Biochemistry* **1992**, *31*, 3645−3652.
(349) Brutscher, B.; Bruschweiler, R.; Ernst, R. R. *Biochemistry* **1997**, *36*, 13043−13053.
(350) Chang, S. L.; Tjandra, N. *J. Magn. Reson.* **2005**, *174*, 43−53.
(351) Kitahara, R.; Yokoyama, S.; Akasaka, K. *J. Mol. Biol.* **2005**, *347*, 277−285.
(352) Mccoy, M. A.; Senior, M. M.; Gesell, J. J.; Ramanathan, L.; Wyss, D. F. *J. Mol. Biol.* **2001**, *305*, 1099−1110.
(353) Nicholson, L. K.; Yamazaki, T.; Torchia, D. A.; Grzesiek, S.; Bax, A.; Stahl, S. J.; Kaufman, J. D.; Wingfield, P. T.; Lam, P. Y. S.; Jadhav, P. K.; Hodge, C. N.; Domaille, P. J.; Chang, C. H. *Nat. Struct. Biol.* **1995**, *2*, 274−280.
(354) Freedberg, D. I.; Wang, Y. X.; Stahl, S. J.; Kaufman, J. D.; Wingfield, P. T.; Kiso, Y.; Torchia, D. A. *J. Am. Chem. Soc.* **1998**, *120*, 7916−7923.
(355) Freedberg, D. I.; Ishima, R.; Jacob, J.; Wang, Y. X.; Kustanovich, I.; Louis, J. M.; Torchia, D. A. *Protein Sci.* **2002**, *11*, 221−232.
(356) Katoh, E.; Louis, J. M.; Yamazaki, T.; Gronenborn, A. M.; Torchia, D. A.; Ishima, R. *Protein Sci.* **2003**, *12*, 1376−1385.
(357) Feng, Y.; Likos, J. J.; Zhu, L.; Woodward, H.; Munie, G.; McDonald, J. J.; Stevens, A. M.; Howard, C. P.; De Crescenzo, G. A.; Welsch, D.; Shieh, H. S.; Stallings, W. C. *Biochim. Biophys. Acta* **2002**, *1598*, 10−23.
(358) Briknarova, K.; Grishaev, A.; Banyai, L.; Tordai, H.; Patthy, L.; Llinas, M. *Struct. Fold. Design* **1999**, *7*, 1235−1245.
(359) Remerowski, M. L.; Pepermans, H. A.; Hilbers, C. W.; Van De Ven, F. J. *Eur. J. Biochem.* **1996**, *235*, 629−640.
(360) Buevich, A. V.; Shinde, U. P.; Inouye, M.; Baum, J. *J. Biomol. NMR* **2001**, *20*, 233−249.
(361) Buevich, A. V.; Baum, J. *J. Am. Chem. Soc.* **1999**, *121*, 8671−8672.
(362) Huang, Y. T.; Liaw, Y. C.; Gorbatyuk, V. Y.; Huang, T. H. *J. Mol. Biol.* **2001**, *307*, 1075−1090.

(363) van Mierlo, C. P.; Darby, N. J.; Keeler, J.; Neuhaus, D.; Creighton, T. E. *J. Mol. Biol.* **1993**, *229*, 1125−1146.
(364) Smith, P. E.; van Schaik, R. C.; Szyperski, T.; Wuthrich, K.; van Gunsteren, W. F. *J. Mol. Biol.* **1995**, *246*, 356−365.
(365) Beeser, S. A.; Oas, T. G.; Goldenberg, D. P. *J. Mol. Biol.* **1998**, *284*, 1581−1596.
(366) Barbar, E.; Hare, M.; Daragan, V.; Barany, G.; Woodward, G. *Biochemistry* **1998**, *37*, 7822−7833.
(367) Shaw, G. L.; Davis, B.; Keeler, J.; Fersht, A. R. *Biochemistry* **1995**, *34*, 2225−2233.
(368) Liu, J.; Prakash, O.; Cai, M.; Gong, Y.; Huang, Y.; Wen, L.; Wen, J. J.; Huang, J. K.; Krishnamoorthi, R. *Biochemistry* **1996**, *35*, 1516−1524.
(369) Cai, M.; Huang, Y.; Prakash, O.; Wen, L.; Dunkelbarger, S. P.; Huang, J. K.; Liu, J.; Krishnamoorthi, R. *Biochemistry* **1996**, *35*, 4784−4794.
(370) Song, J.; Markley, J. L. *Biochemistry* **2003**, *42*, 5186−5194.
(371) Gonzalez, C.; Neira, J. L.; Ventura, S.; Bronsoms, S.; Rico, M.; Aviles, F. X. *Proteins* **2003**, *50*, 410−422.
(372) Szenthe, B.; Gaspari, Z.; Nagy, A.; Perczel, A.; Graf, L. *Biochemistry* **2004**, *43*, 3376−3384.
(373) Gao, G.; Semenchenko, V.; Arumugam, S.; Van, D., Sr. *J. Mol. Biol.* **2000**, *301*, 537−552.
(374) Perez-Canadillas, J. M.; Guenneugues, M.; Campos-Olivas, R.; Santoro, J.; Martinez, D. P.; Gavilanes, J. G.; Rico, M.; Bruix, M. *J. Biomol. NMR* **2002**, *24*, 301−316.
(375) Pang, Y.; Buck, M.; Zuiderweg, E. R. *Biochemistry* **2002**, *41*, 2655−2666.
(376) Cole, R.; Loria, J. P. *Biochemistry* **2002**, *41*, 6072−6081.
(377) Alexandrescu, A. T.; Rathgeb-Szabo, K.; Rumpel, K.; Jahnke, W.; Schulthess, T.; Kammerer, R. A. *Protein Sci.* **1998**, *7*, 389−402.
(378) Powers, R.; Clore, G. M.; Stahl, S. J.; Wingfield, P. T.; Gronenborn, A. *Biochemistry* **1992**, *31*, 9150−9157.
(379) Mueller, G. A.; Pari, K.; Derose, E. F.; Kirby, T. W.; London, R. E. *Biochemistry* **2004**, *43*, 9332−9342.
(380) Yamasaki, K.; Saito, M.; Oobatake, M.; Kanaya, S. *Biochemistry* **1995**, *34*, 6587−6601.
(381) Butterwick, J. A.; Patrick, L. J.; Astrof, N. S.; Kroenke, C. D.; Cole, R.; Rance, M.; Palmer, A. G., III. *J. Mol. Biol.* **2004**, *339*, 855−871.
(382) Laurents, D.; Perez-Canadillas, J. M.; Santoro, J.; Rico, M.; Schell, D.; Pace, C. N.; Bruix, M. *Proteins* **2001**, *44*, 200−211.
(383) Fushman, D.; Ohlenschlager, O.; Ruterjans, H. *J. Biomol. Struct. Dyn.* **1994**, *11*, 1377−1402.
(384) Engelke, J.; Ruterjans, H. *J. Biomol. NMR* **1997**, *9*, 63−78.
(385) Alexandrescu, A. T.; Shortle, D. *J. Mol. Biol.* **1994**, *242*, 527−546.
(386) Alexandrescu, A. T.; Jahnke, W.; Wiltscheck, R.; Blommers, M. J. *J. Mol. Biol.* **1996**, *260*, 570−587.
(387) Sinclair, J. F.; Shortle, D. *Protein Sci.* **1999**, *8*, 991−1000.
(388) Luginbuhl, P.; Pervushin, K. V.; Iwai, H.; Wuthrich, K. *Biochemistry* **1997**, *36*, 7305−7312.
(389) Habazettl, J.; Myers, L. C.; Yuan, F.; Verdine, G. L.; Wagner, G. *Biochemistry* **1996**, *35*, 9335−9348.
(390) Folmer, R. H.; Nilges, M.; Papavoine, C. H.; Harmsen, B. J.; Konings, R. N.; Hilbers, C. W. *Biochemistry* **1997**, *36*, 9120−9135.
(391) Mackay, J. P.; Shaw, G. L.; King, G. F. *Biochemistry* **1996**, *35*, 4867−4877.
(392) Feng, W. Q.; Tejero, R.; Zimmerman, D. E.; Inouye, M.; Montelione, G. T. *Biochemistry* **1998**, *37*, 10881−10896.
(393) Yan, J.; Liu, Y.; Lukasik, S. M.; Speck, N. A.; Bushweller, J. H. *Nat. Struct. Mol. Biol.* **2004**, *11*, 901−906.
(394) Matsuo, H.; Sugeta, H.; Shirakawa, M.; Kyogoku, Y. *J. Mol. Struct.* **1996**, *379*, 143−150.
(395) Clubb, R. T.; Mizuuchi, M.; Huth, J. R.; Omichinski, J. G.; Savilahti, H.; Mizuuchi, K.; Clore, G. M.; Gronenborn, A. M. *Proc. Natl. Acad. Sci. U.S.A.* **1996**, *93*, 1146−1150.
(396) Wikstrom, A.; Berglund, H.; Hambraeus, C.; van den Berg, S.; Hard, T. *J. Mol. Biol.* **1999**, *289*, 963−979.
(397) van Heijenoort, C.; Penin, F.; Guittet, E. *Biochemistry* **1998**, *37*, 5060−5073.
(398) Braddock, D. T.; Louis, J. M.; Baber, J. L.; Levens, D.; Clore, G. M. *Nature* **2002**, *415*, 1051−1056.
(399) Bracken, C.; Carr, P. A.; Cavanagh, J.; Palmer, A. G. *J. Mol. Biol.* **1999**, *285*, 2133−2146.
(400) Jin, C. W.; Marsden, I.; Chen, X. Q.; Liao, X. B. *Biochemistry* **1998**, *37*, 6179−6187.
(401) Berglund, H.; Kovacs, H.; Dahlmanwright, K.; Gustafsson, J. A.; Hard, T. *Biochemistry* **1992**, *31*, 12001−12011.
(402) Damberger, F. F.; Pelton, J. G.; Liu, C.; Cho, H.; Harrison, C. J.; Nelson, H. C.; Wemmer, D. E. *J. Mol. Biol.* **1995**, *254*, 704−719.
(403) Katahira, M.; Miyanoiri, Y.; Enokizono, Y.; Matsuda, G.; Nagata, T.; Ishikawa, F.; Uesugi, S. *J. Mol. Biol.* **2001**, *311*, 973−988.
(404) Baber, J. L.; Levens, D.; Libutti, D.; Tjandra, N. *Biochemistry* **2000**, *39*, 6022−6032.
(405) Broadhurst, R. W.; Hardman, C. H.; Thomas, J. O.; Laue, E. D. *Biochemistry* **1995**, *34*, 16608−16617.
(406) Zhang, X.; Xu, Y.; Zhang, J.; Wu, J.; Shi, Y. *Biochemistry* **2005**, *44*, 8117−8125.
(407) Gao, Y.; Kaluarachchi, K.; Giedroc, D. P. *Protein Sci.* **1998**, *7*, 2265−2280.
(408) Miyanoiri, Y.; Kobayashi, H.; Imai, T.; Watanabe, M.; Nagata, T.; Uesugi, S.; Okano, H.; Katahira, M. *J. Biol. Chem.* **2003**, *278*, 41309−41315.
(409) Poznanski, J.; Bolewska, K.; Zhukov, I.; Wierzchowski, K. L. *Biochemistry* **2003**, *42*, 13438−13448.
(410) Kahsai, M. A.; Martin, E.; Edmondson, S. P.; Shriver, J. W. *Biochemistry* **2005**, *44*, 13500−13509.
(411) Bhattacharya, S.; Botuyan, M. V.; Hsu, F.; Shan, X.; Arunkumar, A. I.; Arrowsmith, C. H.; Edwards, A. M.; Chazin, W. J. *Protein Sci.* **2002**, *11*, 2316−2325.
(412) Cary, P. D.; Read, C. M.; Davis, B.; Driscoll, P. C.; Crane-Robinson, C. *Protein Sci.* **2001**, *10*, 83−98.
(413) Kahsai, M. A.; Vogler, B.; Clark, A. T.; Edmondson, S. P.; Shriver, J. W. *Biochemistry* **2005**, *44*, 2822−2832.
(414) Biyani, K.; Kahsai, M. A.; Clark, A. T.; Armstrong, T. L.; Edmondson, S. P.; Shriver, J. W. *Biochemistry* **2005**, *44*, 14217−14230.
(415) Maguire, M. L.; Guler-Gane, G.; Nietlispach, D.; Raine, A. R.; Zorn, A. M.; Standart, N.; Broadhurst, R. W. *J. Mol. Biol.* **2005**, *348*, 265−279.
(416) Jia, X.; Lee, L. K.; Light, J.; Palmer, A. G.; Assa-Munt, N. *J. Mol. Biol.* **1999**, *292*, 1083−1093.
(417) Fieber, W.; Schneider, M. L.; Matt, T.; Krautler, B.; Konrat, R.; Bister, K. *J. Mol. Biol.* **2001**, *307*, 1395−1410.
(418) Walters, K. J.; Dayie, K. T.; Reece, R. J.; Ptashne, M.; Wagner, G. *Nat. Struct. Biol.* **1997**, *4*, 744−750.
(419) Zheng, Z.; Czaplicki, J.; Jardetzky, O. *Biochemistry* **1995**, *34*, 5212−5223.
(420) Lu, J.; Hall, K. B. *Biochemistry* **1997**, *36*, 10393−10405.
(421) Fausti, S.; Weiler, S.; Cuniberto, C.; Hwang, K. J.; No, K. T.; Gruschus, J. M.; Perico, A.; Nirenberg, M.; Ferretti, J. A. *Biochemistry* **2001**, *40*, 12004−12012.
(422) Laity, J. H.; Dyson, H. J.; Wright, P. E. *Proc. Natl. Acad. Sci. U.S.A.* **2000**, *97*, 11932−11935.
(423) Ikegami, T.; Kuraoka, I.; Saijo, M.; Kodo, N.; Kyogoku, Y.; Morikawa, K.; Tanaka, K.; Shirakawa, M. *J. Biochem.* **1999**, *125*, 495−506.
(424) Buchko, G. W.; Daughdrill, G. W.; de Lorimier, R.; Rao, B. K.; Isern, N. G.; Lingbeck, J. M.; Taylor, J. S.; Wold, M. S.; Gochin, M.; Spicer, L. D.; Lowry, D. F.; Kennedy, M. A. *Biochemistry* **1999**, *38*, 15116−15128.
(425) Kloks, C. P.; Tessari, M.; Vuister, G. W.; Hilbers, C. W. *Biochemistry* **2004**, *43*, 10237−10246.
(426) Guo, X.; Li, Y.; Peng, K.; Hu, Y.; Li, C.; Xia, B.; Jin, C. *J. Biol. Chem.* **2005**, *280*, 39601−39608.
(427) Eletsky, A.; Kienhofer, A.; Hilvert, D.; Pervushin, K. *Biochemistry* **2005**, *44*, 6788−6799.
(428) Banci, L.; Bertini, I.; Cramaro, F.; Del Conte, R.; Rosato, A.; Viezzoli, M. S. *Biochemistry* **2000**, *39*, 9108−9118.
(429) Prompers, J. J.; van Noorloos, B.; Mannesse, M. L. M.; Groenewegen, A.; Egmond, M. R.; Verheij, H. M.; Hilbers, C. W.; Pepermans, H. A. M. *Biochemistry* **1999**, *38*, 5982−5994.
(430) Zhao, Q.; Abeygunawardana, C.; Mildvan, A. S. *Biochemistry* **1996**, *35*, 1525−1532.
(431) Yun, S.; Jang, D. S.; Choi, G.; Kim, K. S.; Choi, K. Y.; Lee, H. C. *J. Biol. Chem.* **2002**, *277*, 23414−23419.
(432) Epstein, D. M.; Benkovic, S. J.; Wright, P. E. *Biochemistry* **1995**, *34*, 11037−11048.
(433) Pitcher, W. H.; Derose, E. F.; Mueller, G. A.; Howell, E. E.; London, R. E. *Biochemistry* **2003**, *42*, 11150−11160.
(434) Krishnan, V. V.; Thornton, K. H.; Thelen, M. P.; Cosman, M. *Biochemistry* **2001**, *40*, 13158−13166.
(435) Maciejewski, M. W.; Liu, D. J.; Prasad, R.; Wilson, S. H.; Mullen, G. P. *J. Mol. Biol.* **2000**, *296*, 229−253.
(436) McCallum, S. A.; Hitchens, T. K.; Torborg, C.; Rule, G. S. *Biochemistry* **2000**, *39*, 7343−7356.
(437) Liu, D. J.; Wang, Y. S.; Gesell, J. J.; Wyss, D. F. *J. Mol. Biol.* **2001**, *314*, 543−561.
(438) Guilhaudis, L.; Simorre, J. P.; Blackledge, M.; Neuburger, M.; Bourguignon, J.; Douce, R.; Marion, D.; Gans, P. *Biochemistry* **1999**, *38*, 8334−8346.
(439) Buck, M.; Boyd, J.; Redfield, C.; MacKenzie, D. A.; Jeenes, D. J.; Archer, D. B.; Dobson, C. M. *Biochemistry* **1995**, *34*, 4041−4055.
(440) Buck, M.; Schwalbe, H.; Dobson, C. M. *J. Mol. Biol.* **1996**, *257*, 669−683.

(441) Johnson, R. J.; Christodoulou, J.; Dumoulin, M.; Caddy, G. L.; Alcocer, M. J.; Murtagh, G. J.; Kumita, J. R.; Larsson, G.; Robinson, C. V.; Archer, D. B.; Luisi, B.; Dobson, C. M. *J. Mol. Biol.* **2005**, *352*, 823−836.
(442) Gorbatyuk, V. Y.; Tsai, C. K.; Chang, C. F.; Huang, T. H. *J. Biol. Chem.* **2004**, *279*, 5772−5780.
(443) Wang, G. P.; Cahill, S. M.; Liu, X. H.; Girvin, M. E.; Grubmeyer, C. *Biochemistry* **1999**, *38*, 284−295.
(444) Uhrinova, S.; Uhrin, D.; Nairn, J.; Price, N. C.; Fothergill-Gilmore, L. A.; Barlow, P. N. *J. Mol. Biol.* **2001**, *306*, 275−290.
(445) Pan, B.; Maciejewski, M. W.; Marintchev, A.; Mullen, G. P. *J. Mol. Biol.* **2001**, *310*, 1089−1107.
(446) Banci, L.; Bertini, I.; Cantini, F.; D'Onofrio, M.; Viezzoli, M. S. *Protein Sci.* **2002**, *11*, 2479−2492.
(447) Shipp, E. L.; Cantini, F.; Bertini, I.; Valentine, J. S.; Banci, L. *Biochemistry* **2003**, *42*, 1890−1899.
(448) Scheuermann, T. H.; Keeler, C.; Hodsdon, M. E. *Biochemistry* **2004**, *43*, 12198−12209.
(449) Connelly, G. P.; Withers, S. G.; McIntosh, L. P. *Protein Sci.* **2000**, *9*, 512−524.
(450) Hill, R. B.; Bracken, C.; DeGrado, W. F.; Palmer, A. G. *J. Am. Chem. Soc.* **2000**, *122*, 11610−11619.
(451) Walsh, S. T. R.; Lee, A. L.; DeGrado, W. F.; Wand, A. J. *Biochemistry* **2001**, *40*, 9560−9569.
(452) Markus, M. A.; Dayie, K. T.; Matsudaira, P.; Wagner, G. *Biochemistry* **1996**, *35*, 1722−1732.
(453) Campos-Olivas, R.; Horr, I.; Bormann, C.; Jung, G.; Gronenborn, A. M. *J. Mol. Biol.* **2001**, *308*, 765−782.
(454) Idiyatullin, D.; Krushelnitsky, A.; Nesmelova, I.; Blanco, F.; Daragan, V. A.; Serrano, L.; Mayo, K. H. *Protein Sci.* **2000**, *9*, 2118−2127.
(455) Mayo, K. H.; Daragan, V. A.; Idiyatullin, D.; Nesmelova, I. *J. Magn. Reson.* **2000**, *146*, 188−195.
(456) Lane, A. N.; Hays, L. M.; Tsvetkova, N.; Feeney, R. E.; Crowe, L. M.; Crowe, J. H. *Biophys. J.* **2000**, *78*, 3195−3207.
(457) Daley, M. E.; Spyracopoulos, L.; Jia, Z.; Davies, P. L.; Sykes, B. D. *Biochemistry* **2002**, *41*, 5515−5525.
(458) Graether, S. P.; Gagne, S. M.; Spyracopoulos, L.; Jia, Z.; Davies, P. L.; Sykes, B. D. *J. Mol. Biol.* **2003**, *327*, 1155−1168.
(459) Raussens, V.; Slupsky, C. M.; Ryan, R. O.; Sykes, B. D. *J. Biol. Chem.* **2002**, *277*, 29172−29180.
(460) Wong, K. B.; Fersht, A. R.; Freund, S. M. V. *J. Mol. Biol.* **1997**, *268*, 494−511.
(461) Sahu, S. C.; Bhuyan, A. K.; Majumdar, A.; Udgaonkar, J. B. *Proteins* **2000**, *41*, 460−474.
(462) Ramirez-Alvarado, M.; Daragan, V. A.; Serrano, L.; Mayo, K. H. *Protein Sci.* **1998**, *7*, 720−729.
(463) Lee, C. S.; Kumar, T. K.; Lian, L. Y.; Cheng, J. W.; Yu, C. *Biochemistry* **1998**, *37*, 155−164.
(464) Favier, A.; Brutscher, B.; Blackledge, M.; Galinier, A.; Deutscher, J.; Penin, F.; Marion, D. *J. Mol. Biol.* **2002**, *317*, 131−144.
(465) Wolf-Watz, M.; Grundstrom, T.; Hard, T. *Biochemistry* **2001**, *40*, 11423−11432.
(466) Griswold, I. J.; Dahlquist, F. W. *Biophys. Chem.* **2002**, *101−102*, 359−373.
(467) Macdonald, C. J.; Tozawa, K.; Collins, E. S.; Penfold, C. N.; James, R.; Kleanthous, C.; Clayden, N. J.; Moore, G. R. *J. Biomol. NMR* **2004**, *30*, 81−96.
(468) Goldenberg, D. P.; Koehn, R. E.; Gilbert, D. E.; Wagner, G. *Protein Sci.* **2001**, *10*, 538−550.
(469) Fan, J. S.; Zhang, Q.; Tochio, H.; Zhang, M. *J. Biomol. NMR* **2002**, *23*, 103−114.
(470) Ilangovan, U.; Ding, W.; Zhong, Y.; Wilson, C. L.; Groppe, J. C.; Trbovich, J. T.; Zuniga, J.; Demeler, B.; Tang, Q.; Gao, G.; Mulder, K. M.; Hinck, A. P. *J. Mol. Biol.* **2005**, *352*, 338−354.
(471) Seifert, M. H.; Georgescu, J.; Ksiazek, D.; Smialowski, P.; Rehm, T.; Steipe, B.; Holak, T. A. *Biochemistry* **2003**, *42*, 2500−2512.
(472) Rothemund, S.; Liou, Y. C.; Davies, P. L.; Sonnichsen, F. D. *Biochemistry* **1997**, *36*, 13791−13801.
(473) Jaroniec, C. P.; Kaufman, J. D.; Stahl, S. J.; Viard, M.; Blumenthal, R.; Wingfield, P. T.; Bax, A. *Biochemistry* **2005**, *44*, 16167−16180.
(474) Cornilescu, C. C.; Bouamr, F.; Carter, C.; Tjandra, N. *Protein Sci.* **2003**, *12*, 973−981.
(475) Bouamr, F.; Cornilescu, C. C.; Goff, S. P.; Tjandra, N.; Carter, C. A. *J. Biol. Chem.* **2005**, *280*, 6792−6801.
(476) Beglova, N.; North, C. L.; Blacklow, S. C. *Biochemistry* **2001**, *40*, 2808−2815.
(477) Kurniawan, N. D.; Aliabadizadeh, K.; Brereton, I. M.; Kroon, P. A.; Smith, R. *J. Mol. Biol.* **2001**, *311*, 341−356.
(478) Papavoine, C. H.; Remerowski, M. L.; Horstink, L. M.; Konings, R. N.; Hilbers, C. W.; Van De Ven, F. J. *Biochemistry* **1997**, *36*, 4015−4026.
(479) Williams, K. A.; Farrow, N. A.; Deber, C. M.; Kay, L. E. *Biochemistry* **1996**, *35*, 5145−5157.
(480) Barthe, P.; Declerck, N.; Delsuc, M. A.; Lefevre, J. F.; Roumestand, C. *J. Chim. Phys. Phys. Chim. Biol.* **1999**, *96*, 1585−1594.
(481) Kemple, M. D.; Buckley, P.; Yuan, P.; Prendergast, F. G. *Biochemistry* **1997**, *36*, 1678−1688.
(482) Sung, Y. H.; Shin, J.; Chang, H. J.; Cho, J. M.; Lee, W. *J. Biol. Chem.* **2001**, *276*, 19624−19630.
(483) Gitti, R. K.; Wright, N. T.; Margolis, J. W.; Varney, K. M.; Weber, D. J.; Margolis, F. L. *Biochemistry* **2005**, *44*, 9673−9679.
(484) Campbell, A. P.; Spyracopoulos, L.; Irvin, R. T.; Sykes, B. D. *J. Biomol. NMR* **2000**, *17*, 239−255.
(485) Campbell, A. P.; Spyracopoulos, L.; Wong, W. Y.; Irvin, R. T.; Sykes, B. D. *Biochemistry* **2003**, *42*, 11334−11346.
(486) Suh, J. Y.; Spyracopoulos, L.; Keizer, D. W.; Irvin, R. T.; Sykes, B. D. *Biochemistry* **2001**, *40*, 3985−3995.
(487) Berjanskii, M.; Riley, M.; Van Doren, S. R. *J. Mol. Biol.* **2002**, *321*, 503−516.
(488) Viles, J. H.; Donne, D.; Kroon, G.; Prusiner, S. B.; Cohen, F. E.; Dyson, H. J.; Wright, P. E. *Biochemistry* **2001**, *40*, 2743−2753.
(489) McDonnell, J. M.; Fushman, D.; Cahill, S. M.; Zhou, W. J.; Wolven, A.; Wilson, C. B.; Nelle, T. D.; Resh, M. D.; Wills, J.; Cowburn, D. *J. Mol. Biol.* **1998**, *279*, 921−928.
(490) Williams, C.; Galyov, E. E.; Bagby, S. *Biochemistry* **2004**, *43*, 11998−12008.
(491) Feher, V. A.; Zapf, J. W.; Hoch, J. A.; Whiteley, J. M.; McIntosh, L. P.; Rance, M.; Skelton, N. J.; Dahlquist, F. W.; Cavanagh, J. *Biochemistry* **1997**, *36*, 10015−10025.
(492) Allard, P.; Haerd, T. *J. Magn. Reson.* **1997**, *126*, 48−57.
(493) Prieto, J. H.; Sampoli Benitez, B. A.; Melacini, G.; Johnson, D. A.; Wood, M. J.; Komives, E. A. *Biochemistry* **2005**, *44*, 1225−1233.
(494) Guenneugues, M.; Gilquin, B.; Wolff, N.; Menez, A.; Zinn-Justin, S. *J. Biomol. NMR* **1999**, *14*, 47−66.
(495) Botuyan, M. V.; Mer, G.; Yi, G. S.; Koth, C. M.; Case, D. A.; Edwards, A. M.; Chazin, W. J.; Arrowsmith, C. H. *J. Mol. Biol.* **2001**, *312*, 177−186.
(496) Grey, M. J.; Tang, Y.; Alexov, E.; McKnight, C. J.; Raleigh, D. P.; Palmer, A. G., III. *J. Mol. Biol.* **2006**, *355*, 1078−1094.
(497) Korzhnev, D. M.; Bocharov, E. V.; Zhuravlyova, A. V.; Orekhov, V. Y.; Ovchinnikova, T. V.; Billeter, M.; Arseniev, A. S. *FEBS Lett.* **2001**, *495*, 52−55.

CR040421P